ıia Water Resources Research Center
ıia Polytechnic Institute and State University

Bulletin 164

riable Source Area Concept for Identifying Critical Runoff-Generating Areas in a Watershed

G.V. Loganathan, S.P. Shrestha, T.A. Dillaha, and B.B. Ross

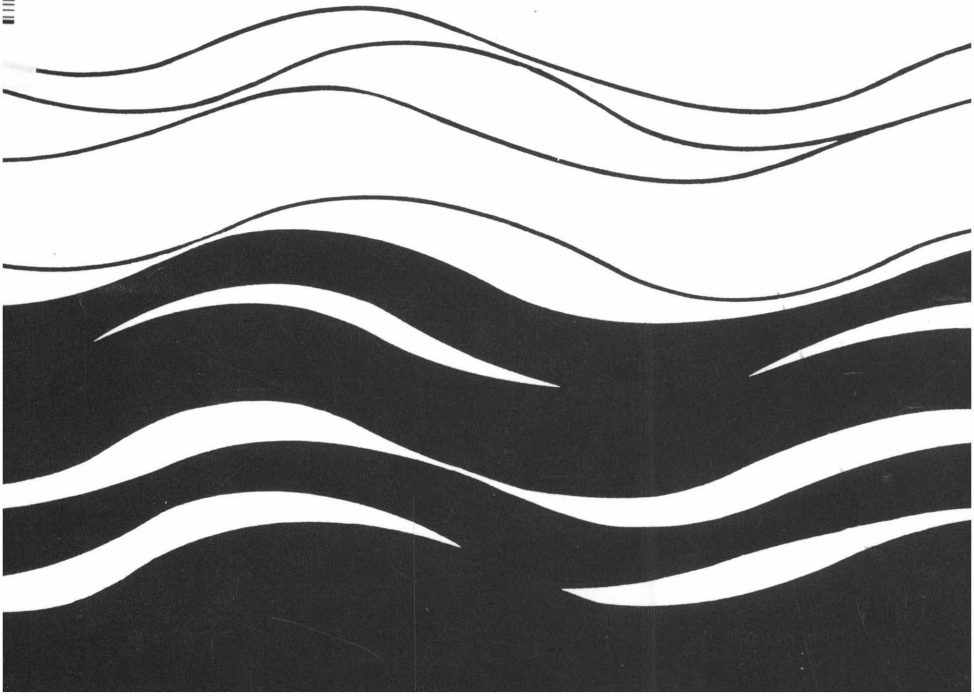

Bulletin 164
May 1989

Variable Source Area Concept for Identifying Critical Runoff-Generating Areas in a Watershed

G.V. Loganathan
S.P. Shrestha
Department of Civil Engineering
T.A. Dillaha
B.B. Ross
Department of Agricultural Engineering
Virginia Polytechnic Institute and State University

VPI-VWRRC-BULL 164

Virginia Water Resources Research Center
Virginia Polytechnic Institute and State University
Blacksburg • 1989

This Bulletin is published with funds provided in part by the
U.S Geological Survey, Department of the Interior,
as authorized by the Water Resources Research Act of 1984.

Additional copies of this publication, while the supply lasts,
may be obtained from the Virginia Water Resources Research Center.
Single copies are provided free to persons and organizations within
Virginia. For those out-of-state, the charge is $8 a copy.
Payment or purchase order must accompany the order.

CONTENTS

LIST OF FIGURES

LIST OF TABLES

ACKNOWLEDGMENTS

The authors express their appreciation to William R. Walker, Director of the Virginia Water Resources Research Center for his support and valuable suggestions in setting the guidelines for the project. We thank Margaret S. Hrezo and Diana Weigmann of the Water Center for coordinating advisory committee meetings and for general administration of the project. Our thanks go to P. Y. Bernier of the Northern Forest Research Center, Alberta, Canada, for providing the VSAS2 computer program. The authors thank Jan Karr of the Agricultural Engineering Department for providing the data used in this study. We also thank the technical reviewers for their constructive comments.

ABSTRACT

Nonpoint source pollution from agricultural areas is a major water quality concern in the rivers, lakes, and estuaries of Virginia. It has also been identified as a major problem in the Chesapeake Bay with the Environmental Protection Agency estimating that agricultural nonpoint sources account for 40 to 70 percent of the phosphorus and nitrogen loading to the bay. To address this problem, the use of conservation tillage and other best management practices (BMPs) is being promoted in Virginia. In fact, a state cost-sharing program has been implemented to encourage farmers to install BMPs specifically for water quality improvement. Since funds are severely limited, it is essential that some mechanism be developed to target cost-sharing funds to the farms and fields which have the most significant impact on downstream water quality. This will greatly improve the cost effectiveness of the program and would result in far greater water quality improvements. One possible means for targeting BMPs is identifying the portions of watersheds that are responsible for generating runoff since runoff is the primary transport vehicle for pollutants from watersheds.

A general methodology has been developed to identify the critical areas within a watershed that contribute to surface and subsurface runoff and thus to pollutant transport. The surface runoff is viewed as an extension of the surface saturation process which occurs because of the soil's inability to transmit subsurface flow further downstream. The subsurface flow emerging to the surface (return flow), combined with rainfall, generates the surface runoff. In the absence of surface saturation, no surface runoff is generated but subsurface flow may still contribute to runoff. The methodology was applied to Pony Mountain Branch watershed in Virginia. It was found that subsurface flow does account for a significant part of total runoff. The critical areas were identified based on their relative contributions to total runoff production. To account for its variability, hydraulic conductivity was treated as a lognormally distributed random variable. A Monte Carlo simulation procedure was adopted to compute water content values for varying hydraulic conductivities. The saturated water content values at different times decide the expansion and contraction of critical areas. The mean growth pattern for the critical areas from the simulations was adopted as the required critical region. It is also found that deterministic simulation may not be representative of the critical area growth pattern where large standard deviations in hydraulic conductivity occur.

Key Words: Partial Watershed Hydrology, Subsurface Flow, Numerical Analysis, Monte Carlo Simulation

INTRODUCTION

I. Problem Definition

Nonpoint source pollution from agricultural areas is a major water quality concern in the rivers, lakes, and estuaries of Virginia. It has also been identified as a major source of pollution in the Chesapeake Bay. According to an Environmental Protection Agency (EPA) estimate, nonpoint sources account for 40 to 70 percent of phosphorus and nitrogen loading to the bay. At present, Virginia is promoting the use of best management practices (BMPs) to abate the problem of nonpoint source pollution and there is a need to identify the particular fields responsible for water quality problems. It has been demonstrated that only portions of watersheds contribute a significant proportion of runoff (Betson 1964; Ragan 1968; Engman and Rogowski 1974; Gburek et al. 1977; Beven and Kirkby 1979). The identification of these source areas provides an excellent strategy for the placement of BMPs to control agricultural runoff. This, in turn, will reduce the water quality degradation since runoff is the primary transport vehicle for pollutants from watersheds. Concentrating BMPs in these source areas will result in maximum water quality improvements at minimum cost. It should be noted that the control of runoff within the source areas is important not only from the aspect of surface runoff (Betson 1964), which transports sediment and agricultural chemicals, but also because of its intimate connection to subsurface flow or interflow (Hewlett 1961) which carries soluble pollutants.

II. Study Objectives

Agricultural runoff can be controlled with the use of BMPs. The efficient selection and positioning of BMPs requires an understanding of the runoff generation phenomena within a watershed. A number of processes may be involved; some of these mechanisms are shown in Figure 1. In urban areas, runoff primarily occurs as overland flow. The classic concept of the Horton overland flow theory (Horton 1933), called *infiltration excess mechanism* states that whenever rainfall intensity exceeds the infiltration capacity of the soil (the maximum rate at which water can be absorbed) overland flow occurs (see path 1, Figure 1). In periods of continued intense rainfall, the moisture content at the surface increases and the surface becomes saturated. At this point, the infiltration rate equals the saturated hydraulic conductivity and overland flow will continue if rainfall intensity exceeds the saturation rate. It is seen that only the vertical hydraulic conductivity is used. Therefore, the maximum runoff rate equals the difference of the rainfall rate and the saturated hydraulic conductivity. This theory, while adequately predicting runoff quantities from poorly vegetated areas, did not fare well when applied to well-vegetated slopes (Hewlett 1961). He observed that it was rather rare for rainfall intensity to exceed infiltration in vegetated areas. In the Coweeta watershed of North Carolina, a 100-year storm delivering more than 20 inches of rain in five

days did not generate any overland flow (Hewlett and Nutter 1970). Hewlett and Hibbert (1967) and Hewlett and Nutter (1970) found interflow to be the primary source of runoff in such areas. This mechanism, known as *saturation excess mechanism,* is based on the hypothesis that as rainfall continues to soak the slopes, the capacity of the soil mantle near the stream to transmit subsurface flow is exceeded and the water emerges at the surface (see path 3, Figure 1). Both this emergence of subsurface flow to the surface and the inability of soil to transmit subsurface flow downstream are related to the lateral hydraulic conductivity of the soil. Zaslavsky and Rogowski (1969) attributed the deviation of the infiltration flux from the vertical to the downslope to the soil anisotropy. Zaslavsky and Sinai (1981) present more details of the role played by soil anisotropy in determining the lateral flow along with the splashing of raindrops as an additional cause. This emerging subsurface flow also leads to expanding saturated areas, typically starting from the stream sides. Once the rain ceases, these saturated areas begin to contract. These expanding and contracting saturated areas are called the *variable source areas.* The overland flow is generated by the combination of rainfall and subsurface flow emerging to the surface. It is also noted that in the absence of overland flow, the runoff generated by subsurface flow will be lagged by several days compared to only a few hours for overland flow. This is because of the tremendous discrepancy in the speeds of these flows; overland flow speed is about 15,000 ft./day whereas subsurface flow speed is only about 15 ft./day. Dunne and Black (1970a, 1970b) observed overland flow from the water table rising to the surface and named it *saturation overland flow*; this tends to occur in thickly vegetated landscapes with thin soils, regions with high water tables, and concave hill slopes. Dunne (1983) presents a comprehensive review of the various mechanisms of runoff generation.

The actual runoff production mechanisms in a particular watershed depend on such factors as topography, hydrogeologic properties of soil, and land use. Betson (1964) proposed the *partial area concept*, stating that only certain fixed portions of the watershed regularly contribute to runoff whereas other portions rarely do. The main differences are that the partial areas are almost fixed whereas the variable source areas expand and contract; the partial areas generate Hortonian overland flow whereas the variable source areas combine rainfall and subsurface flow; the partial areas result from the extreme variability in infiltration rates and irregular patterns of rainfall in time and space whereas the variable source areas are the result of the soil's inability to transmit interflow further downstream (Freeze 1974).

The traditional approach to predicting runoff is based on the unit hydrograph theory (Sherman 1932) which considers surface runoff only and ignores subsurface flow. Therefore, it is readily seen that such a method will be of little use in predicting runoff in well-vegetated areas that generate hardly any surface runoff. It should also be noted that the unit hydrograph theory is a black box method in that it gives very little consideration to watershed characteristics and therefore lacks

the ability to capture the growth patterns of the critical source areas contributing the maximum runoff quantity.

Even though the theories on runoff generation seem to be quite varied, they can be unified by observing that all of these theories relate rainfall to soil saturation conditions. By coupling unsaturated and saturated groundwater flow with surface flow, a unified theory can be developed. Leite (1985) has found that interflow not only can exceed overland flow in terms of discharge but also can transport soluble pollutants such as nitrates in large quantities. Therefore, a unified theory is required to identify the origin and pathways (source areas) of overland flow and interflow. This study is directed towards developing a methodology for identifying these source areas. Any BMPs placed across these paths will have significant impact on runoff and on nonpoint source pollution.

Another crucial point is the variation in hydraulic conductivity values. El-Kadi (1984) presents a comprehensive review of modeling variability in groundwater flow and Gelhar (1986) reviews stochastic groundwater flow analysis. In this study, the Monte Carlo simulation is used to account for the randomness of the hydraulic conductivity. A detailed description of the Monte Carlo simulation as applied to groundwater flow can be found in Smith and Freeze (1979a, 1979b), Smith and Schwartz (1980, 1981a, 1981b), and Silliman and Wright (1988). The hydraulic conductivities at different depths are assumed to be correlated, lognormally distributed random variables. In order to incorporate the spatial variations of hydraulic conductivity values, a Monte Carlo simulation analysis is performed and the growth patterns of the source areas are predicted.

III. Organization of the Report

The chapter on subsurface flow presents the relevant equations together with the boundary conditions and a brief description of the numerical scheme employed. The chapter on the computer program Variable Source Area Simulator (VSAS2) describes the model assumptions, input requirements, and interpretation of the output. It also explains the coupling between the surface and subsurface flows. The chapter on the Monte Carlo simulation analysis for identifying the critical regions of a watershed in terms of runoff generation presents the relevant statistical analysis. Also, a step-by-step procedure for implementation of the analysis is presented. The application chapter contains the Monte Carlo analysis for a real watershed, Pony Mountain Branch watershed in Virginia. A comparison between the Monte Carlo analysis and deterministic simulation is made. A summary of the findings is provided. Appendix A presents a detailed description of the numerical scheme used in the computer program. Appendix B is the users' manual for the model used in this study and offers an example with detailed descriptions of input and output. Figures and tables used in the study are provided at the end of the report.

SUBSURFACE FLOW

I. Introduction

Identification of the source areas requires a clear understanding of flow principles. The path by which water reaches a stream depends upon various factors such as topography, soil type, land use, etc. In different watersheds — and even in various parts of the same watershed — different processes may govern runoff, and the relative contributions towards total runoff will differ. This chapter discusses the subsurface flow part of the runoff. The governing equation is derived and finite difference approximations to the governing equation are reviewed.

II. Governing Equation

The movement of water in the subsurface zone occurs through both saturated and unsaturated regions. The governing flow equation is derived using the continuity equation for flow through porous medium and Darcy's law for groundwater movement.

A. Preliminaries

Groundwater denotes the subsurface water that occurs beneath the water table in soils and geologic formations that are fully saturated. The primary source of groundwater is precipitation. Water from precipitation infiltrates the ground surface; moves downward, primarily under the influence of gravity; and accumulates, filling all the interstices of the porous medium above some impervious stratum. A porous medium consists of pore space (voids) and solid matrix. The pore space is that portion of the porous medium which is not occupied by solid matter. In general, the pore space contains a liquid (e.g. water) and/or gas (e.g. air). The total volume occupied by the pore space in a porous medium is termed volume of voids and the total volume occupied by the solid particles alone is called volume of solids. In Figure 2, the crosshatched portion represents the volume of solids, the dotted portion represents the volume of water, and the unshaded portion represents the void space. It is observed that

$$V_T = V_V + V_s \tag{2.1}$$

where: V_T is the bulk volume of the porous medium.

The following notation is used in the ensuing sections:

V_v = Volume of voids (L^3)
V_s = Volume of solids (L^3)
V_w = Volume of water (L^3)

V_T = Bulk volume of the porous medium (L^3)
$= V_v + V_s$
K = hydraulic conductivity of the porous medium (LT^{-1})
p = pore water pressure ($ML^{-1}T^{-2}$)
z = elevation head (L)
ρ = fluid density (ML^{-3})
ψ = pressure head (L)
$= p/\Gamma$
Γ = specific weight of the fluid ($ML^{-2}T^{-2}$)
σ_z = stress borne by the solids ($ML^{-1}T^{-2}$)
σ_T = total stress acting downward on a plane ($ML^{-1}T^{-2}$); the total stress acting on a subsurface plane is due to the overburden load that includes the total load of soil, water, and everything that adds load at the ground surface including atmospheric pressure
$= \sigma_z + p$

The following definitions are formed with the aid of the above notation:

$$\text{Porosity, } n = \frac{V_v}{V_T}$$

$$\text{Void ratio , } e = \frac{V_v}{V_s}$$

$$\text{Moisture content, } \theta = \frac{V_w}{V_T} \quad \text{(also known as water content)}$$

$$\text{Degree of saturation, } S = \frac{V_w}{V_v}$$

$$\text{Fluid compressibility, } \xi = \frac{-\Delta V_w/V_w}{\Delta p} = \frac{\Delta\rho/\rho}{\Delta p}$$

$$\text{Porous medium compressibility, } \zeta = \frac{-\Delta V_T/V_T}{\Delta\sigma_z}$$

$$\text{Hydraulic head, } \phi = \frac{p}{\Gamma} + z = \psi + z$$

Mathematically, moisture content, θ, can vary between zero and porosity, n. However, there exists a lower threshold limit for θ known as the residual water content, θ_r. This is due to the adhesive forces that hold the moisture around the soil particles and cannot be removed by usual hydraulic gradients. The upper and lower limits for the degree of saturation, S, are zero for fully dry soils to unity for a fully saturated matrix. The void ratio, e, can be greater than unity indicating that the

volume of voids, V_v, can be larger than the volume of solids, V_s. The fluid compressibility, ξ, indicates the relative change in the volume of water due to the change in imparted stress on water, namely, the change in pore water pressure, Δp. The porous medium compressibility, ζ, indicates the relative change in bulk volume for a relative change in the stress borne by the solid skeleton, $\Delta\sigma_z$.

B. Darcy's Law

The specific discharge or superficial velocity, q, through a porous medium can be described by Darcy's law (1856) which can be written as

$$q = -K\frac{\Delta\phi}{\Delta l} \tag{2.2}$$

where: q = specific discharge (LT^{-1})

K = hydraulic conductivity of the porous medium (LT^{-1})

$\frac{\Delta\phi}{\Delta l}$ = hydraulic gradient (LL^{-1})

Equation (2.2) assumes that the velocity head is negligible and uses the hydraulic head, ϕ (sum of pressure head and elevation head), instead of the total energy head which is the sum of hydraulic head and velocity head. The specific discharge, q, has the dimensions of velocity. However, note that this superficial velocity is different from the actual velocity of flow, v (Figure 3). This is because the flow can take place only through the interstices. That is, the actual area available for flow is nA. Therefore, the actual average velocity of flow should be

$$v = \frac{Q}{n\,A} = \frac{q}{n} \tag{2.3}$$

It is further noted that v is still an average velocity in the sense that it reflects the average of individual pore fluid velocities. Because of the uncertainties involved in estimating n, it is generally preferred to use Darcy's superficial velocity, q, in groundwater flow analysis with the area of flow as A.

The constant of proportionality in Darcy's law, known as the hydraulic conductivity, expresses the ease with which a fluid moves through a porous matrix. It depends on both the solid matrix and the fluid properties. The fluid properties of major concern are the density, ρ, and the viscosity, η; the relevant matrix properties are the pore size distribution and porosity. From dimensional analysis one can show that the hydraulic conductivity has the form (De Wiest 1965)

$$K = \frac{k\,\rho\,g}{\eta} \tag{2.4}$$

where k is called the intrinsic permeability and is a function of the characteristic of the porous medium alone and has the form

$$k = C\, d_{eff}^2 \tag{2.5}$$

where C is a dimensionless coefficient in the range between 45 for clayey sand and 140 for pure sand (often an average value C = 100 is used), and d_{eff} is the effective grain diameter (Bear 1979). These suggested values are applicable only when k is in cm^2 and d_{eff} is in cm.

In three dimensions, Darcy's law can be written as

$$q_x = -K_x \frac{\partial \phi}{\partial x} \tag{2.6}$$

$$q_y = -K_y \frac{\partial \phi}{\partial y} \tag{2.7}$$

$$q_z = -K_z \frac{\partial \phi}{\partial z} \tag{2.8}$$

where K_x, K_y, and K_z are hydraulic conductivities in the x, y, and z directions, respectively.

It should be noted that the most general form of Darcy's law for three-dimensional flow contains nine components of hydraulic conductivity and is of the form

$$q_x = -K_{xx} \frac{\partial \phi}{\partial x} - K_{xy} \frac{\partial \phi}{\partial y} - K_{xz} \frac{\partial \phi}{\partial z} \tag{2.6a}$$

$$q_y = -K_{yx} \frac{\partial \phi}{\partial x} - K_{yy} \frac{\partial \phi}{\partial y} - K_{yz} \frac{\partial \phi}{\partial z} \tag{2.7a}$$

$$q_z = -K_{zx} \frac{\partial \phi}{\partial x} - K_{zy} \frac{\partial \phi}{\partial y} - K_{zz} \frac{\partial \phi}{\partial z} \tag{2.8a}$$

If the x, y, z axes coincide with the principal axes, then by the definition of the principal axes, $K_{xy} = K_{yx} = K_{yz} = K_{zy} = K_{zx} = K_{xz} = 0$. In this report equations (2.6), (2.7), and (2.8) are assumed to describe the three-dimensional flow adequately and are used in the sections to follow.

Experience shows that Darcy's law is valid only for laminar flow with low Reynolds numbers (De Wiest 1965). Bear (1979) recommends the range for Reynolds number to be between 1 and 10. The Reynolds number is defined as

$$R_e = \frac{\rho\, q\, d_{rep}}{\eta} \tag{2.9}$$

where: η = dynamic viscosity of water ($M L^{-1} T^{-1}$)

d_{rep} = representative length dimension for the porous medium (L)

ρ = fluid density (ML^{-3})

q = Darcy superficial velocity (LT^{-1})

It should be noted that the computation of the Reynolds number uses Darcy's superficial velocity and not the actual pore fluid velocity. The representative length dimension is a subject of controversy in the sense that there is no definite way to quantify its value as in pipe flows. It is clear that d_{rep} should be a measure of the cross section of an elemental channel of the porous medium or pore size. However, because of the difficulty involved in quantifying the pore size, usually the mean grain diameter, d_{10} (which is the diameter such that 10 percent by weight of the grains are smaller than that diameter), is taken as the representative value. Collins (1961) suggests the following relationship to determine the representative length

$$d_{rep} = (k/n)^{1/2} \tag{2.10}$$

where k is the intrinsic permeability, and n is the porosity.

C. Unsaturated-Saturated Groundwater Flow Equation

Assuming a representative elementary volume (REV) of sides Δx,Δy, and Δz in three principal coordinate directions (Figure 4), the mass inflow in the x-direction is

$$I_x = \rho\, q_x\, \Delta y\, \Delta z \tag{2.11}$$

The mass outflow in the x-direction is

$$O_x = \rho\, q_x\, \Delta y\, \Delta z + \frac{\partial}{\partial x}(\rho\, q_x)\, \Delta x\, \Delta y\, \Delta z \tag{2.12}$$

Thus, the net mass inflow in the x-direction is

$$I_x - O_x = -\frac{\partial}{\partial x}(\rho\, q_x)\, \Delta x\, \Delta y\, \Delta z, \tag{2.13}$$

Adding the contributions to the inflow and outflow in the x, y, and z directions, the net mass flow is

$$-\left[\frac{\partial}{\partial x}(\rho\, q_x) + \frac{\partial}{\partial y}(\rho\, q_y) + \frac{\partial}{\partial z}(\rho\, q_z)\right]\Delta x\, \Delta y\, \Delta z \tag{2.14}$$

The total mass of fluid contained in the REV is ($\rho\theta\Delta x\Delta y\Delta z$). Thus, we have

$$\text{the rate of change of mass storage} = \frac{\partial}{\partial t}(\rho\,\theta)\,\Delta x\,\Delta y\,\Delta z \tag{2.15}$$

Using the principle of conservation of mass

$$\text{Rate of change of mass storage} = \text{mass inflow rate - mass outflow rate} \tag{2.16}$$

we obtain

$$\frac{\partial}{\partial t}(\rho\,\theta)\,\Delta x\,\Delta y\,\Delta z = -\left[\frac{\partial}{\partial x}(\rho\,q_x) + \frac{\partial}{\partial y}(\rho\,q_y) + \frac{\partial}{\partial z}(\rho\,q_z)\right]\Delta x\,\Delta y\,\Delta z \tag{2.17}$$

which becomes

$$\frac{\partial}{\partial t}(\rho\,\theta) = -\left[\frac{\partial}{\partial x}(\rho\,q_x) + \frac{\partial}{\partial y}(\rho\,q_y) + \frac{\partial}{\partial z}(\rho\,q_z)\right] \tag{2.18}$$

which is the basic governing continuity equation. For partially saturated flow by using the definition of water content

$$\theta = n\,S \tag{2.19}$$

equation (2.18) becomes

$$\frac{\partial}{\partial t}(\rho\,n\,S) = -\left[\frac{\partial}{\partial x}(\rho\,q_x) + \frac{\partial}{\partial y}(\rho\,q_y) + \frac{\partial}{\partial z}(\rho\,q_z)\right] \tag{2.20}$$

The term on the left-hand side of equation (2.20) can be expanded as

$$\frac{\partial}{\partial t}(\rho\,n\,S) = \left[S\,\frac{\partial(\rho\,n)}{\partial t}\right] + \left[(\rho\,n)\,\frac{\partial S}{\partial t}\right] \tag{2.21}$$

The first term on the right-hand side of equation (2.21) can be expanded as

$$S\,\frac{\partial(\rho n)}{\partial t} = nS\,\frac{\partial \rho}{\partial t} + \rho S\,\frac{\partial n}{\partial t} \tag{2.22}$$

Within an elementary volume, the volume of solids is fixed and therefore

$$V_s = (1 - n)V_T = \text{constant} \tag{2.23}$$

The stress borne by the solid skeleton is σ_z. The change in solid skeleton volume

as the result of the change in σ_z must be zero because of the fixed constant volume, V_s.

Therefore

$$\frac{\partial V_s}{\partial \sigma_z} = 0 \tag{2.24}$$

By using equation (2.23) we obtain

$$\frac{\partial V_s}{\partial \sigma_z} = (1 - n)\frac{\partial V_T}{\partial \sigma_z} - V_T \frac{\partial n}{\partial \sigma_z} = 0 \tag{2.25}$$

which is written as

$$\frac{1}{V_T}\frac{\partial V_T}{\partial \sigma_z} = \frac{1}{(1 - n)}\frac{\partial n}{\partial \sigma_z} \tag{2.26}$$

By using the definition of the porous medium compressibility, ζ, equation (2.26) can be written as

$$-\zeta = \frac{1}{(1 - n)}\frac{\partial n}{\partial \sigma_z} \tag{2.27}$$

and therefore

$$\frac{\partial n}{\partial t} = -\zeta(1 - n)\frac{\partial \sigma_z}{\partial t} \tag{2.28}$$

Also, because the pore water pressure is the only stress on the pore water we have, the density is the function of pore pressure only and can be written as

$$\rho = \rho(p) \tag{2.29}$$

From the definition of fluid compressibility, ζ, we obtain

$$\frac{\partial \rho}{\partial t} = \xi \rho \frac{\partial p}{\partial t} \tag{2.30}$$

By substituting equations (2.28) and (2.30) into equation (2.22), we obtain

$$S\frac{\partial(\rho n)}{\partial t} = n S \rho\left[\xi \frac{\partial p}{\partial t} - \frac{(1 - n)}{n}\zeta \frac{\partial \sigma_z}{\partial t}\right] \tag{2.31}$$

which is substituted into the right-hand side of equation (2.21). This newly formed equation (2.21) is used for the left-hand side of equation (2.20) to yield the valid governing equation for saturated-unsaturated, unsteady flow in an elastic porous medium which may be deforming. The right-hand side of equation (2.21) can be simplified by assuming a nondeforming elementary volume with a constant porosity, n, for which

$$\frac{\partial \theta}{\partial t} = n \frac{\partial S}{\partial t} \qquad \text{for fixed } n \tag{2.32}$$

Eagleson (1970) points out that the compressibility terms of equation (2.31) are relatively unimportant and the whole right-hand side of equation (2.31) becomes zero; therefore, the first term of equation (2.21) may be ignored and water is treated as incompressible which implies ρ is a constant. For an incompressible, unsteady flow in a deforming porous medium, equation (2.18) can be written as

$$\frac{\partial \theta}{\partial t} = -\left[\frac{\partial}{\partial x}(q_x) + \frac{\partial}{\partial y}(q_y) + \frac{\partial}{\partial z}(q_z) \right] \tag{2.33}$$

Based on experiments (Figure 5) it has been found

$$\theta = \theta(\psi) \qquad \text{function of } \psi \text{ only} \tag{2.34}$$

and therefore

$$\frac{\partial \theta}{\partial t} = \frac{\partial \theta}{\partial \psi} \cdot \frac{\partial \psi}{\partial t} \tag{2.35}$$

Using Darcy's law for incompressible, unsaturated, unsteady flow in a non-deforming control volume in equation (2.33) we obtain the Richards equation given as

$$C(\psi) \frac{\partial \psi}{\partial t} = \frac{\partial}{\partial x}\left[K_x(\psi)\left(\frac{\partial \psi}{\partial x}\right) \right] + \frac{\partial}{\partial y}\left[K_y(\psi)\left(\frac{\partial \psi}{\partial y}\right) \right] + \frac{\partial}{\partial z}\left[K_z(\psi)\left(\frac{\partial \psi}{\partial z} + 1\right) \right] \tag{2.36}$$

where: $C(\psi) = \dfrac{\partial \theta}{\partial \psi}$

$= \text{specific moisture capacity}$

It is noted that equation (2.34) provides a unique relation between ψ and θ only for the unsaturated flow case, i.e. for $0 < \theta < n$. For saturated flow $\psi > 0$, and $\theta = n$ for all $\psi > 0$. The quantity $\partial\theta/\partial\psi = 0$ for saturated flow in a nondeforming porous

medium and therefore $C(\psi)$ is undefined. The implication is that equation (2.36) is valid only for unsaturated flow regime.

The nondeforming elementary volume is necessary to express Darcy's law in its original terms [equation (2.2)]; for a deforming elementary volume, the relative Darcy velocity with respect to the velocity of the solid grains should be used. However, if one assumes the relative velocity is close to the original Darcy expression, then equation (2.36) can be used for the deforming elementary volume as well.

The soil moisture diffusivity is defined as

$$D(\theta) = K \frac{\partial \psi}{\partial \theta}$$

It is pointed out that $D(\theta)$ is undefined for saturated flow. We can rewrite equation (2.18) for incompressible, unsaturated, unsteady flow in a nondeforming porous medium as

$$\frac{\partial \theta}{\partial t} = \frac{\partial}{\partial x}\left[D_x(\theta)\frac{\partial \theta}{\partial x}\right] + \frac{\partial}{\partial y}\left[D_y(\theta)\frac{\partial \theta}{\partial y}\right] + \left[D_z(\theta)\frac{\partial \theta}{\partial z}\right] + \frac{\partial K_z(\theta)}{\partial z} \qquad (2.37)$$

in which D_x, D_y, and D_z are functions of θ. Assuming a two-dimensional flow in x and z directions for an isotropic, homogeneous porous medium which implies $K_x = K_z$ at each and every point in the xz plane, equation (2.37) can be simplified as

$$\frac{\partial \theta}{\partial t} = \frac{\partial}{\partial x}\left[D(\theta)\left(\frac{\partial \theta}{\partial x}\right)\right] + \left[D(\theta)\left(\frac{\partial \theta}{\partial z}\right)\right] + \frac{\partial K_z(\theta)}{\partial z} \qquad (2.38)$$

in which $D = D(\theta)$ only and does not depend on x or z directions. Substituting the hydraulic heat, $\phi = \psi + z$, for the two-dimmensional (in x and z directions), incompressible, unsteady flow in a nondeforming porous medium, in equation (2.33) yields

$$\frac{\partial \theta}{\partial t} = \frac{\partial}{\partial x}\left[K_x(\theta)\left(\frac{\partial \phi}{\partial x}\right)\right] + \frac{\partial}{\partial z}\left[K_z(\theta)\left(\frac{\partial \phi}{\partial z}\right)\right] \qquad (2.39)$$

It should be noted that in a nondeforming porous medium for *saturated flow,* $\theta = n$ = constant, and therefore $\partial\theta/\partial t = 0$. For *unsaturated flow,* solution of (2.39) requires the information on characteristic curves $K(\theta)$ and $\psi(\theta)$. These curves have been observed to be hysteric, i.e. these have different shapes depending on wetting or drying phase. Figure 5 shows a typical hysteric relationship between θ and ψ for a soil. If the soil were saturated at a pressure head greater than zero and the pressure was then lowered, the moisture content would follow the drying curve. If water were then added to the dry soil, pressure heads would follow the

wetting curve. A similar hysteric functional relationship exists between K and ψ as shown in Figure 6. The nonlinear functions of ψ-θ and K-ψ have been approximated by various researchers with empirical relations. One such widely used function is the van Genuchten model (1980). This function neglects the hysteric effects of capacity and hydraulic conductivity and is given as

$$C = \frac{A\, m\, (\theta_s - \theta_r)}{(1 - m)} S_e^{1/m} (1 - S_e^{1/m})^m \tag{2.40}$$

$$K = K_s S_e^{1/2} \left[1 - (1 - S_e^{1/m})^m\right]^2 \tag{2.41}$$

$$\begin{aligned} S_e &= \left[1 + (A|\psi|)^M\right]^{-m} \\ &= \frac{\theta - \theta_r}{\theta_s - \theta_r} \\ &= \text{degree of effective saturation} \end{aligned} \tag{2.42}$$

where: θ_s = saturated water content (L^3L^{-3})

θ_r = residual water content (L^3L^{-3})

K_s = saturated hydraulic conductivity (LT^{-1})

$$M = \frac{1}{(1 - m)}$$

A and M are parameters (dimensionless)

Information on the parameter values θ_s, θ_r and K_s for various soil types can be obtained from Carsel and Parrish (1988). This function is used in the next chapter to obtain the relations between K, θ, and ψ.

III. Boundary Conditions

The solution of (2.39) requires information on initial and boundary conditions. The boundary conditions impose a specified spatial and temporal variation of the water content and pressure head or its derivatives at the boundaries of the flow domain. The following three types of boundary conditions normally occur:

- Dirichlet boundary condition (specify dependent function value on the boundary)
- Neumann boundary condition (specify normal derivatives of the dependent function on the boundary)

- Mixed boundary conditions (mixture of dependent function and its derivatives)

For the Dirichlet boundary condition the water content is prescribed at all points on the system boundaries. This occurs when there is ponded water on the soil surface. For the system boundary Γ, a Dirichlet-type boundary condition can be expressed as:

$$\theta(x, z, t) = \theta_0(t) \quad \text{for} \quad (x, z) \in \Gamma \tag{2.43}$$

where: θ_0 is a known function of time for all t over Γ

When the water flux rate is known at the boundary of the flow domain, a Neumann-type boundary condition is said to exist. For impermeable boundaries, a Neumann-type boundary condition states the flux across the boundary to be zero.

There are cases when the boundary condition changes from one type to another. For example, the ground surface may be dry at the beginning of a rainfall event. Therefore, a Neumann-type boundary condition prevails with flux equal to infiltration rate. As time progresses and the hydraulic conductivity of the soil layer reaches its saturated value, water will start ponding at the boundary and the Dirichlet-type boundary condition takes over. After the cessation of the storm, as the time progresses, a Neumann-type boundary condition once again will prevail.

IV. Initial Conditions

In addition to boundary conditions, initial conditions must also be specified in order to solve the boundary value problem. This can be expressed as

$$\theta(x, z, 0) = \theta_i(x, z) \tag{2.44}$$

where θ_i defines the initial water content (i.e. for a fixed time) at all points in the interior of the soil system.

V. Solution Procedure

Once the initial and boundary conditions are specified, the boundary value problem can be solved to obtain $\psi(x,z,t)$ and/or $\theta(x,z,t)$. However, the nonlinear partial differential equation cannot be solved analytically except perhaps for trivial geometries. Therefore, numerical techniques have to be resorted to for solving groundwater flow problems. These techniques usually transform the partial differential equations of the groundwater system into systems of ordinary differential or algebraic equations. The solution of these equations determines the values of the dependent variables at a predetermined set of discrete nodal points within the flow domain.

The finite difference methods are widely used for solution of the groundwater flow equations. The main advantage of the finite difference methods is that they reduce the differential equations to algebraic equations which can be solved much more easily compared to their parent differential equations. In finite difference methods, the partial derivatives such as $\partial\theta/\partial z$ in the governing flow equations are replaced by ratios of the differences $\delta\theta/\delta z$. The solution domain is first divided into a set of grids formed by lines representing space and time. The finite difference equations use the distance between grid points as the increments for the independent variables in respective directions which in turn form the denominators for the difference approximation of the derivatives. The set of finite difference equations thus obtained are solved numerically on a digital computer, which results in the values of the dependent variables at the predetermined grid points.

If θ_E is the exact solution of the partial differential equation, θ_D is the exact solution of the difference equation, θ_N is the numerical solution of the difference equation, the difference $|\theta_D - \theta_N|$ is called the numerical or round-off error and the difference $|\theta_E - \theta_D|$ is called the truncation error. The solution is said to converge if $|\theta_E - \theta_D| \rightarrow 0$ everywhere in the solution domain. Similarly, the stability criterion requires $|\theta_D - \theta_N| \rightarrow 0$ everywhere in the solution domain.

There are two broad classes of finite difference solution schemes, namely explicit scheme and implicit scheme. In an *explicit scheme*, one can solve for the dependent variable, θ, at some grid point (nodal point), for time $t + \Delta t$ from the knowledge of θ at the *preceding time*, t, corresponding to the neighboring grid (nodal) points. Therefore, the determination of a nodal dependent function value at some time is *independent* of dependent function values at other nodes for the *same time* (see Figure 7). In an *implicit scheme* the dependent function value at a particular node at some time depends on the function values at its adjoining nodes for the same time which is in general unknown. Therefore, to determine the unknown nodal function values at $t + \Delta t$, one is forced to solve *all nodal equations* corresponding to the time $t + \Delta t$ simultaneously; and a single value of the dependent variable at a particular node cannot be computed explicitly at time $t + \Delta t$. The complete solution would then require *simultaneously* solving the nodal equations *at each time* $t + \Delta t$, $t + 2\Delta t$, ... until the specified final time is reached (see Figure 7).

Even though the implicit schemes are computationally complex they are unconditionally stable, implying that the dependent function remains bounded as time passes. The explicit scheme requires certain conditions related to the discretization scheme to remain stable; these conditions can be overly restrictive if long time periods are involved. However, owing to the simplicity in formulation and programming ease, an explicit finite difference scheme is used to solve the Richards equation (2.39) with appropriate initial and boundary conditions. Using the explicit scheme of Bernier (1985) in equation (2.39), we obtain

$$\theta_{i,j}^{t+\Delta t} = \theta_{i,j}^{t} + \left(\frac{\Delta t}{V_{(i,j)}}\right)\left[\overline{K}_1 A_1\left(\frac{\phi^t_{(i+1,j)} - \phi^t_{(i,j)} + z_{(i+1,j)} - z_{(i,j)}}{X_{(i+1,j)} - X_{(i,j)}}\right)\right]$$

$$-\left(\frac{\Delta t}{V_{(i,j)}}\right)\left[\overline{K}_3 A_3\left(\frac{\phi^t_{(i,j)} - \phi^t_{(i-1,j)} + z_{(i,j)} - z_{(i-1,j)}}{X_{(i,j)} - X_{(i-1,j)}}\right)\right] \qquad (2.45)$$

$$+\left(\frac{\Delta t}{V_{(i,j)}}\right)\left[\overline{K}_2 A_2\left(\frac{\phi^t_{(i,j-1)} - \phi^t_{(i,j)}}{z_{(i,j-1)} - z_{(i,j)}} + 1\right) - \overline{K}_4 A_4\left(\frac{\phi^t_{(i,j)} - \phi^t_{(i,j+1)}}{z_{(i,j)} - z_{(i,j+1)}} + 1\right)\right]$$

where: A_i's are the cross-sectional areas for flow through the face i and $V_{(i,j)}$ is the bulk volume of the element (i,j) (see Figure 9). The hydraulic conductivity, $\overline{K}_1$ is computed as

$$\overline{K}_1 = \frac{\Delta x_{(i+1,j)} + \Delta x_{(i,j)}}{\dfrac{\Delta x_{(i+1,j)}}{K(\theta^t_{(i+1,j)})} + \dfrac{\Delta x_{(i,j)}}{K(\theta^t_{(i,j)})}} \qquad (2.45a)$$

In equation (2.45a) the subscript pairs (i,j-1) and (i,j) determine $\overline{K}_2$; (i,j) and (i-1,j) determine $\overline{K}_3$; (i,j) and (i,j+1) determine $\overline{K}_4$. In equation (2.45), subscripts i, j, and superscript, t, represent the x, z, and t variables of the governing flow equation. The time level $t + \Delta t$ is represented by the superscript $t + \Delta t$. Equation (2.45) can also be written as

$$\theta^{t+\Delta t} = \theta^t + \frac{\Delta t}{V_T}(Q_1 + Q_2 - Q_3 - Q_4) \qquad (2.46)$$

where:

$\theta^{t+\Delta t}$ = moisture content at time $(t + \Delta t)$

θ^t = moisture content at time t

V_T = bulk volume of the soil element

Δt = time step size

Q_i = Darcy flux through face i; i = 1,2,3,4

The solution progresses by setting t = 0 for which $\theta^t_{i,j}$ is known (from initial conditions) for all (i,j). Equations (2.41) and (2.42) are now used, with known $\theta^t_{i,j}$, to compute $\psi_{i,j}(\theta)$ and $K_{i,j}(\theta)$. When the elevation head $z_{i,j}$ is added to the pressure head $\psi_{i,j}(\theta)$ one obtains the hydraulic head $\phi^t_{i,j}(\theta)$. At the impervious boundaries there is no flow and therefore ϕ values are assigned the same values as of the

adjoining element, i.e. $\partial\phi/\partial x = 0$ and $\partial\phi/\partial z = 0$. This is shown in Figure 8. Darcy's law, equation (2.2), is used to obtain the flow between the adjoining elements. The moisture content at time step $t + \Delta t$ denoted as $\theta^{t+\Delta t}_{(i,j)}$ is obtained by solving equation (2.45) or equation (2.46).

The numerical procedure is carried out to a prespecified simulation period. The result of the simulation is a time history of states of each element, i.e. whether the soil element is saturated or not. If saturation spreads to upstream areas, expansion is said to occur; contraction occurs when saturation recedes toward downstream elements (upstream and downstream are defined relative to the channel location). Therefore, with the aid of the time history of θ at all grid points, it can be determined whether the source area is expanding or contracting. A computer model, Variable Source Area Simulator (VSAS2), which models the expansion and contraction of source areas, is described in the next chapter. The numerical procedure is described in detail in Appendix A.

VARIABLE SOURCE AREA SIMULATOR (VSAS2)

I. Introduction

The area of a drainage basin contributing to runoff varies with time even within a single storm event. The expansion and contraction of contributing areas during and following a storm are generally influenced by the subsurface flow. Once the top surface of the soil gets saturated, continuation of rainfall results in exfiltration (emergence of subsurface flow to the surface) which leads to the saturation of upslope areas. This is termed the *expansion* of source areas. After the cessation of rainfall, downstream moisture movement results in the *contraction* of source areas. These contributing areas, which change with time, are known as the *variable source areas*. The expansion and contraction of source areas for a storm event are shown in Figure 10. It is readily seen that the peak discharge is attained when the growth of the source areas is a maximum which occurs on day three. As the source areas contract, the discharge decreases.

Coupled surface (overland and open-channel flows) and subsurface flow (saturated and unsaturated regions) equations, along with the appropriate initial and boundary conditions, need to be solved to predict the variable source areas. A computer program called the Variable Source Area Simulator, VSAS2, (Bernier 1985) is one such attempt and is used in this study. A simplified users' manual is given in Appendix B.

II. Description of the Model

VSAS2 is a physically based mathematical model which simulates the formation of source areas in watersheds. It couples both the surface and the subsurface flows using appropriate initial and boundary conditions. The basin is divided into a number of independent segments based on the channel system, the topography, and the soil variability. The segments are the subregions bounded at the upstream boundary by a drainage divide and at the base by a perennial or an intermittent stream (Figure 11). Each segment is described by a pair of polynomials running from the stream to the ridge (Figure 12). One polynomial describes the surface elevation as a function of the distance from the channel whereas the other describes the depth of the porous medium as a function of the distance. The coefficients of the polynomials are obtained by substituting known depths at known distances into these equations and solving for the unknown coefficients. Each segment is divided into increments paralleling the stream. To obtain greater sensitivity along the stream end of segments, smaller increments are used near the stream and progressively larger increments are used away from the stream. Each increment thus obtained is further subdivided vertically into layers to obtain volumetric soil elements. Each soil element extends throughout the width of the segment. A simplified segment cross section is shown in Figure 13. Within each

segment, centers of mass of the elements form a variable, nonorthogonal, two-dimensional grid system and act as the solution points for the two-dimensional saturated-unsaturated flow described by the Richards equation. The model uses the following simplifying assumptions:

1. Segments are independent.
   It is assumed that for a segment all boundaries except the top surface and the region above the channel water surface are impervious (Figure 8).

2. Soil hysteresis is neglected.
   This assumption aids in the selection of the parameters of the moisture-hydraulic conductivity and the moisture-pressure head curves. Soil is always assumed to be in the desorption phase.

3. Soil is assumed to be isotropic within a layer.
   This assumption eliminates the necessity of dealing with different hydraulic conductivity values in the x and the z directions. These are assumed to be equal within a layer. Nevertheless, saturated hydraulic conductivities may be different for different layers.

4. Surface water generated within one iteration reaches the channel during that iteration.
   Any excess water generated on the surface layer at the end of one iteration (refer to Appendix A) is added to the channel as the flow from the element on the top layer adjacent to the stream. This flow consists of both the overland flow component, if any, and the subsurface flow component from the top layer. It should be noted that no routing is performed on the overland flow generated within a segment. VSAS2 uses 15 minutes as the time interval between iterations.

5. Channel routing is simplified by a simple lag function.
   The hydrograph depicting the runoff due to channel and impervious area precipitation and the pervious area runoff is assumed to occur at the center of the channel, midway between the respective segment boundaries shown as point C in Figure 11, for example. This hydrograph is lagged by the time of travel of a flood wave to move from point C to the watershed outlet. It should be noted that the shape of the hydrograph remains unchanged during the lag process except for the shift in time equal to the time of travel.

6. Variations in channel water level are neglected.
   The channel water level is assumed to be constant throughout the simulation period.

7. Fluid is assumed to be incompressible.

8. Porous medium is nondeforming.

A. Computation of Runoff

In VSAS2, the runoff is taken to be composed of (1) channel precipitation (2) impervious area runoff, and (3) pervious area runoff. The channel precipitation and runoff from impervious areas are computed by multiplying the precipitation and the corresponding surface areas. The net precipitation required for these purposes is obtained by subtracting interception loss from gross precipitation. VSAS2 uses an interception loss of 0.05 inches for dormant season and 0.10 inches for growing season. The pervious area runoff is obtained by solving the Richards two-dimensional equation for a homogeneous, isotropic, nondeforming porous medium, which may be stated as

$$\frac{\partial \theta}{\partial t} = \frac{\partial}{\partial x}\left[K(\theta)\frac{\partial \phi}{\partial x}\right] + \frac{\partial}{\partial z}\left[K(\theta)\frac{\partial \phi}{\partial z}\right] \quad \text{for} \quad 0 < \theta \leq \theta_s \tag{3.1}$$

where: $\theta = \theta(x,z,t)$

= volumetric water content of the porous medium (L^3/L^3)

$\phi = \phi(\theta;x,z,t)$

= total head (L)

$\psi = \psi(\theta;x,z,t)$

= pressure head (L)

$K = K(\theta)$

= hydraulic conductivity of the porous medium (L/T)

The explicit finite difference scheme discussed in the previous chapter is used to solve equation (3.1). This equation is solved for $\theta(x,z,t)$ with the known initial $\theta(x,z,0)$. The solution of equation (3.1) also requires the relationship between the unsaturated hydraulic conductivity, $K(\theta)$, and the pressure head, $\psi(\theta)$, which are functions of water content, θ. By neglecting the effect of soil hysteresis and assuming K-θ and ψ-θ to be uniquely related, single-valued functions relating K and ψ to θ can be formed (van Genuchten 1980). The specific K-θ and ψ-θ functions used in VSAS2 are

$$\psi(\theta) = \alpha\,\theta^{\beta} + c \tag{3.2}$$

$$K(\theta) = \gamma\,\theta^{\omega} \tag{3.3}$$

where α, β, and γ are the parameters of the $\psi(\theta)$ and $K(\theta)$ functions. The parameter 'c' in equation (3.2) is used as a correction factor to force the ψ-θ curve to pass through the origin when the soil element is fully saturated. Value of c, therefore, is obtained as

$$c = -\alpha n^{\beta} \tag{3.4}$$

where n is the porosity of the soil element.

In this study, van Genuchten's model (1980) is used to obtain $\psi(\theta)$ and $K(\theta)$ curves for different soil types. The five parameters θ_s, θ_r, m, K_s, and α required for the solution of equations (2.41) and (2.42) are obtained from Carsel and Parrish (1988). The ψ and K values obtained from the van Genuchten model are used to find the best regression estimates for the parameters $\alpha, \beta, \gamma, \omega$ and c in equations (3.2) and (3.3). This regression analysis is performed by using the SYSNLIN routine of the Statistical Analysis System (SAS) package. The parameter values obtained from the regression analysis for the four types of soils are shown in Table 1.

It is assumed that all faces of a segment are impermeable except for the top soil surface and the stream side region located above the prespecified channel level (see Figure 8). At the impervious boundaries the flux is zero, i.e. $\partial\phi/\partial x = 0$ and $\partial\phi/\partial z = 0$. At the beginning of the simulation, $\theta_{i,j}$'s are known for all (i,j) from the known initial conditions. The corresponding hydraulic heads, $\phi_{i,j}$'s are computed as the sum of the pressure head, $\psi(\theta)$, equation (3.2), and the elevation head, z. The one time step ahead moisture content denoted as $\theta^{t+\Delta t}_{ij}$ is computed from equation (2.45).

When the surface elements get saturated (i.e. $\theta = \theta_s = n$), the soil element is said to have reached its storage capacity. Additional input to a surface element, at a rate greater than the infiltration rate, produces overland flow. Computation of overland flow begins at the top of the slope and proceeds towards the stream side. The overland flow is routed to the adjoining downstream surface element and eventually reaches the stream. The procedure is repeated for a desired simulation period. A detailed description of the procedure is given in Appendix A.

The pervious area runoff (overland and subsurface flow components) is added to the channel precipitation and the impervious area runoff. The obtained flow is lagged to the watershed outlet which is then combined with the hydrographs from other segments to yield the composite outlet hydrograph for the entire basin.

B. Input Data Requirements

VSAS2 requires information on:

1. Topography of the basin
   obtained from topographical and contour maps.

2. Hydrologic properties of the porous medium
   soil porosity
   saturated hydraulic conductivity
   unsaturated hydraulic conductivity coefficients (γ and ω)
   moisture release coefficients (α and β)
   correction factor for moisture release curve (c)
   Soil survey maps and handbooks are used to obtain the soil porosities and the saturated hydraulic conductivities. The parameters $\alpha, \beta, \gamma, \omega$, and c are computed from regression analysis (see Table 1 for some calibrated values).

3. Top surface area of channels
   This is required to compute the channel flow component from precipitation directly falling on channels.

4. Initial moisture contents of soil elements
   The following procedure is used to obtain the initial moisture contents of soil elements required by the model.
   VSAS2 is run by assuming all the soil elements to be fully saturated and no precipitation. Simulation is performed until a prespecified outflow rate is achieved (VSAS2 assumes the outflow rate of 0.05 cu. ft. per sq. mile per hour). The moisture contents at the end of this simulation are used as the initial moisture contents required by the model for the desired simulation.

5. Rainfall information
   Hourly precipitation in inches. In Virginia, HISARS (Hydrologic Information Storage and Retrieval System 1988) can be used to obtain this information.

6. Time of travel
   This is required to lag the hydrograph from the segment to the watershed outlet.

Two input data files are used to provide the information needed. The first file provides the detailed information on the watershed characteristics and the precipitation for which the simulation is to be performed. The second file provides information on the initial moisture contents of the elements in the subsurface domain. Appendix B provides a detailed description of input preparation for an example problem along with the output.

C. Output

Using the above information, the model generates the outflow hydrograph at the watershed outlet. It also prints out the moisture contents for each element at prespecified times (see Appendix B, section III). If the moisture content of an element is equal to its porosity, that element is considered saturated and becomes a part of the source area. By observing the saturated elements at different times, expansion and contraction of the source area within the basin are delineated. Thus, saturated widths of various segments at different times can be plotted to visualize the source area dynamics. The output also contains the overland flow component, channel precipitation, and flows from different soil layers. These aid in determining the surface and the subsurface flow components of runoff. The surface flow component is obtained as the sum of the overland flow component and the channel precipitation, whereas the subsurface flow component is computed by summing up the flows from all the soil layers. Appendix B presents a simple example with comprehensive input and output.

MONTE CARLO SIMULATION OF VARIABLE SOURCE AREAS

I. Introduction

Traditional approaches to solving groundwater flow problems are based on mathematical solutions to deterministic models of flow through porous media. These methods model the flow by partial differential equations with appropriate initial and boundary conditions. The soil properties are represented by deterministic empirical functional relationships between hydraulic parameters. The validation of these models is carried out in a controlled environment (laboratory experiments). The application to field conditions is valid only under the assumption that the field can be regarded as a homogeneous medium characterized by some equivalent properties (Dagan and Bresler 1983). These equivalent properties are determined by sampling from a few locations and by appropriate averaging techniques. On a watershed scale, however, soil mass is truly a heterogeneous medium and the use of the equivalent properties is restrictive. Because of the heterogeneity, the hydraulic properties of soil exhibit a large degree of spatial variability. Assorted experimental and field studies support the existence of such variability (Rogowski 1972; Nielsen et al. 1973; Carvallo et al. 1976; Sharma et al. 1980; Gelhar 1986). Therefore, any sound groundwater modeling approach should incorporate these variabilities. One approach is to treat the relevant hydraulic parameters as random variables. In this study, saturated hydraulic conductivities at different depths are treated as lognormally distributed random variables. A Monte Carlo simulation is carried out to predict the source areas based on the surface water content in response to the random variation in the parameters.

II. Monte Carlo Simulation

A. Introduction

The Monte Carlo methods comprise that branch of experimental mathematics concerned with random numbers. The procedure involves the generation of random numbers from a known probability distribution. The generated random numbers are used as inputs to governing equations, and the corresponding outputs are computed. This process is repeated a specified number of times to obtain a set of system outputs that is then analyzed statistically to define the output distribution. Well-detailed accounts of a Monte Carlo simulation analysis of groundwater flow can be found in Smith and Freeze (1979a, 1979b), Smith and Schwartz (1980, 1981a, 1981b) and Silliman and Wright (1988). Following Nielsen et al. (1973), Freeze (1975), and Smith and Schwartz (1980), it is assumed that the saturated hydraulic conductivity of the porous medium is lognormally distributed. This distribution is also implied by the observation that hydraulic conductivity can be estimated as an exponential function of porosity, which is generally taken to be

normally distributed (Bennion and Griffiths 1966). The assumption of lognormally distributed hydraulic conductivity can also be supported based on small-particle statistics (Aitchison and Brown 1957).

B. Lognormal Distribution

Let K be the hydraulic conductivity which is lognormally distributed. A random variable K is said to be lognormally distributed only when its logarithms are normally distributed. That is, if we denote $X = \ln K$, then X is normally distributed. It is clear that K must be positive which is true for hydraulic conductivity. Let μ and σ^2 be the mean and variance of X, respectively. Then, the probability density function (pdf) of X is given as

$$f_X(x) = \frac{1}{\sigma\sqrt{2\pi}} \exp\left[-\frac{1}{2}\left(\frac{x-\mu}{\sigma}\right)^2\right]; \qquad -\infty < x < \infty \tag{4.1}$$

It also follows that the pdf of K should be

$$f_K(k) = \frac{1}{k\,\sigma\sqrt{2\pi}} \exp\left[-\frac{1}{2}\left(\frac{\ln k-\mu}{\sigma}\right)^2\right]; \qquad k > 0 \tag{4.2}$$

In general, the estimates of mean and variance for K only are available, and the parameters of X have to be computed from these. Let κ and ε^2 be the mean and variance of K, respectively. Then one can use the following formulas to estimate μ and σ from κ and ε. (Aitchison and Brown 1957)

$$\kappa = \exp\left[\mu + \frac{\sigma^2}{2}\right] \tag{4.3}$$

$$\varepsilon^2 = \exp\,(2\mu + \sigma^2)\left[\exp\,(\sigma^2) - 1\right] \tag{4.4}$$

It is also seen that $K = e^X$ provides the inverse transformation to draw pertinent inferences on K based on the results of X.

C. Generation of Bivariate Normal Random Vectors

For the Monte Carlo simulation, the soil medium is assumed to be composed of two layers with different saturated hydraulic conductivities. In general, these two conductivities are correlated. In this study, it is assumed that these hydraulic conductivities follow a bivariate normal pdf.

A random vector $X = (X_1, X_2)$ is bivariate normally distributed if the pdf $N(\mu, \Sigma)$ is given as

$$f_X(x) = \frac{1}{(2\pi)^{1/2} |\Sigma|^{1/2}} \exp\left[-\frac{1}{2}(x-\mu)^T \Sigma^{-1}(x-\mu)\right] \tag{4.5}$$

$$-\infty < x_1 < \infty$$

$$-\infty < x_2 < \infty$$

in which $x = (x_1, x_2)$; $\mu = (\mu_1, \mu_2)$ the mean vector; and Σ the covariance matrix

$$\Sigma = \begin{bmatrix} \text{Var}\, X_1 & \text{Cov}(X_1, X_2) \\ \text{Cov}(X_2, X_1) & \text{Var} X_2 \end{bmatrix} \tag{4.6}$$

which is positive definite and symmetric, $|\Sigma|$ is the determinant of Σ, and Σ^{-1} is the inverse of matrix of Σ and

$$\text{Var} X_1 = E[X_1 - \mu_1]^2 \tag{4.7}$$

$$\text{Cov}(X_1, X_2) = E[(X_1 - \mu_1)(X_2 - \mu_2)] \tag{4.8}$$

$$\text{Var} X_2 = E[X_2 - \mu_2]^2 \tag{4.9}$$

where E [.] is the Expected value.

Since Σ is positive definite and symmetric, there exists a unique lower triangular matrix (Scheuer and Stoller 1972)

$$C = \begin{bmatrix} c_{11} & 0 \\ c_{21} & c_{22} \end{bmatrix} \tag{4.10}$$

such that

$$\Sigma = C\, C^T \tag{4.11}$$

Then the vector X can be represented as

$$X = C\, Z + \mu \tag{4.12}$$

where $Z = (Z_1, Z_2)$ is a normal vector with a zero mean and covariance matrix equal to the identity matrix, that is, both the components Z_1 and Z_2 have the standard normal distribution N(0,1) and are independent random variables.

The elements of C can be obtained by using the following relationships:

$$c_{11} = (\mathrm{Var}X_1)^{0.5} \tag{4.13}$$

$$c_{21} = \frac{\mathrm{Cov}(X_1, X_2)}{c_{11}} \tag{4.14}$$

$$c_{22} = \left[\mathrm{Var}(X_2) - \frac{[\mathrm{Cov}(X_1, X_2)]^2}{\mathrm{Var}(X_1)} \right]^{0.5} \tag{4.15}$$

Equation (4.12) is based on the following theorem (Johnson and Wichern 1982)

Theorem 1. If $X = (X_1, ..., X_p)$ is normally distributed as $N_p(\mu, \Sigma)$, the q linear combinations $A_{(qxp)}X_{(px1)}$ are distributed as $N_q(A\mu, A\Sigma A^T)$. Also, $X + d$, where d is a vector of constants, is distributed as $N_p(\mu + d, \Sigma)$.

By applying Theorem 1 with $Z = (Z_1, Z_2)$ normally distributed $N_2(0, I_2)$ (I_2 is the identity matrix of size 2), the distribution of $X = C Z$ is $N_2(0, CC^T)$. Further, by the second part of the Theorem, for $X + d$ with $d = \mu$ the pdf is given as $N_2(\mu, CC^T)$. Therefore, the bivariate normal vector can be generated by using the following three steps:

1. Compute C matrix from equations (4.13), (4.14) and (4.15)
2. Generate the Z_1 and Z_2 independently from N(0,1)
3. Compute $X = C Z + \mu$ from equation (4.12)

D. Determination of Sample Size

One important question that remains to be answered is the sample size, i.e. how many random variates one should generate before terminating the simulation. It is assumed that the logarithms of hydraulic conductivities are normally distributed with mean μ and variance σ^2. We would like to determine the minimum value of the sample size, λ, for which the probability of the sample average being different from the true mean by a certain amount should meet a prespecified limit. For example consider

$$P[\,|\bar{x} - \mu| \leq 1\,] \geq 0.9 \tag{4.16}$$

where: $\bar{x}$ is the sample average

It is known (DeGroot 1986) that the sample mean $\bar{x}$ will have a normal distribution $N(\mu, \sigma^2/\lambda)$. Therefore, if one lets

$$Y = \left(\frac{\bar{x} - \mu}{\sigma} \right) \sqrt{\lambda} \tag{4.17}$$

then Y will have a standard normal distribution. Therefore,

$$P[|\bar{x} - \mu| \leq 1] = P\left[|Y| \leq \frac{\sqrt{\lambda}}{\sigma}\right] \geq 0.9 \tag{4.18}$$

which implies

$$P\left[Y > \frac{\sqrt{\lambda}}{\sigma}\right] \leq 0.05 \tag{4.19}$$

and therefore from standard normal tables one obtains

$$\frac{\sqrt{\lambda}}{\sigma} \geq 1.64 \tag{4.20}$$

and

$$\lambda \geq 2.69\,\sigma^2 \tag{4.21}$$

In this analysis, it has been assumed that the true variance is known. If both the true mean and variance are unknowns, the following approach may be followed (DeGroot 1986):

Let

$$\hat{\mu} = \bar{x} = \frac{\sum_{i=1}^{\lambda} X_i}{\lambda} \tag{4.22}$$

and

$$\hat{\sigma}^2 = \frac{1}{\lambda}\sum_{i=1}^{\lambda}(X_i - \bar{x})^2 \tag{4.23}$$

We would like to determine the minimum sample size, λ, for which the probability will be at least 'a' that neither $\hat{\mu}$ nor $\hat{\sigma}$ will differ from the unknown value it is estimating by more than $g\sigma$, where g is a given number. Since $\hat{\mu}$ and $\hat{\sigma}^2$ are independent

$$P[|\hat{\mu} - \mu| \leq g\sigma \text{ and } |\hat{\sigma} - \sigma| \leq g\sigma] \geq a \tag{4.24}$$

becomes

$$P[|\hat{\mu} - \mu| \leq g\sigma]\ P[|\hat{\sigma} - \sigma| \leq g\sigma] \geq a \tag{4.25}$$

By letting

$$p_1 = P\left[\,|U| \le g\sqrt{\lambda}\,\right] \tag{4.26}$$

and

$$p_2 = P\left[(1-g)^2\lambda < V < (1+g)^2\lambda\right] \tag{4.27}$$

where:

$U = \left(\frac{\hat{\mu}-\mu}{\sigma}\right)\sqrt{\lambda}$ which is a Standard normal variate

$V = \frac{\lambda\,\hat{\sigma}^2}{\sigma^2}$ which is a Chi-Square variate with (λ-1) degrees of freedom

For any given value of λ, the values of p_1 and p_2 can be found by using Standard normal and Chi-Square tables. The task is to choose a λ such that $p_1p_2 = a$. Because there are two hydraulic conductivities used in the present study, two sample sizes should be computed and the maximum of these sample sizes may be adopted for the actual simulation.

The above procedure would suffice for practical purposes. However, a more accurate procedure will be to consider the joint distribution (bivariate normal) of the logarithm of hydraulic conductivities in deriving the test procedure for estimating the sample size. Johnson and Wichern (1982) showed that the squared distance involving $\bar{X}$ of the form

$$\Omega^2 = \lambda(\bar{X}-\vec{\mu})'S^{-1}(\bar{X}-\vec{\mu}) \tag{4.28}$$

is Chi-square distributed with two degrees of freedom, χ^2_2.

Here,

$$\bar{X} = \begin{pmatrix}\bar{X}_1\\ \bar{X}_2\end{pmatrix} \tag{4.29}$$

is the vector of average values for random variables X_1 and X_2, which are bivariate normally distributed; S^{-1} is the inverse of the sample Variance-Covariance matrix; and $\vec{\mu}$ is the vector of population means. Therefore, by considering

$$P\left[(\bar{X}-\vec{\mu})'S^{-1}(\bar{X}-\vec{\mu}) \le 1\right] \ge p \tag{4.30}$$

which can be written as

$$P\left[\lambda(\bar{X}-\vec{\mu})'S^{-1}(\bar{X}-\vec{\mu}) \le \lambda\right] \ge p \tag{4.31}$$

we obtain

$$\lambda \geq \chi^2_2(1 - p) \tag{4.32}$$

where: $\chi^2_2(1 - p)$ is the Chi-square cutoff value with an area of (1-p) to the left of it under the density function. For $p = 0.9$, we have $\lambda \geq 4.61$; and for $p = 0.99$, we obtain $\lambda \geq 9.21$.

E. Simulation Analysis

Once the sample size is determined, that many random vectors using the procedure described earlier are generated. Each such random vector is used for saturated hydraulic conductivities (after using the inverse transformation) within the simulation model VSAS2. This process is repeated for all random vectors. The mean water content of the simulation outputs is declared as the desired solution which also determines the extent of the source areas. A step-by-step description of the Monte Carlo simulation procedure is given below:

Step 1. Determine the sample size for a prespecified probability limit using the procedure described in section D above.

Step 2. The elements of the C matrix, equation (4.10), are generated from equations (4.13), (4.14), and (4.15). Estimates of the needed variances of X_1 and X_2 are obtained from the estimator (4.23). An estimate of the covariance, $Cov(X_1, X_2)$ is computed using the relationship:

$$Cov(X_1, X_2) = \left(\frac{1}{\lambda - 1}\right)\sum_{i=1}^{\lambda}(X_{1i} - \bar{x}_1)(X_{2i} - \bar{x}_2) \tag{4.33}$$

These estimators are to be used when core samples are available. In this study, the means and the variances of saturated hydraulic conductivities were obtained from USDA (1952). An estimator of the $Cov(X_1, X_2)$ was obtained by assuming a correlation coefficient of 0.5 and using the relationship:

$$Cov(X_1, X_2) = 0.5\left[Var[X_1]Var[X_2]\right]^{0.5} \tag{4.34}$$

Step 3. Pick components Z_1 and Z_2 of Z, independently, for N(0,1) from the standard normal random number table (Fiering and Jackson 1971).

Step 4. Use the vector Z generated in step 3 to compute the vector X from equation (4.12) by using the estimates of C and μ.

Step 5. Run VSAS2 using the saturated hydraulic conductivity vector obtained in step 4.

Step 6. Tabulate moisture content, overland flow, subsurface flow and total flow values.

Step 7. Steps 3 through 6 are repeated as many times as the sample size obtained in the first step.

Step 8. Compute the mean of the values obtained in step 6. These are the mean overland flow, subsurface flow, and the total runoff volumes from the watershed.

Also, the International Mathematical and Statistical Libraries (IMSL) contain the subroutine RNMVN which generates the bivariate normal random vectors directly. Use of the computer program RNMVN is described in the next chapter. This chapter also contains complete descriptions of the deterministic and stochastic simulation analyses for a real watershed.

MODEL APPLICATION

I. Watershed Selection

The model has been applied to the Pony Mountain Branch watershed located in Culpeper County in Northern Virginia. The watershed is on the Piedmont Plateau, about three miles southeast of Culpeper. It is a second order drainage basin with an area of 192 acres; 53 percent is forested, 29 percent is pasture, about 16 percent is cultivated, and roads account for the remaining two percent (Watershed Engineering Project 1968).

The watershed has an outlet near the stream gaging station number 1312 (Figure 14). The station consists of a 4 feet wide by 8 feet high box culvert modified with a V-notch weir. Average annual precipitation on the watershed is 36.23 inches, and the average annual streamflow is 7.5 inches with a maximum peak discharge of 92.9 cfs (Watershed Engineering Project 1968). Elevation of the study area ranges from 340 feet to 780 feet. The upstream region of the watershed has steeper slopes reducing to gentle towards the downstream region (Figure 14).

II. Application

The watershed is divided into 24 segments (Figure 15), each with three layers, following the procedure described in Chapter 3. The segment areas range from 84,380 $ft.^2$ to 966,520 $ft.^2$ (Table 2). The land-use types, by segments, are presented in Table 3. Information on soil profiles was obtained from the soil survey manual (USDA 1952). Based on these soil types, porosities and saturated hydraulic conductivities were obtained from the USDA (1952) soil survey manual and are given in Table 4. The parameters required to fit the pressure head and hydraulic conductivity functions, equations (3.2) and (3.3), were obtained by using van Genuchten's model and the SYSNLIN package from SAS. To obtain the initial moisture contents for the actual run, VSAS2 was run assuming that there was no rainfall during the entire simulation period and $\theta_i = \theta_s$ for all elements. The simulation was continued until a prespecified outflow rate, assumed to be 0.05 cubic feet per hour per square mile, was achieved. The moisture contents of elements at the end of this simulation period were used as initial moisture contents for actual simulation. It should be noted that VSAS2 was run segment by segment to arrive at these initial moisture contents. Complete input data sets for the actual simulation are given in Tables 11 and 12.

Simulations were performed for two storm events:

- a 4-hour storm on June 12, 1958, with total rainfall volume of 2.37 inches;
- a 13-hour storm February 18, 1960, with total rainfall volume of 1.40 inches.

III. Results and Discussions

For the first storm event, the simulation was performed for 24 hours. The observed and the simulated hydrographs at the watershed outlet are shown in Figure 16 along with the rainfall hyetograph. The response of the individual segments are summarized in Table 5. These volumes are further divided into channel precipitation, overland flow component, and subsurface flow component and are given in Table 6. It is clear from Figure 16 that the simulated peak flow is very close to the observed peak flow. However, the simulator overpredicted the total outflow volume.

Observation of Tables 5 and 6 indicate that segments 1, 12, 13, 16, 18, 22, 23, and 24 contribute most of the runoff volume. Further analyses show that just over 40 percent of the total area of the basin contributes more than 67 percent of the total runoff volume. Segment 18, which has less than 4 percent of the total area, accounts for more than 13 percent of the total runoff volume (maximum) whereas segment 6, with more than 4.5 percent of the total area, accounts for less than 0.5 percent of the total runoff volume (the minimum volume contributed). These numbers agree with the structure of the model. The model uses Richards' equation (3.1) to simulate the flow in the subsurface zone. It uses Darcy's law, equation (2.2), in which the flow is directly related to the hydraulic conductivity of the porous medium. Therefore, the segments with higher hydraulic conductivities are expected to contribute more flow volume than the segments with lower hydraulic conductivities. Table 4 indicates that the hydraulic conductivities of soils in segment 18 are much higher than that of soils in segment 6. Therefore, water movement through segment 18 should be expected to be much faster than that through segment 6. The results of the simulation exemplify this intuition. From the results, it can be concluded that segment 18 is more important by far than segment 6 for the selection and placement of BMPs.

It is evident from Table 6 that the subsurface flow component is a substantial portion of the total runoff volume (see columns d and e, Table 6). If this component had been neglected, the total runoff volume would have been only about one-half what was obtained in this simulation. The model computes the surface flow components by using the impervious surface areas and the channel surface area along with rainfall information. The only other way the surface flow may be generated is by exfiltration, i.e. by saturating the surface layer. It is noted that the model does not account for evaporation and transpiration. For exfiltration to occur, the hydraulic gradient should be such that when Darcy's law, equation (2.2), is applied, the flow should be towards the top surface. In the present model, this is possible because of the bucket effect. Here, all the faces of a segment, except the top surface and the face above the channel level, are assumed to be impermeable. Hence, the rainfall input has nowhere to escape other than through the channel face (above the channel level) and/or to increase the water content of elements in

the subsurface flow zone. In this study, impervious surface areas were assumed to be nonexistent. Thus the only possible way, other than channel precipitation, for surface flow to occur is by exfiltration. Therefore, the model results of relatively lesser surface flow contribution is to be expected. For cases like this, the importance of the subsurface flow component is readily recognized. The traditional unit hydrograph approach that emphasizes the overland flow will not be able to predict the hydrograph properly.

For the second storm event, the simulation was performed for 48 hours. Outflow hydrographs are shown in Figure 17. Segment responses and volumes are presented in Tables 7 and 8, respectively. Here again, the peak flow was well predicted but the total outflow volume was overpredicted. Tables 7 and 8 indicate that the segments 12, 13, 16, 18, 22, 23, and 24 contribute most of the runoff volume. Less than 40 percent of the total area of the watershed accounted for more than 67 percent of the total runoff volume. Segment 18, with less than 4 percent of the total area, accounted for more than 20 percent of the total runoff volume and segment 6, with more than 4.5 percent of the total basin area, contributed less than 0.5 percent of the total outflow volume. Once again, a deduction can be made by observing the saturated hydraulic conductivities of segments 18 and 6. The importance of the subsurface flow contribution to the total runoff volume is evident.

For the stochastic simulation, the porous medium was assumed to comprise only two layers. A correlation coefficient of 0.5 was used to compute the covariance matrix needed for the generation of bivariate normal random vectors. The random hydraulic conductivity vectors for the two layers were generated using the IMSL subroutine RNMVN which requires the variance-covariance matrix as the input, and yields pseudorandom bivariate normal random vectors as the output. The conductivities so generated were used in VSAS2 to observe the variations in the watershed response in terms of flow and water content. A probability limit of 99 percent was chosen for the Monte Carlo simulation in this study. For this probability limit, and for $|\bar{x}-\mu| \leq 1$, the procedure outlined in chapter 4 results in

$$\lambda \geq 6.63\sigma^2 \tag{5.1}$$

For the two layers with $\kappa_1 = 16.767$ cm/day, $\varepsilon_1 = 76.259$ cm/day; and $\kappa_2 = 40.568$ cm/day, $\varepsilon_2 = 8.83$ cm/day (USDA 1952), equations (4.3) and (4.4) are solved for σ^2 using the equation

$$\sigma^2 = \ln\left(\left(\frac{\varepsilon}{\kappa}\right)^2 + 1\right) \tag{5.2}$$

Using the values of κ and ε in equation (5.2), we get ${\sigma_1}^2 = 0.355$, and ${\sigma_2}^2 = 0.046$. The sample sizes λ_1 and λ_2 were then computed using equation (5.1) and were found to be 3 and 1, respectively. This shows the necessity of at least three

samples to perform the Monte Carlo simulation. Based on bivariate normal distribution for the log-transformed hydraulic conductivities, $\lambda \geq \chi^2_2(0.01)$ for the 99 percent probability limit, i.e. $\lambda \geq 9.21$. A step-by-step procedure used in the present study is described below.

Step 1. Determination of the sample size:
For $\kappa_1 = 116.767$ cm/day and $\varepsilon_1 = 76.259$ cm/day, equation (5.2) results in $\sigma_1^2 = 0.355$. Therefore, from equation (5.1), $\lambda_1 \geq 3$. Similarly, for $\kappa_2 = 40.568$ cm/day and $\varepsilon_2 = 8.83$ cm/day $\sigma_2^2 = 0.046$ and $\lambda_2 \geq 1$. Based on the bivariate normal distribution for a 99 percent probability limit, $\lambda \geq 9.21$. However, in the present study, 25 simulations were performed.

Step 2. Generation of random vectors:
Assuming a correlation coefficient of 0.5 between the two layers and using the known estimates of variances of X_1 and X_2 (USDA 1952), the covariance matrix was estimated using the relationship (4.34). The IMSL subroutine RNMVN was used with the estimated covariance matrix to generate the saturated hydrauiic conductivity vector for the two layer system. This step was repeated for all 24 segments.

Step 3. The simulator VSAS2 was run using the saturated hydraulic conductivities generated in step 2.

Step 4. The watershed response in terms of channel precipitation, overland flow, and subsurface flow components of each segment were noted.

Step 5. Steps 2 through 4 were repeated 25 times corresponding to the chosen sample size.

Step 6. Mean values of channel precipitation, overland flow, subsurface flow, and total outflow volumes were computed by taking the average of the results obtained in step 4. This is the mean watershed response.

The mean runoff volumes for different segments are presented in Tables 9 and 10. It is seen from Table 10 that the segments 12, 13, 18, and 23 —with a combined area of about 21 percent of the total basin area —contribute about 53 percent of the total runoff volume. Segment 13, with less than 5 percent of the total area, contributes more than 18 percent of the total runoff volume whereas segment 6, with almost the same area, contributes less than 0.5 percent of the total runoff volume. As in the deterministic case, the reason for this may be attributed to the saturated hydraulic conductivities of the respective segments (see Table 4).

IV. Conclusion

It is obvious from the results presented previously that segments 12, 13, 18, and 23 consistently generate greater runoff volumes. The deterministic approach results show that segment 16 accounted for 10 percent of the total runoff volume (for the storm event of February 18, 1960) whereas the Monte Carlo technique indicates that this segment accounts for less than 6 percent of the total runoff volume. The

deterministic approach indicates that segment 18 produces the highest runoff volume, but the Monte Carlo method results indicate segment 13 produces the maximum runoff volume. This discrepancy may be attributed to the following difference between the two methods.

The Monte Carlo approach accounts for a variety of hydraulic conductivity values for different segments and the results are averaged; in the deterministic simulation, only one hydraulic conductivity vector is used to obtain a single realization of the output. However, for this example application, the deterministic simulation results are more or less consistent with those of the Monte Carlo simulation, which may be attributed to the relatively small standard deviations. In cases with large standard deviations, the results of the deterministic simulation may not be consistent with those of the Monte Carlo simulation. It is recommended that one use the Monte Carlo simulation results because this method accounts for the statistical nature of the hydraulic parameters; in the deterministic simulation, only one realization of the hydraulic parameter values is used and in the field one may not know the best estimates of the hydraulic conductivities.

SUMMARY

This study presents a unified procedure for runoff generation by simultaneously considering the surface and subsurface flows. Therefore, the procedure is able to identify the critical areas of a watershed that are primarily responsible for runoff generation. The important implication is that one can install proper runoff control measures in these critical regions to reduce undesired effects.

The procedure also points out that a significant part of the runoff need not be generated by overland flow but might be due to subsurface flow. The procedure, therefore, not only identifies the critical regions but also indicates the type of BMP measure needed to appropriately control the surface runoff and/or the subsurface runoff. It should, however, be remembered that the placement of BMPs may alter the surface-subsurface flow relationship. Therefore, effects of the placement of BMPs should be carefully investigated before arriving at any decision.

It is noted that the present methodology is a useful tool in identifying the critical regions in vegetated areas. Erosion and other related water quality problems are dominant in agricultural and rural areas and the methodology can provide better results in such areas. In urban areas, such a detailed procedure may not be needed and the classical unit hydrograph theory that ignores the subsurface component may be applied.

Another point of interest is the Monte Carlo simulation analysis. Based on the application to the Pony Mountain Branch watershed, it is readily seen that the deterministic simulation may not be able to identify the critical source regions because it generates one set of outputs only. Because the field hydraulic conductivity is not precisely known, it seems proper to use a distribution for such a parameter. Such a distribution leads to the generation of an ensemble of outputs which can be used for further inference. An average of the outputs is used in this study. This procedure provides a better guideline for assessing the source area patterns compared to a single realization generated from a deterministic simulation run. Pronounced dissimilarities will be observed if the variances are too large.

FIGURES

FIGURE 1
Runoff Generation

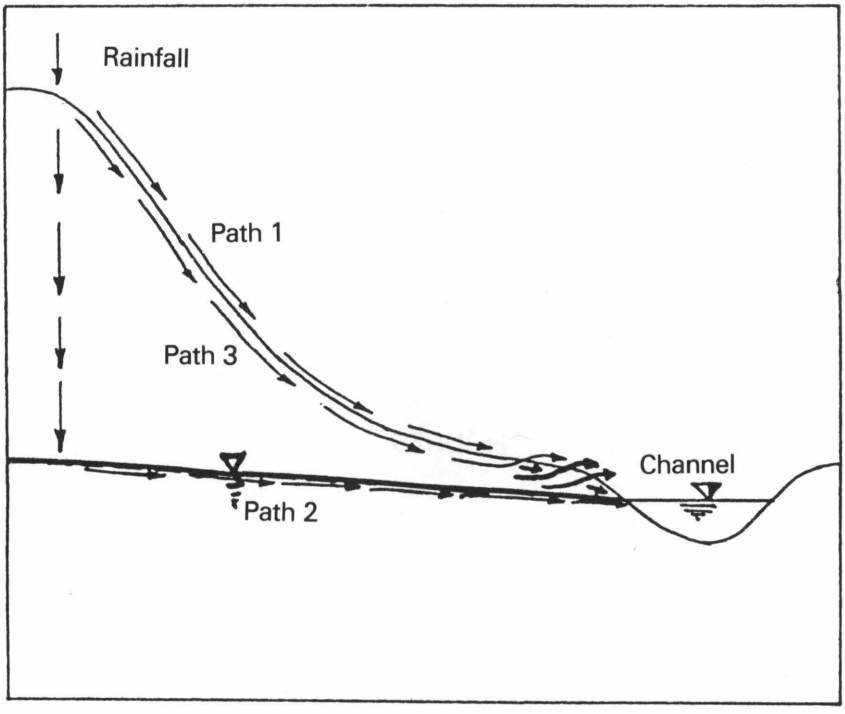

Path 1: Horton Overland Flow
Path 2: Groundwater Flow
Path 3: Subsurface Stormflow

FIGURE 2
Porous Medium

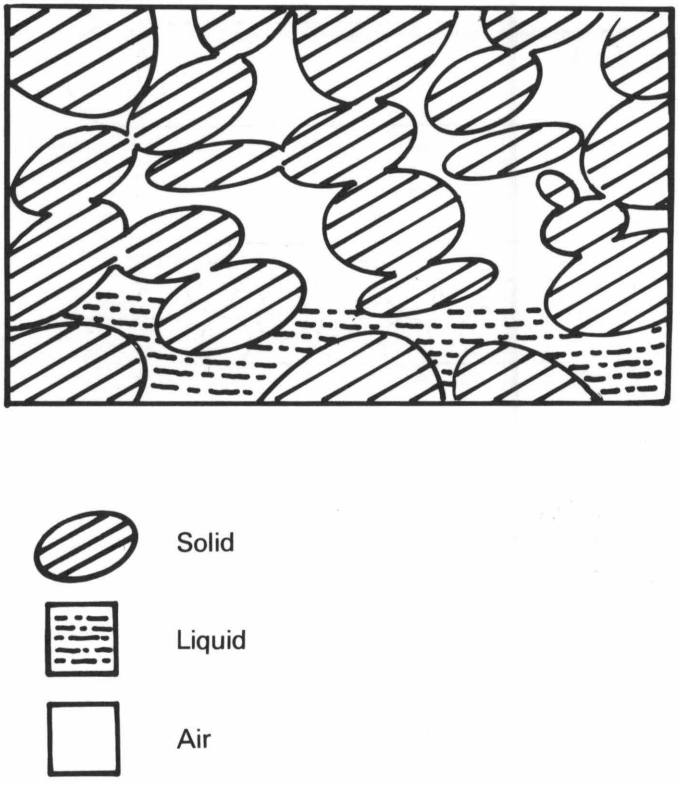

FIGURE 3
Superficial and Actual Velocities

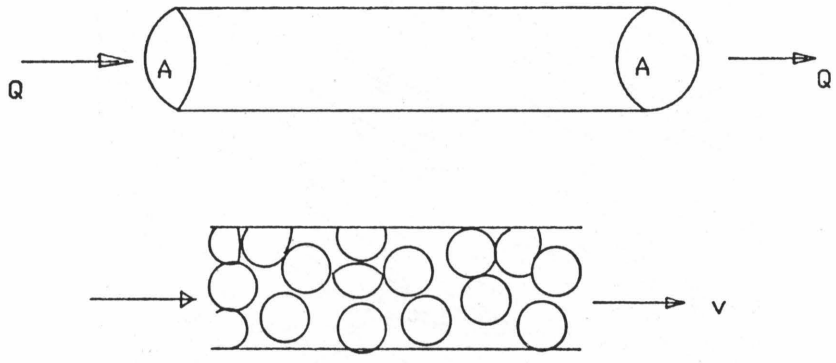

Flow area = A
Discharge = Q
Darcy velocity, q = Q/A
Pore water velocity, v = q/n
(actual velocity)

FIGURE 4
Control Volume for a Porous Medium

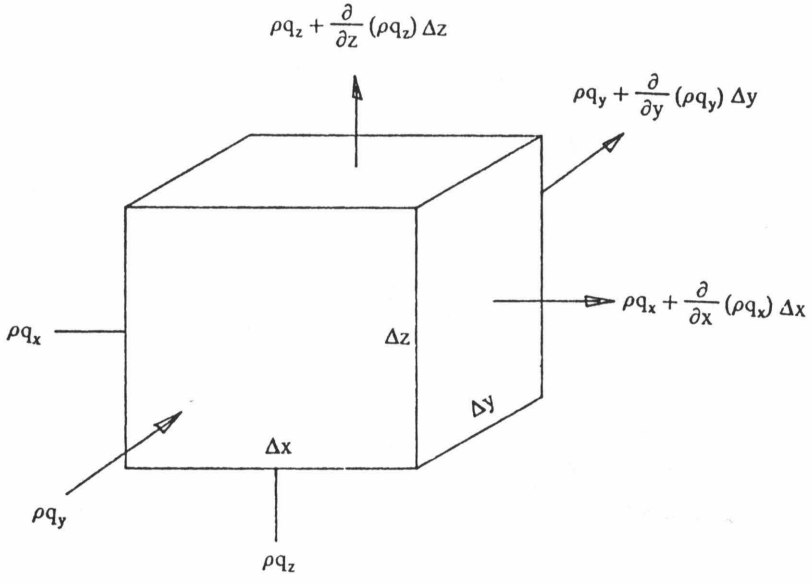

ρ = Fluid Density
q = Superficial Velocity

FIGURE 5
Moisture Content - Pressure Head Curve

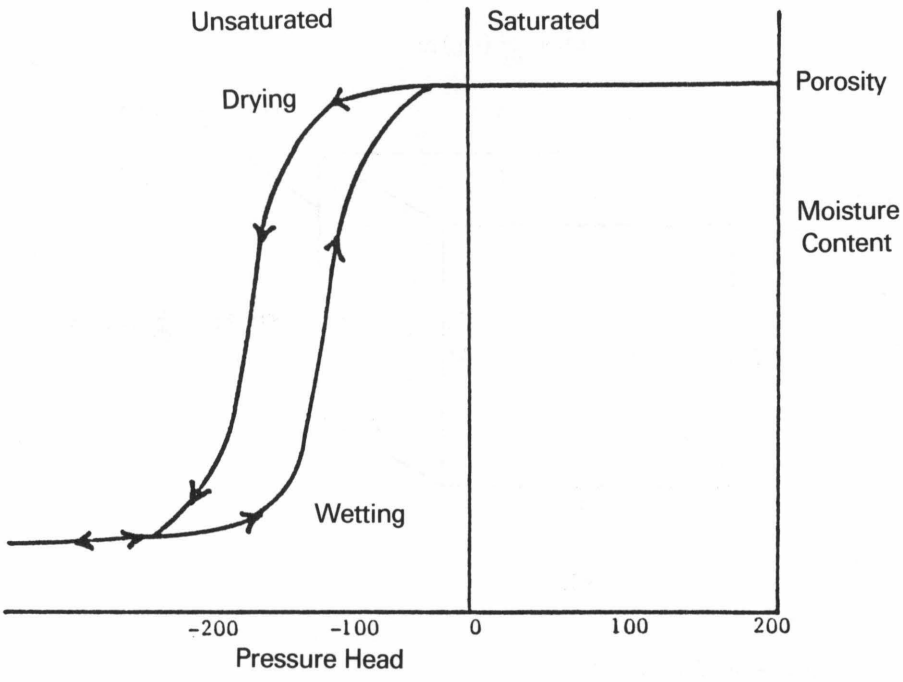

FIGURE 6
Hydraulic Conductivity - Pressure Head Curve

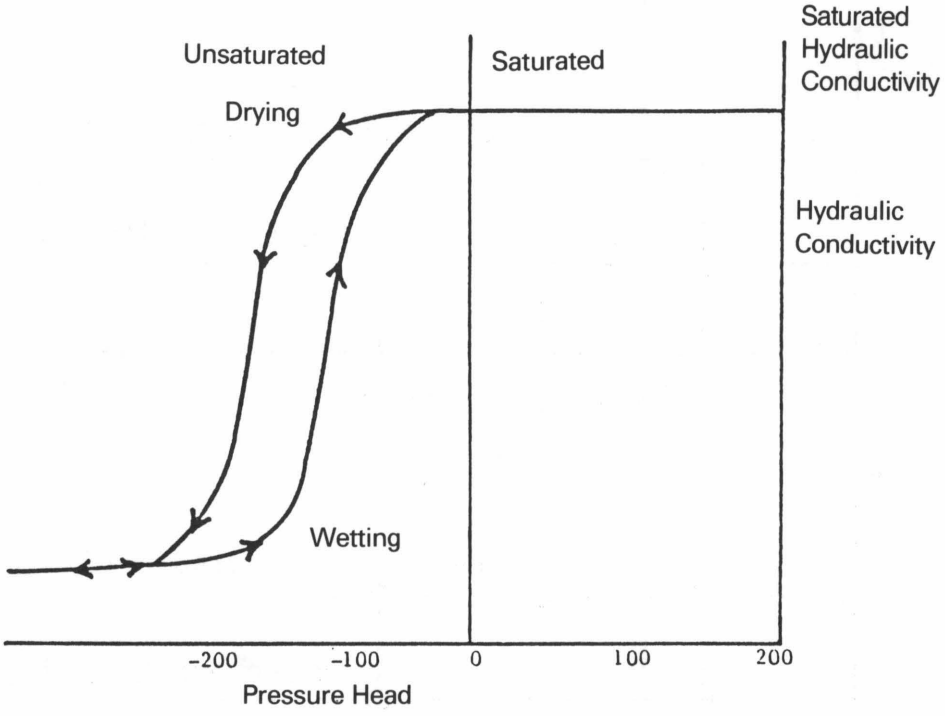

FIGURE 7
Schematic of Explicit and Implicit Schemes

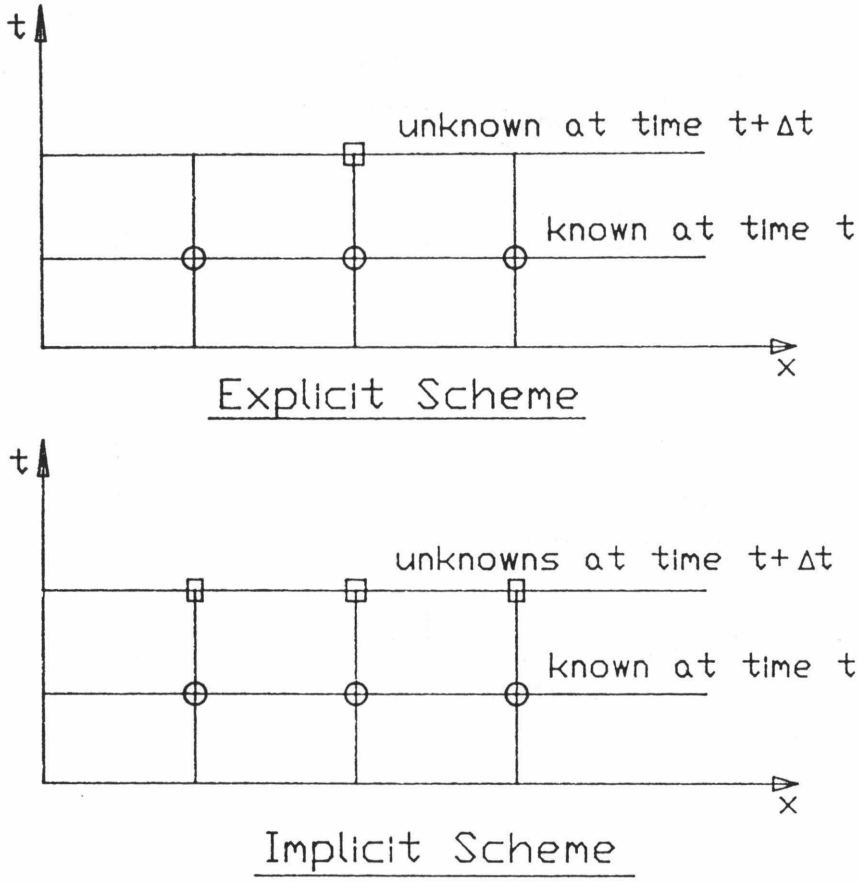

FIGURE 8
Boundary Conditions for a Typical Segment

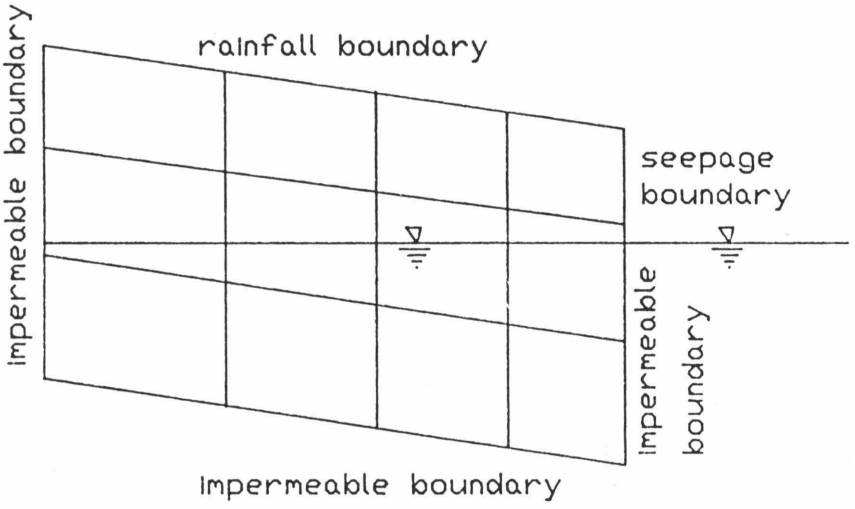

FIGURE 9
Fluxes through a Nonboundary Element

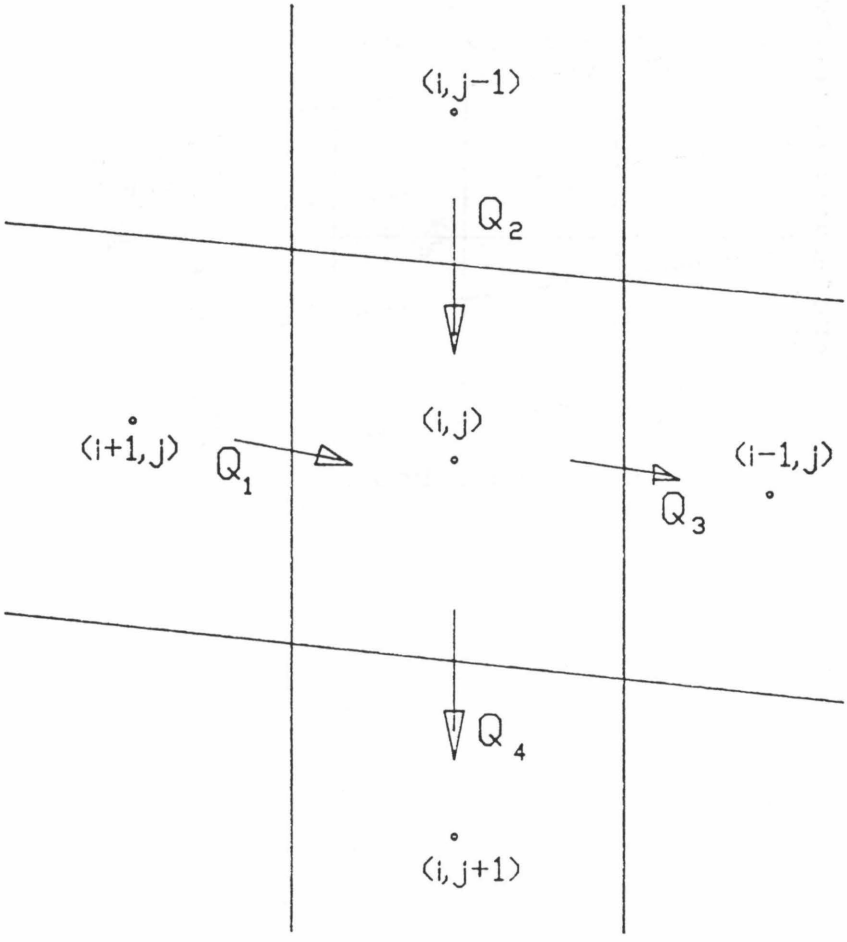

FIGURE 10
Source Area Expansion and Contraction

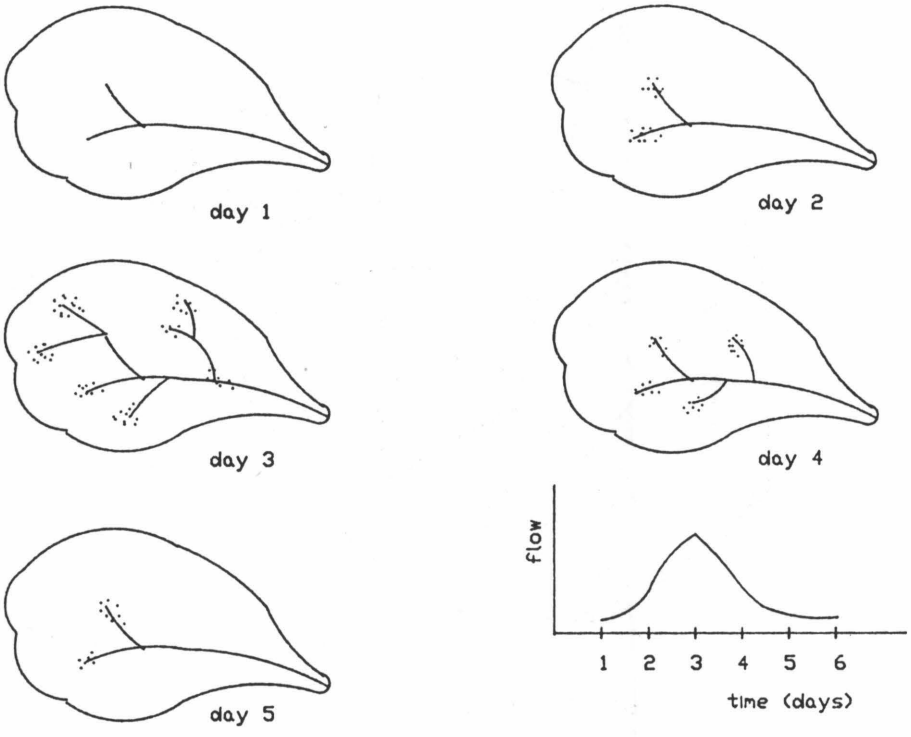

FIGURE 11
Segmentation of a Watershed

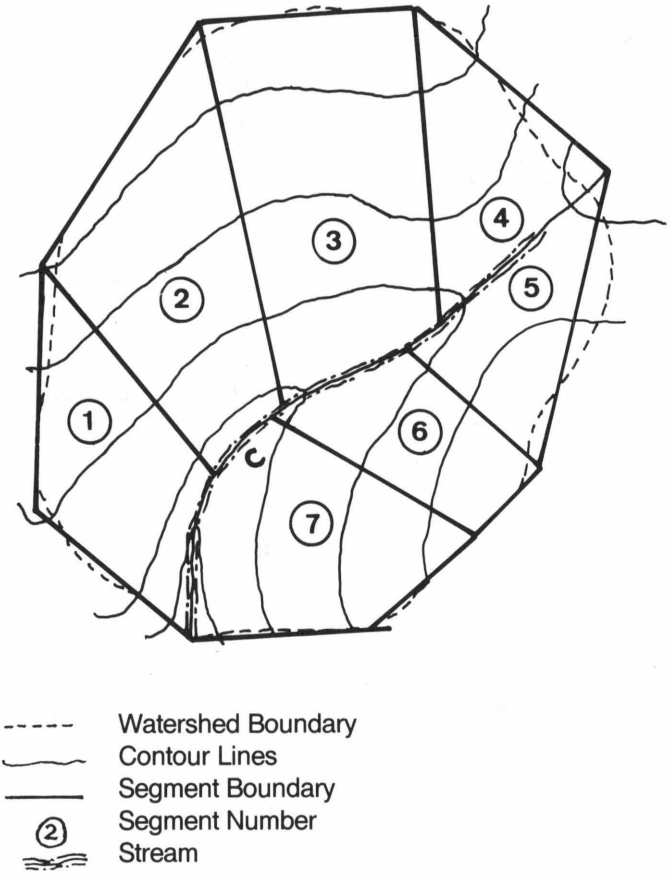

FIGURE 12
Segment Description

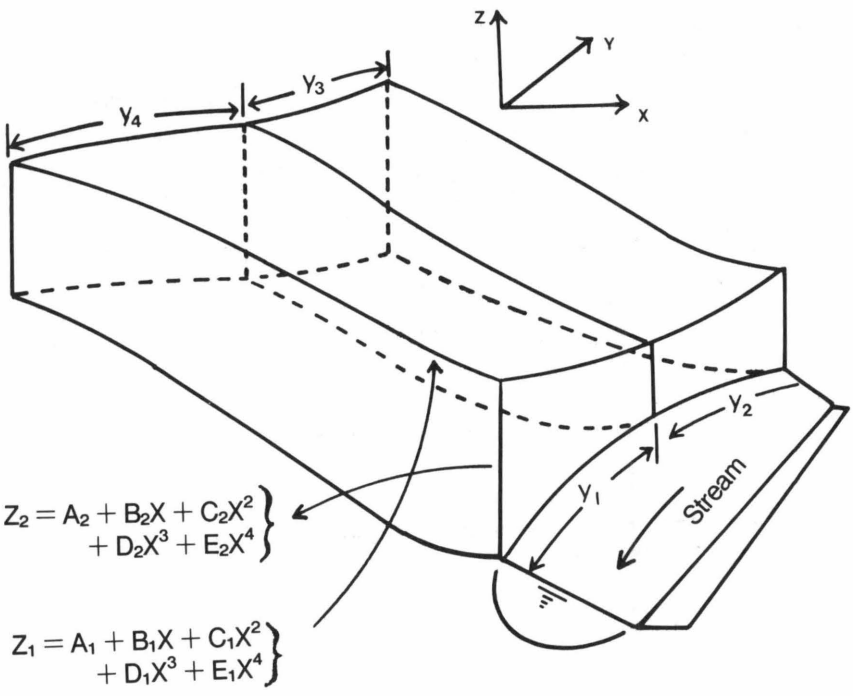

FIGURE 13
Segment Cross-Section

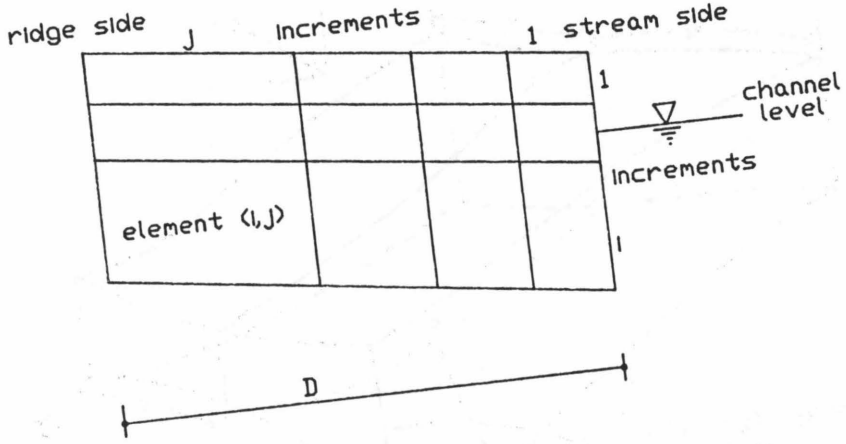

D = horizontal stream to ridge length of a segment

FIGURE 14
Pony Mountain Branch Watershed

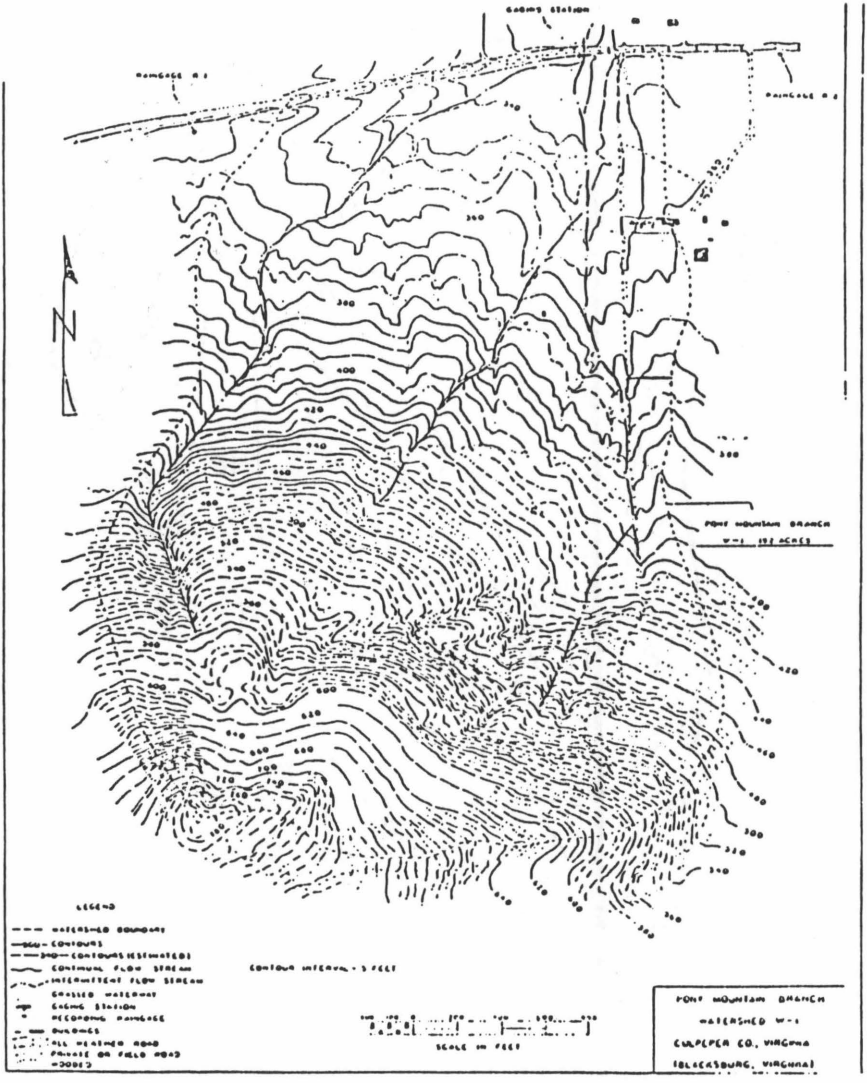

FIGURE 15
Segmentation - Pony Mountain Branch Watershed

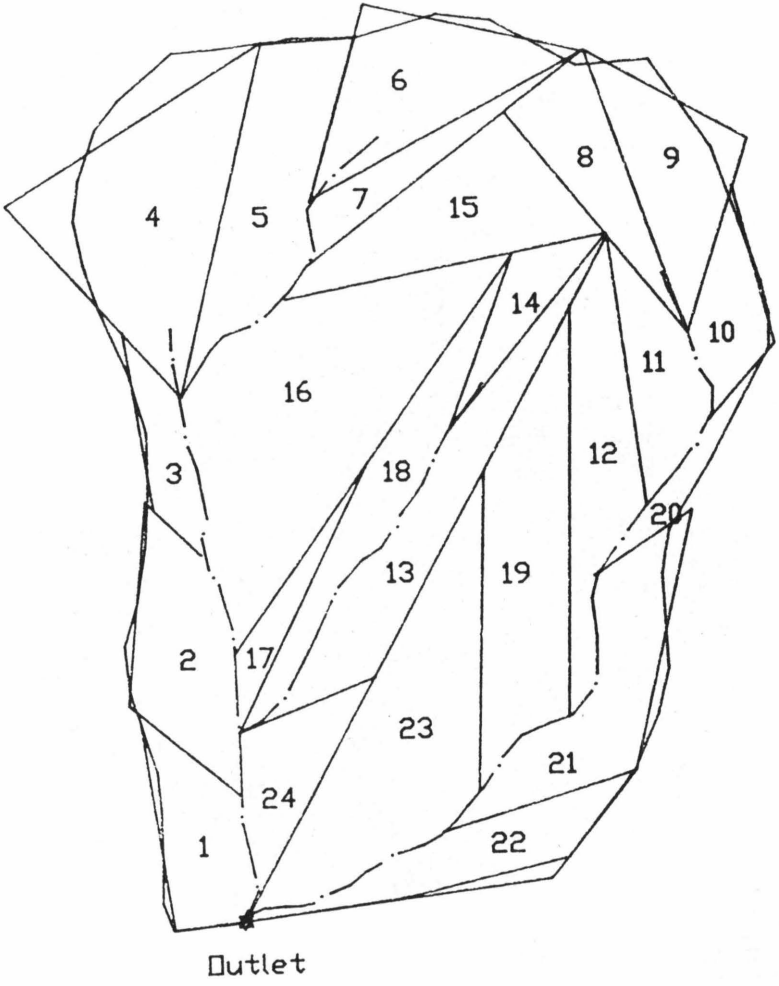

FIGURE 16
Hyetograph and Outflow Hydrograph (June 12, 1958)

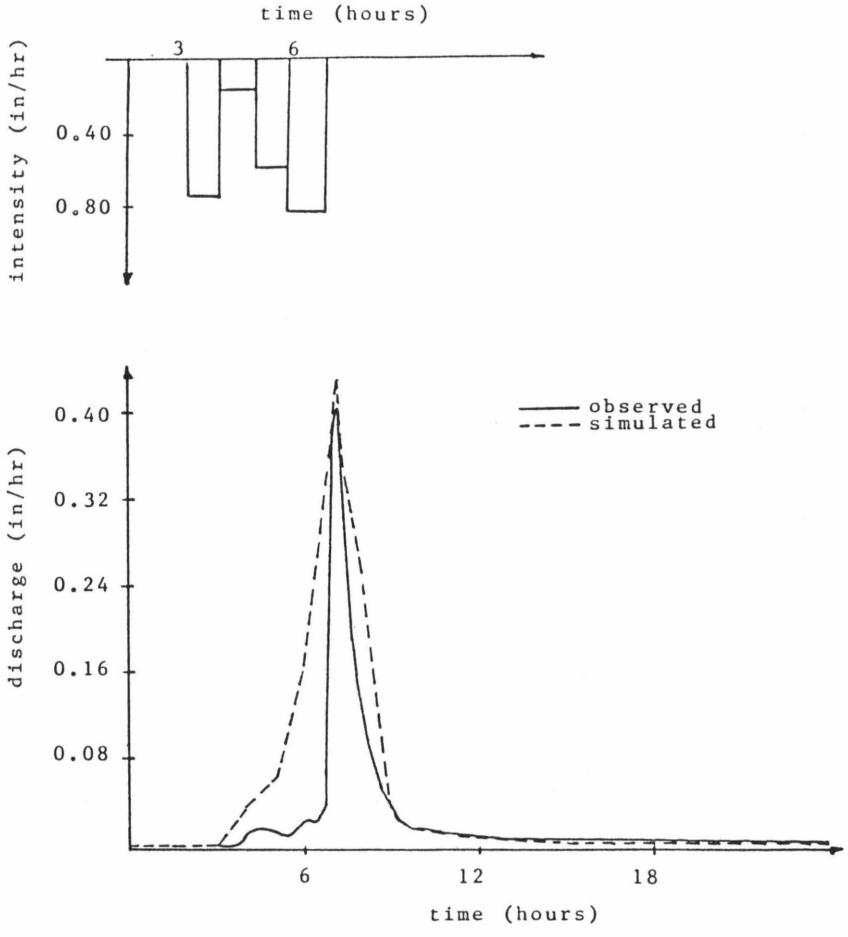

FIGURE 17
Hyetograph and Outflow Hydrograph (February 18, 1960)

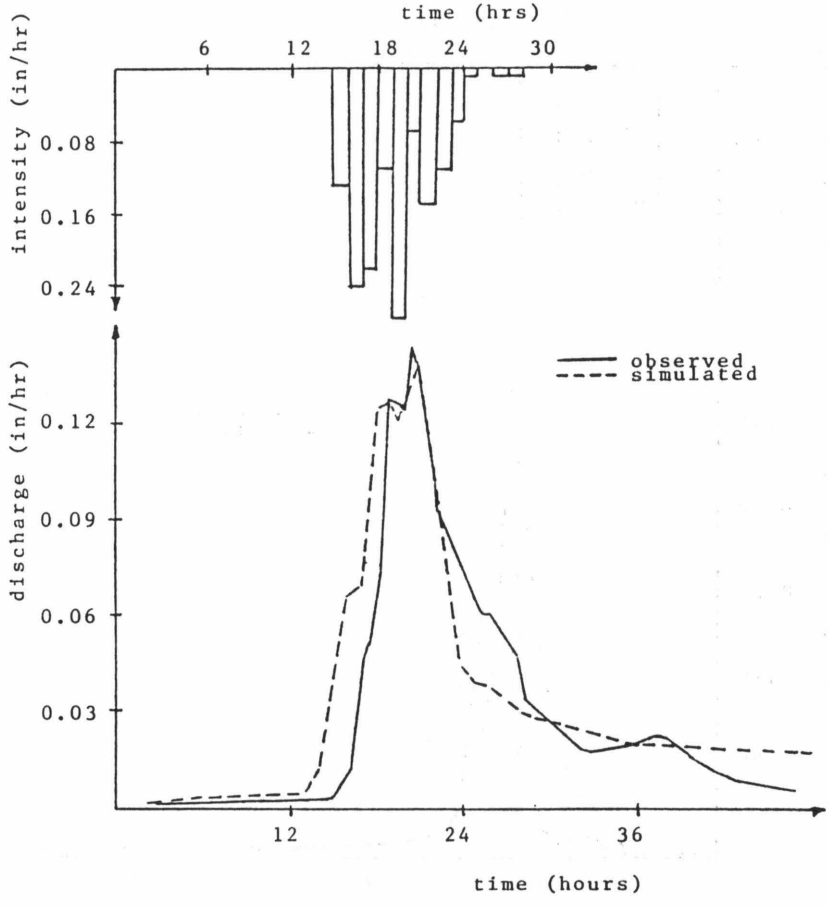

TABLES

TABLE 1
Parameters for Hydraulic Conductivity and Pressure Head (Equations 3.2 and 3.3)

Soil Type	Parameters				
	α (cm)	β	γ (cm/day)	ω	c (cm)
Silty clay loam	2.98×10^{-1}	-4.79	1.88×10^{10}	33.12	16.93
Silt loam	1.09×10^{-1}	-5.45	1.39×10^{7}	22.13	8.39
Sandy loam	6.49×10^{-4}	-9.19	1.07×10^{5}	14.01	2.35
Sand	2.50×10^{-3}	-7.74	7.46×10^{3}	6.87	1.72

TABLE 2
Segment Areas

Segment No.	Area (sq. ft.)	Percentage
1	253140	3.06
2	345190	4.17
3	138070	1.67
4	632850	7.65
5	444920	5.38
6	378430	4.57
7	148300	1.79
8	230130	2.78
9	455160	5.50
10	168760	2.04
11	230130	2.78
12	355420	4.30
13	406560	4.91
14	132960	1.61
15	419360	5.07
16	966520	11.68
17	97160	1.17
18	294050	3.55
19	503720	6.09
20	84380	1.02
21	398890	4.82
22	258250	3.12
23	702960	8.50
24	204560	2.47

Stream Area = 89600 sq. ft.
Total Area of Watershed = 192 acres
1 acre = 43,560 sq. ft.

TABLE 3
Land-Use Types by Segments

Segment No.	Land-use Type	Segment No.	Land-use Type
1	Cultivated	13	Pasture
2	Cultivated	14	Wooded
3	Cultivated	15	Wooded
4	Wooded	16	Wooded
5	Wooded	17	Pasture
6	Wooded	18	Wooded
7	Wooded	19	Pasture
8	Wooded	20	Pasture
9	Wooded	21	Pasture
10	Wooded	22	Pasture
11	Wooded	23	Pasture
12	Cultivated	24	Pasture

Source: Watershed Engineering Project (1968)

TABLE 4
Porosities and Saturated Hydraulic Conductivities by Segments

Segment No.	Porosity			Saturated Hydraulic Conductivity*		
	Layer 1	Layer 2	Layer 3	Layer 1	Layer 2	Layer 3
1	0.486	0.486	0.428	116.767	40.568	116.767
2	0.486	0.486	0.428	116.767	40.568	116.767
3	0.486	0.486	0.428	116.767	40.568	116.767
4	0.459	0.498	0.490	51.548	9.960	0.100
5	0.459	0.498	0.490	51.548	9.960	0.100
6	0.459	0.498	0.490	51.548	9.960	0.100
7	0.459	0.498	0.490	51.548	9.960	0.100
8	0.459	0.498	0.490	51.548	9.960	0.100
9	0.459	0.498	0.490	51.548	9.960	0.100
10	0.459	0.498	0.490	51.548	9.960	0.100
11	0.459	0.498	0.490	51.548	9.960	0.100
12	0.489	0.459	0.498	125.258	51.548	9.960
13	0.489	0.459	0.498	125.258	51.548	9.960
14	0.459	0.498	0.490	51.548	9.960	0.100
15	0.459	0.498	0.490	51.548	9.960	0.100
16	0.486	0.486	0.428	116.767	40.568	116.767
17	0.486	0.486	0.428	116.767	40.568	116.767
18	0.486	0.486	0.428	116.767	40.568	116.767
19	0.486	0.486	0.428	116.767	40.568	116.767
20	0.489	0.459	0.498	125.258	51.548	9.960
21	0.486	0.486	0.428	116.767	40.568	116.767
22	0.486	0.486	0.428	116.767	40.568	116.767
23	0.486	0.486	0.428	116.767	40.568	116.767
24	0.486	0.486	0.428	116.767	40.568	116.767

* cm/day

Source:U.S. Department of Agriculture (1952)

TABLE 5
Runoff Distribution by Segments (June 12, 1958)

Segment No.	Runoff	
	(a) Volume (inches)	(b) Percentage of Rainfall Volume
1	0.138	5.877
2	0.074	3.163
3	0.120	5.152
4	0.017	0.722
5	0.047	2.004
6	0.007	0.293
7	0.093	3.951
8	0.009	0.385
9	0.020	0.822
10	0.046	1.986
11	0.110	4.626
12	0.178	8.190
13	0.170	7.233
14	0.011	0.428
15	0.026	1.104
16	0.118	4.991
17	0.173	7.346
18	0.352	14.856
19	0.059	2.520
20	0.314	13.169
21	0.080	3.360
22	0.141	5.951
23	0.111	4.636
24	0.128	5.337

(a): From VSAS2 output (for example, see line 100 of output in Appendix B)
(b): Percentage of total rainfall volume (2.37 inches)

TABLE 6
Surface and Subsurface Flow Volumes by Segments (June 12, 1958)

(a) Segment No.	(b) Channel Precip. (in.)	(c) Overland Flow (in.)	(d) Subsurface Flow (in.)	(e) Total Flow (in.)	(f) Total Volume of Flow (cu. ft.)
1	0.010	0.041	0.087	0.138	2911
2	0.011	0.025	0.039	0.074	2129
3	0.022	0.034	0.064	0.120	1381
4	0.004	0.005	0.008	0.017	897
5	0.007	0.014	0.027	0.047	1743
6	0.003	0.002	0.002	0.007	221
7	0.020	0.023	0.050	0.093	1149
8	0.006	0.001	0.002	0.009	173
9	0.003	0.006	0.011	0.020	759
10	0.008	0.009	0.029	0.046	647
11	0.019	0.025	0.066	0.110	2109
12	0.012	0.046	0.119	0.178	5272
13	0.019	0.034	0.118	0.170	5760
14	0.007	0.002	0.002	0.011	122
15	0.007	0.007	0.012	0.026	909
16	0.008	0.032	0.078	0.118	9504
17	0.014	0.053	0.106	0.173	1401
18	0.020	0.073	0.259	0.352	8625
19	0.005	0.022	0.033	0.059	2477
20	0.024	0.037	0.253	0.314	2208
21	0.011	0.026	0.043	0.080	2659
22	0.019	0.047	0.075	0.141	3034
23	0.008	0.037	0.066	0.111	6502
24	0.018	0.035	0.074	0.128	2182

(b): Channel precipitation = rainfall volume x stream Area

(c): Overland flow volume is obtained by summing hourly values from VSAS2 output (see lines 45, 50, etc. in the sample output in Appendix B for hourly overland flow volumes) for the entire simulation period.

(d): Subsurface flow = Total flow – Overland flow – Channel precipitation. Total flow (e) is obtained from VSAS2 (for a sample problem, see line 100 under streamflow in the sample output of Appendix B).

(f): Total volume of flow is obtained by multiplying column (e) and the segment area from Table 2.

TABLE 7
Runoff Distribution by Segments (February 18, 1960)

Segment No.	Runoff	
	(a) Volume (inches)	(b) Percentage of Rainfall Volume
1	0.027	1.926
2	0.013	0.938
3	0.027	1.964
4	0.003	0.223
5	0.012	0.887
6	0.001	0.078
7	0.029	2.078
8	0.0002	0.146
9	0.004	0.252
10	0.012	0.848
11	0.031	2.225
12	0.053	3.807
13	0.052	3.690
14	0.002	0.173
15	0.006	0.458
16	0.021	1.469
17	0.047	3.349
18	0.047	10.503
19	0.012	0.853
20	0.095	6.765
21	0.020	1.402
22	0.038	2.699
23	0.027	1.931
24	0.035	2.524

(a): From VSAS2 output (for an example, see line 100 of output in Appendix B)
(b): Percentage of total rainfall volume (1.40 inches)

TABLE 8
Surface and Subsurface Flow Volumes by Segments (February 18, 1960)

(a) Segment No.	(b) Channel Precip. (in.)	(c) Overland Flow (in.)	(d) Subsurface Flow (in.)	(e) Total Flow (in.)	(f) Total Volume (cu. ft.)
1	0.006	0.003	0.018	0.027	570
2	0.006	0.001	0.006	0.013	374
3	0.012	0.003	0.012	0.027	311
4	0.001	0.000	0.002	0.003	158
5	0.003	0.001	0.009	0.012	445
6	0.001	0.000	0.000	0.001	32
7	0.009	0.002	0.018	0.029	358
8	0.002	0.000	0.000	0.002	38
9	0.001	0.001	0.002	0.004	152
10	0.003	0.000	0.009	0.012	169
11	0.008	0.001	0.022	0.031	595
12	0.006	0.005	0.043	0.053	1570
13	0.009	0.003	0.041	0.052	1762
14	0.002	0.000	0.000	0.002	22
15	0.002	0.001	0.004	0.006	210
16	0.003	0.003	0.015	0.021	1691
17	0.007	0.008	0.032	0.047	381
18	0.011	0.016	0.120	0.147	3602
19	0.002	0.002	0.008	0.012	504
20	0.013	0.000	0.082	0.095	668
21	0.005	0.004	0.011	0.020	665
22	0.008	0.006	0.024	0.038	818
23	0.004	0.006	0.018	0.027	1582
24	0.009	0.007	0.019	0.035	597

(b): Channel precipitation = rainfall volume x stream Area

(c): Overland flow volume is obtained by summing hourly values from VSAS2 output (see lines 45, 50, etc. in the sample output in Appendix B for hourly overland flow volumes) for the entire simulation period.

(d): Subsurface flow = Total flow – Overland flow – Channel precipitation. Total flow (e) is obtained from VSAS2 (for a sample problem, see line 100 under streamflow in the sample output of Appendix B).

(f): Total volume of flow is obtained by multiplying column (e) and the segment area from Table 2.

TABLE 9
Mean Runoff Distribution
Monte Carlo Simulation (February 18, 1960)

Segment No.	Runoff	
	(a) Volume (inches)	(b) Percentage of rainfall volume
1	0.013	0.913
2	0.009	0.686
3	0.019	1.364
4	0.002	0.147
5	0.005	0.365
6	0.001	0.072
7	0.017	1.213
8	0.002	0.130
9	0.001	0.076
10	0.008	0.588
11	0.021	1.491
12	0.051	3.623
13	0.057	4.060
14	0.002	0.161
15	0.003	0.223
16	0.008	0.588
17	0.021	1.478
18	0.044	3.712
19	0.005	0.349
20	0.106	7.583
21	0.014	1.026
22	0.015	1.067
23	0.017	1.195
24	0.020	1.445

Total Rainfall Volume = 1.40 inches

TABLE 10
Surface and Subsurface Flow Volumes by Segments
Monte Carlo Simulation (February 18, 1960)

Segment No.	Channel Precip. (in.)	Overland Flow (in.)	Subsurface Flow (in.)	Total Flow (in.)	Total Volume (cu. ft.)
1	0.006	0.001	0.006	0.013	274
2	0.006	0.000	0.003	0.009	259
3	0.012	0.001	0.006	0.019	219
4	0.001	0.000	0.001	0.002	105
5	0.003	0.000	0.002	0.005	185
6	0.001	0.000	0.000	0.001	32
7	0.009	0.002	0.006	0.017	210
8	0.002	0.000	0.000	0.002	38
9	0.001	0.000	0.000	0.001	38
10	0.003	0.001	0.004	0.008	113
11	0.008	0.002	0.011	0.021	403
12	0.006	0.005	0.040	0.051	1511
13	0.009	0.004	0.044	0.057	1931
14	0.002	0.000	0.000	0.002	22
15	0.002	0.000	0.001	0.003	105
16	0.003	0.001	0.004	0.008	644
17	0.007	0.004	0.010	0.021	170
18	0.011	0.010	0.023	0.044	1078
19	0.002	0.000	0.003	0.005	210
20	0.013	0.011	0.082	0.106	745
21	0.005	0.002	0.007	0.014	465
22	0.008	0.002	0.005	0.015	323
23	0.004	0.004	0.009	0.017	996
24	0.009	0.002	0.009	0.020	341

TABLE 11
Data File for Input Deck 1 (Pony Mountain Branch Watershed)

```
SIMULATION OF PONY MOUNTAIN BRANCH FOR 06/12/58
580612
            .74 .18 .60 .85

  9.
 1   3   3    4   253140.
0.3
  3.360E02  5.313E-2  1.950E-5                          3.200E02  2.600E02
  1.500E00                                             3.200E02  3.000E02
  3.380E02  7.455E-2 -4.380E-5                         3.800E02  3.000E02
  1.500E00                                             3.800E02  6.200E02
  3.430E02  4.834E-2 -2.870E-5                         5.000E02
  1.500E00                                             5.000E02
   0.50    0.500   0.500
  2800.
    1.0
    5.220E-2     -5.14637
    9.179E06     12.75683
    1.387E-2     -6.44750
    6.153E07     15.44120
    8.161E-2     -4.39137
    6.927E06     11.2131
116.7670   0.486400   2.13055
 40.5675   0.486400   1.44610
116.7670   0.427500   3.41173
 2   4   3   19   345190.
0.4
  3.430E02  4.180E-2 -1.910E-5                          6.000E02  2.800E02
  1.500E00                                             6.000E02  3.400E02
  3.500E02  3.357E-2 -1.424E-5                         6.000E02  3.000E02
  1.500E00                                             6.000E02  2.000E02
  3.580E02  6.670E-3  4.440E-5                         5.200E02  4.400E02
  1.500E00                                             5.200E02  3.000E02
  3.680E02  7.500E-3  1.250E-4                         3.000E02
  1.500E00                                             3.000E02
   0.50    0.500   0.500
  4000.
    1.0
    5.220E-2     -5.14637
    9.179E06     12.75683
    1.387E-2     -6.44750
    6.153E07     15.44120
    8.161E-2     -4.39137
    6.927E06     11.2131
116.7670   0.486400   2.13055
 40.5675   0.486400   1.44610
116.7670   0.427500   3.41173
```

```
 3   4   3   27   138070.
0.3
  3.680E02  1.357E-2  1.071E-4                    3.000E02  2.200E02
  1.500E00                                        3.000E02  2.800E02
  3.780E02 -7.575E-3  1.791E-4                    3.600E02  3.000E02
  1.500E00                                        3.600E02  2.600E02
  3.890E02  5.890E-2 -7.410E-5                    3.000E02  1.600E02
  1.500E00                                        3.000E02  1.000E02
  3.950E02  2.590E-2  1.010E-5                    3.600E02
  1.500E00                                        3.600E02
   0.50     0.500    0.500
  3300.
    1.0
    5.220E-2     -5.14637
    9.179E06     12.75683
    1.387E-2     -6.44750
    6.153E07     15.44120
    8.161E-2     -4.39137
    6.927E06     11.2131
116.7670    0.486400    2.13055
 40.5675    0.486400    1.44610
116.7670    0.427500    3.41173
 4   3   3   29   632850.
0.4
  3.950E02  4.496E-2  2.500E-6                    3.200E02  2.600E02
  1.500E00                                        3.200E02  3.000E02
  3.950E02  7.106E-2  3.789E-5                    3.800E02  3.000E02
  1.500E00                                        3.800E02  6.200E02
  3.950E02  7.740E-2  5.062E-5                    5.000E02
  1.500E00                                        5.000E02
   0.50     0.500    0.500
  3000.
    1.0
    4.608E-3     -8.05885
    2.921E07     18.81997
    4.416E-3     -8.19369
    6.525E07     19.13503
    1.289E-2     -9.19313
    3.295E06     21.7547
 51.5475    0.458500    2.47038
  9.9600    0.497917    1.33789
  0.1000    0.490400    9.02102
 5   2   3   34   444920.
0.4
  3.950E02  7.740E-2  5.062E-5                    1.480E03  5.400E02
  1.500E00                                        1.480E03  4.000E02
  5.100E02  2.847E-1 -9.430E-5                    7.000E02
  1.500E00                                        7.000E02
   0.50     0.500    0.500
```

TABLE 11 continued

```
 3300.
   1.0
   4.608E-3     -8.05885
   2.921E07     18.81997
   4.416E-3     -8.19369
   6.525E07     19.13503
   1.289E-2     -9.19313
   3.295E06     21.7547
51.5475    0.458500    2.47038
 9.9600    0.497917    1.33789
 0.1000    0.490400    9.02102

 6    2    3    37    378430.
0.4
  5.100E02  2.847E-1 -9.430E-5                    8.200E02  0.000E02
  1.500E00                                       8.200E02  9.200E02
  5.100E02  1.869E-1  3.667E-5                    1.280E03
  1.500E00                                       1.280E03
   0.50     0.500    0.500
  1500.
    1.0
    4.608E-3     -8.05885
    2.921E07     18.81997
    4.416E-3     -8.19369
    6.525E07     19.13503
    1.289E-2     -9.19313
    3.295E06     21.7547
 51.5475    0.458500    2.47038
  9.9600    0.497917    1.33789
  0.1000    0.490400    9.02102
 7    2    3    34    148300.
0.4
  5.100E02  1.869E-1  3.667E-5                    1.260E03  2.600E02
  1.500E00                                       1.260E03  0.000E00
  4.550E02  2.367E-1  5.150E-6                    1.420E03
  1.500E00                                       1.420E03
   0.50     0.500    0.500
  3300.
    1.0
    4.608E-3     -8.05885
    2.921E07     18.81997
    4.416E-3     -8.19369
    6.525E07     19.13503
    1.289E-2     -9.19313
    3.295E06     21.7547
 51.5475    0.458500    2.47038
  9.9600    0.497917    1.33789
  0.1000    0.490400    9.02102
 8    2    3    46    230130.
```

```
0.4
  5.150E02  1.003E-1  5.500E-5                    1.180E03  0.000E02
  1.500E00                                      1.180E03  4.000E02
  5.150E02  1.748E-2  1.485E-4                  1.240E03
  1.500E00                                      1.240E03
   0.50     0.500    0.500
  1500.
    1.0
    4.608E-3     -8.05885
    2.921E07     18.81997
    4.416E-3     -8.19369
    6.525E07     19.13503
    1.289E-2     -9.19313
    3.295E06     21.7547
 51.5475   0.458500    2.47038
  9.9600   0.497917    1.33789
  0.1000   0.490400    9.02102
 9   2   3   46   455160.
0.4
  5.150E02  1.748E-2  1.485E-4                  1.240E03  2.400E02
  1.500E00                                      1.240E03  8.000E02
  5.150E02  2.458E-1 -1.458E-4                  6.000E02
  1.500E00                                      6.000E02
   0.50     0.500    0.500
  1500.
    1.0
    4.608E-3     -8.05885
    2.921E07     18.81997
    4.416E-3     -8.19369
    6.525E07     19.13503
    1.289E-2     -9.19313
    3.295E06     21.7547
 51.5475   0.458500    2.47038
  9.9600   0.497917    1.33789
  0.1000   0.490400    9.02102
10   2   3   44   168760.
0.4
  5.150E02  2.458E-1 -1.580E-4                  6.000E02  3.600E02
  1.500E00                                      6.000E02  5.600E02
  4.500E02  1.806E-1 -7.716E-5                  3.600E02
  1.500E00                                      3.600E02
   0.50     0.500    0.500
  1500.
    1.0
    4.608E-3     -8.05885
    2.921E07     18.81997
    4.416E-3     -8.19369
    6.525E07     19.13503
    1.289E-2     -9.19313
    3.295E06     21.7547
 51.5475   0.458500    2.47038
  9.9600   0.497917    1.33789
  0.1000   0.490400    9.02102
```

TABLE 11 continued

```
11   2   3   44   230130.
0.4
  5.150E02  2.417E-1 -1.690E-4                    5.200E02  7.400E02
  1.500E00                                       5.200E02  0.000E00
  4.150E02  2.050E-1 -4.132E-5                   1.140E03
  1.500E00                                       1.140E03
   0.50     0.500    0.500
  4700.
    1.0
    4.608E-3     -8.05885
    2.921E07     18.81997
    4.416E-3     -8.19369
    6.525E07     19.13503
    1.289E-2     -9.19313
    3.295E06     21.7547
 51.5475    0.458500    2.47038
  9.9600    0.497917    1.33789
  0.1000    0.490400    9.02102

12   2   3   34   355420.
0.3
  4.150E02  2.050E-1 -4.132E-5                   1.140E03  9.000E02
  1.500E00                                       1.140E03  3.400E02
  3.670E02  2.822E-2  4.981E-5                   1.680E03
  1.500E00                                       1.680E03
   0.50     0.500    0.500
  4800.
    1.0
    3.023E-2     -7.47757
    2.363E07     20.73710
    2.409E-2     -5.44682
    1.761E06     13.38040
    1.125E-4    -14.78649
    1.906E10     33.53633
125.2583    0.489222    6.34169
 51.5475    0.458500    1.68473
  9.9600    0.497917    3.82849
13   2   3   30   406560.
0.4
  4.800E02  1.642E-1 -3.540E-5                   8.600E02  1.540E03
  1.500E00                                       8.600E02  2.100E03
  3.500E02  3.051E-2  1.859E-5                   6.000E02
  1.500E00                                       6.000E02
   0.50     0.500    0.500
  8300.
    1.0
    3.023E-2     -7.47757
    2.363E07     20.73710
    2.409E-2     -5.44682
    1.761E06     13.38040
    1.125E-4    -14.78649
    1.906E10     33.53633
125.2583    0.489222    6.34169
 51.5475    0.458500    1.68473
  9.9600    0.497917    3.82849
```

```
14   2   3   30   132960.
0.4
  4.800E02  1.642E-1 -3.540E-5                    8.600E02  0.000E02
  1.500E00                                        8.600E02  4.000E02
  4.550E02  1.601E-1 -4.094E-5                    7.800E02
  1.500E00                                        7.800E02
   0.50     0.500    0.500
  1000.
    1.0
    4.608E-3     -8.05885
    2.921E07     18.81997
    4.416E-3     -8.19369
    6.525E07     19.13503
    1.289E-2     -9.19313
    3.295E06     21.7547
 51.5475   0.458500   2.47038
  9.9600   0.497917   1.33789
  0.1000   0.490400   9.02102

15   2   3   38   419360.
0.4
  4.600E02  2.445E-1 -1.867E-5                    1.020E03  2.000E02
  1.500E00                                        1.020E03  5.400E02
  4.250E02  1.479E-1 -1.793E-5                    1.380E03
  1.500E00                                        1.380E03
   0.50     0.500    0.500
  3300.
    1.0
    4.608E-3     -8.05885
    2.921E07     18.81997
    4.416E-3     -8.19369
    6.525E07     19.13503
    1.289E-2     -9.19313
    3.295E06     21.7547
 51.5475   0.458500   2.47038
  9.9600   0.497917   1.33789
  0.1000   0.490400   9.02102
16   2   3   36   966520.
0.4
  4.250E02  1.493E-1 -1.932E-5                    1.000E03  1.440E03
  1.500E00                                        1.000E03  0.000E00
  3.580E02  3.857E-2  2.843E-5                    2.040E03
  1.500E00                                        2.040E03
   0.50     0.500    0.500
  8700.
    1.0
    5.220E-2     -5.14637
    9.179E06     12.75683
    1.387E-2     -6.44750
    6.153E07     15.44120
    8.161E-2     -4.39137
    6.927E06     11.2131
116.7670   0.486400   2.13055
 40.5675   0.486400   1.44610
116.7670   0.427500   3.41173
```

TABLE 11 continued

```
17    2    3    14     97160.
0.4
  3.580E02  4.700E-2  2.000E-5                    1.000E03  3.200E02
  1.500E00                                       1.000E03  0.000E00
  3.480E02  3.710E-2  2.016E-5                    1.240E03
  1.500E00                                       1.240E03
   0.50     0.500    0.500
  1500.
    1.0
    5.220E-2     -5.14637
    9.179E06     12.75683
    1.387E-2     -6.44750
    6.153E07     15.44120
    8.161E-2     -4.39137
    6.927E06     11.2131
116.7670    0.486400    2.13055
 40.5675    0.486400    1.44610
116.7670    0.427500    3.41173

18    2    3    30    294050.
0.4
  3.480E02  3.710E-2  2.016E-5                    1.240E03  1.540E03
  1.500E00                                       1.240E03  1.060E03
  4.550E02  1.601E-1 -4.094E-5                    7.800E02
  1.500E00                                       7.800E02
   0.50     0.500    0.500
  6300.
    1.0
    5.220E-2     -5.14637
    9.179E06     12.75683
    1.387E-2     -6.44750
    6.153E07     15.44120
    8.161E-2     -4.39137
    6.927E06     11.2131
116.7670    0.486400    2.13055
 40.5675    0.486400    1.44610
116.7670    0.427500    3.41173
19    2    3    22    503720.
0.3
  3.670E02  2.822E-2  4.981E-5                    1.680E03  4.800E02
  1.500E00                                       1.680E03  7.800E02
  3.500E02  2.6547-2  3.350E-5                    1.290E03
  1.500E00                                       1.290E03
   0.50     0.500    0.500
  2500.
    1.0
    5.943E-2     -4.76597
    7.322E06     12.01307
    1.543E-2     -6.37197
    3.480E07     15.27147
    6.310E-3     -6.99323
    7.220E07     16.53747
116.7670    0.486400    2.13055
 40.5675    0.486400    1.44610
116.7670    0.427500    3.41173
```

```
20   2   3   34    84380.
0.3
  4.500E02  1.806E-1 -7.716E-5                    3.600E02  8.000E02
  1.500E00                                       3.600E02  8.400E02
  3.940E02  5.159E-2  1.705E-5                   4.400E02
  1.500E00                                       4.400E02
   0.50    0.500   0.500
  2200.
    1.0
    3.023E-2    -7.47757
    2.363E07    20.73710
    2.409E-2    -5.44682
    1.761E06    13.38040
    1.125E-4   -14.78649
    1.906E10    33.53633
125.2583   0.489222   6.34169
 51.5475   0.458500   1.68473
  9.9600   0.497917   3.82849

21   2   3   15   398890.
0.2
  3.940E02  5.159E-2  1.705E-5                   4.400E02  9.000E02
  1.500E00                                       4.400E02  5.400E02
  3.450E02  2.874E-2 -6.375E-6                   8.600E02
  1.500E00                                       8.600E02
   0.50    0.500   0.500
  5000.
    1.0
    5.943E-2    -4.76597
    7.322E06    12.01307
    1.543E-2    -6.37197
    3.480E07    15.27147
    6.310E-3    -6.99323
    7.220E07    16.53747
116.7670   0.486400   2.13055
 40.5675   0.486400   1.44610
116.7670   0.427500   3.41173
22   2   3   29   258250.
0.3
  3.450E02  2.874E-2 -6.375E-6                   8.600E02  1.600E03
  1.500E00                                       8.600E02  2.420E03
  3.360E02  1.986E-2 -1.265E-6                   1.320E03
  1.500E00                                       1.320E03
   0.50    0.500   0.500
  5500.
    1.0
    5.943E-2    -4.76597
    7.322E06    12.01307
    1.543E-2    -6.37197
    3.480E07    15.27147
    6.310E-3    -6.99323
    7.220E07    16.53747
116.7670   0.486400   2.13055
 40.5675   0.486400   1.44610
116.7670   0.427500   3.41173
```

TABLE 11 continued

```
23    2    3    15    702960.
0.3
  3.500E02  2.655E-2  3.350E-5                    1.290E03  1.600E03
  1.500E00                                        1.290E03  2.420E03
  3.360E02                                        2.100E03
  1.500E00                                        2.100E03
   0.50     0.500    0.500
  6000.
    1.0
    5.943E-2      -4.76597
    7.322E06      12.01307
    1.543E-2      -6.37197
    3.480E07      15.27147
    6.310E-3      -6.99323
    7.220E07      16.53747
116.7670    0.486400    2.13055
 40.5675    0.486400    1.44610
116.7670    0.427500    3.41173

24    2    3    10    204560.
0.2
  3.360E02                                        0.000E00  8.000E02
  1.500E00                                        0.000E00  1.100E03
  3.480E02  4.098E-2  6.696E-6                    6.000E02
  1.500E00                                        6.600E02
   0.50     0.500    0.500
  4100.
    1.0
    5.220E-2      -5.14637
    9.179E06      12.75683
    1.387E-2      -6.44750
    6.153E07      15.44120
    8.161E-2      -4.39137
    6.927E06      11.2131
116.7670    0.486400    2.13055
 40.5675    0.486400    1.44610
116.7670    0.427500    3.41173
```

TABLE 12
Data File for Input Deck 2 (Pony Mountain Branch Watershed)

.411	.346	.312	.303	.217	.201	.201	.170	.160	.160
.486	.473	.401	.383	.383	.356	.344	.341	.341	.329
.428	.420	.419	.404	.400	.378	.378	.376	.373	.373
.428	.420	.419	.404	.400	.378	.378	.376	.373	.373
.428	.428	.395	.335	.331	.326	.320	.307	.302	.296
.411	.346	.312	.303	.217	.201	.201	.170	.160	.160
.486	.473	.401	.383	.383	.356	.344	.341	.341	.329
.428	.420	.419	.404	.400	.378	.378	.376	.373	.373
.428	.420	.419	.404	.400	.378	.378	.376	.373	.373
.428	.428	.395	.335	.331	.326	.320	.307	.302	.296
.411	.346	.312	.303	.217	.201	.201	.170	.160	.160
.486	.473	.401	.383	.383	.356	.344	.341	.341	.329
.428	.420	.419	.404	.400	.378	.378	.376	.373	.373
.428	.420	.419	.404	.400	.378	.378	.376	.373	.373
.428	.428	.395	.335	.331	.326	.320	.307	.302	.296
.411	.346	.312	.303	.217	.201	.201	.170	.160	.160
.498	.473	.401	.383	.383	.356	.341	.341	.303	.303
.490	.490	.439	.404	.400	.378	.378	.376	.373	.373
.490	.428	.395	.335	.331	.326	.320	.307	.302	.296
.490	.428	.395	.335	.331	.326	.320	.307	.302	.296
.411	.346	.312	.303	.217	.201	.201	.170	.160	.160
.498	.473	.401	.383	.383	.356	.341	.341	.303	.303
.490	.490	.439	.404	.400	.378	.378	.376	.373	.373
.490	.428	.395	.335	.331	.326	.320	.307	.302	.296
.490	.428	.395	.335	.331	.326	.320	.307	.302	.296
.411	.346	.312	.303	.217	.201	.201	.170	.160	.160
.498	.473	.401	.383	.383	.356	.341	.341	.303	.303
.490	.490	.439	.404	.400	.378	.378	.376	.373	.373
.490	.428	.395	.335	.331	.326	.320	.307	.302	.296
.490	.428	.395	.335	.331	.326	.320	.307	.302	.296
.411	.346	.312	.303	.217	.201	.201	.170	.160	.160
.498	.473	.401	.383	.383	.356	.341	.341	.303	.303
.490	.490	.439	.404	.400	.378	.378	.376	.373	.373
.490	.428	.395	.335	.331	.326	.320	.307	.302	.296
.490	.428	.395	.335	.331	.326	.320	.307	.302	.296
.411	.346	.312	.303	.217	.201	.201	.170	.160	.160
.498	.473	.401	.383	.383	.356	.341	.341	.303	.303
.490	.490	.439	.404	.400	.378	.378	.376	.373	.373
.490	.428	.395	.335	.331	.326	.320	.307	.302	.296
.490	.428	.395	.335	.331	.326	.320	.307	.302	.296
.411	.346	.312	.303	.217	.201	.201	.170	.160	.160
.498	.473	.401	.383	.383	.356	.341	.341	.303	.303
.490	.490	.439	.404	.400	.378	.378	.376	.373	.373
.490	.428	.395	.335	.331	.326	.320	.307	.302	.296
.490	.428	.395	.335	.331	.326	.320	.307	.302	.296
.411	.346	.312	.303	.217	.201	.201	.170	.160	.160
.498	.473	.401	.383	.383	.356	.341	.341	.303	.303
.490	.490	.439	.404	.400	.378	.378	.376	.373	.373
.490	.428	.395	.335	.331	.326	.320	.307	.302	.296
.490	.428	.395	.335	.331	.326	.320	.307	.302	.296
.411	.346	.312	.303	.217	.201	.201	.170	.160	.160
.498	.473	.401	.383	.383	.356	.341	.341	.303	.303
.490	.490	.439	.404	.400	.378	.378	.376	.373	.373
.490	.428	.395	.335	.331	.326	.320	.307	.302	.296
.490	.428	.395	.335	.331	.326	.320	.307	.302	.296

TABLE 12 continued

.428	.425	.375	.303	.217	.201	.201	.170	.160	.160
.458	.437	.401	.384	.383	.383	.356	.341	.341	.329
.497	.490	.439	.404	.400	.378	.378	.376	.373	.373
.428	.428	.395	.335	.331	.326	.320	.307	.302	.296
.428	.428	.428	.382	.382	.374	.357	.326	.309	.296
.428	.425	.375	.303	.217	.201	.201	.170	.160	.160
.458	.437	.401	.384	.383	.383	.356	.341	.341	.329
.497	.490	.439	.404	.400	.378	.378	.376	.373	.373
.428	.428	.395	.335	.331	.326	.320	.307	.302	.296
.428	.428	.428	.382	.382	.374	.357	.326	.309	.296
.411	.346	.312	.303	.217	.201	.201	.170	.160	.160
.498	.473	.401	.383	.383	.356	.341	.341	.303	.303
.490	.490	.439	.404	.400	.378	.378	.376	.373	.373
.490	.428	.395	.335	.331	.326	.320	.307	.302	.296
.490	.428	.395	.335	.331	.326	.320	.307	.302	.296
.411	.346	.312	.303	.217	.201	.201	.170	.160	.160
.498	.473	.401	.383	.383	.356	.341	.341	.303	.303
.490	.490	.439	.404	.400	.378	.378	.376	.373	.373
.490	.428	.395	.335	.331	.326	.320	.307	.302	.296
.490	.428	.395	.335	.331	.326	.320	.307	.302	.296
.411	.346	.312	.303	.217	.201	.201	.170	.160	.160
.486	.473	.401	.383	.383	.356	.344	.341	.341	.329
.428	.420	.419	.404	.400	.378	.378	.376	.373	.373
.428	.420	.419	.404	.400	.378	.378	.376	.373	.373
.428	.428	.395	.335	.331	.326	.320	.307	.302	.296
.411	.346	.312	.303	.217	.201	.201	.170	.160	.160
.486	.473	.401	.383	.383	.356	.344	.341	.341	.329
.428	.420	.419	.404	.400	.378	.378	.376	.373	.373
.428	.420	.419	.404	.400	.378	.378	.376	.373	.373
.428	.428	.395	.335	.331	.326	.320	.307	.302	.296
.411	.346	.312	.303	.217	.201	.201	.170	.160	.160
.486	.473	.401	.383	.383	.356	.344	.341	.341	.329
.428	.420	.419	.404	.400	.378	.378	.376	.373	.373
.428	.420	.419	.404	.400	.378	.378	.376	.373	.373
.428	.428	.395	.335	.331	.326	.320	.307	.302	.296
.411	.346	.312	.303	.217	.201	.201	.170	.160	.160
.486	.473	.401	.383	.383	.356	.344	.341	.341	.329
.428	.420	.419	.404	.400	.378	.378	.376	.373	.373
.428	.420	.419	.404	.400	.378	.378	.376	.373	.373
.428	.428	.395	.335	.331	.326	.320	.307	.302	.296
.428	.425	.375	.303	.217	.201	.201	.170	.160	.160
.458	.437	.401	.384	.383	.383	.356	.341	.341	.329
.497	.490	.439	.404	.400	.378	.378	.376	.373	.373
.428	.428	.395	.335	.331	.326	.320	.307	.302	.296
.428	.428	.428	.382	.382	.374	.357	.326	.309	.296
.411	.346	.312	.303	.217	.201	.201	.170	.160	.160
.486	.473	.401	.383	.383	.356	.344	.341	.341	.329
.428	.420	.419	.404	.400	.378	.378	.376	.373	.373
.428	.420	.419	.404	.400	.378	.378	.376	.373	.373
.428	.428	.395	.335	.331	.326	.320	.307	.302	.296
.411	.346	.312	.303	.217	.201	.201	.170	.160	.160
.486	.473	.401	.383	.383	.356	.344	.341	.341	.329
.428	.420	.419	.404	.400	.378	.378	.376	.373	.373

.428	.420	.419	.404	.400	.378	.378	.376	.373	.373
.428	.428	.395	.335	.331	.326	.320	.307	.302	.296
.411	.346	.312	.303	.217	.201	.201	.170	.160	.160
.486	.473	.401	.383	.383	.356	.344	.341	.341	.329
.428	.420	.419	.404	.400	.378	.378	.376	.373	.373
.428	.420	.419	.404	.400	.378	.378	.376	.373	.373
.428	.428	.395	.335	.331	.326	.320	.307	.302	.296
.411	.346	.312	.303	.217	.201	.201	.170	.160	.160
.486	.473	.401	.383	.383	.356	.344	.341	.341	.329
.428	.420	.419	.404	.400	.378	.378	.376	.373	.373
.428	.420	.419	.404	.400	.378	.378	.376	.373	.373
.428	.428	.395	.335	.331	.326	.320	.307	.302	.296

APPENDICES

APPENDIX A: COMPUTATIONAL PROCEDURE OF VSAS2

The computational procedure used in VSAS2 is explained with the following simplified example.

Figure A1 is the subsurface flow domain which is divided into nine elements. It is assumed that the channel level is fixed and does not vary with time. The input data required are:

- soil porosity of each element, n(x,z)
- saturated hydraulic conductivity of each element, K_s (x,z)
- unsaturated hydraulic conductivity coefficients (γ and ω)
- moisture release coefficients (α and β)
- correction factor for moisture release curve (c)
- elevation of each element
- location of channel level
- top surface area of top layer (layer 1) elements
- rainfall information

The boundary value problem — equations (2.39), (2.43), and (2.44) — consists of solving for moisture contents one step ahead, say at time $t + \Delta t$, *given the initial moisture contents at time t and the boundary conditions.*

Initial Conditions: Initial moisture contents at time t for all (x,z) are given as

$$\theta(x,z,t) = \theta_i(x,z)$$

Boundary Conditions: All faces of the porous medium except for the top (ground surface) layer and the channel side above the channel level are impermeable. These are indicated by zero flux gradients as shown in Figure A1.

Information is provided on rain falling on the rainfall boundary (ground surface), which is used in computing the rainfall contribution during the time interval Δt.

Purpose: To compute moisture content values one time step ahead

$$\theta(x,z,t + \Delta t) \quad \text{for all} \quad (x,z)$$

Solution Procedure: In VSAS2, the computation of $\theta(x,z,t + \Delta t)$ is carried out in two stages: lateral flow computation and vertical flow computation. Both the computation schemes are carried out within the same Δt. The slopewise flow (lateral) is computed first, starting from the lowermost element of the bottom layer — element (1,3) in Figure A1 — and moving to the left until the left boundary is reached. With regard to Figure A1, for the element (1,3) $\partial\phi/\partial x$ at the boundary is zero because of the boundary condition. The computation begins with the pair [(1,3),(2,3)] and then moves to the pair [(2,3),(3,3)]. Once the left boundary is reached, the computation again starts from the right for the next layer from the channel side and moves to the left boundary. In Figure A1, for the second layer the computation considers the pairs [channel (1,2)], [(1,2),(2,2)] and [(2,2),(3,2)] in that order. For the top surface layer, the computation moves in the same order from the right to the left. However, the rainfall contribution is also accounted for in the computation of initial moisture contents of the top layer. Once the slopewise flow computation reaches the leftmost element of the uppermost layer, the vertical flow computations begin. First the flow between pairs (1,3),(1,2) is computed. The computation then moves to the left with the computation of flow between pairs (2,3),(2,2) and (3,3),(3,2) in that order. For the next row, the solution proceeds by computing the flow between the pairs (1,2),(1,1), (2,2),(2,1) and (3,2),(3,1) in that order. Note that no rainfall contribution to the surface layer elements (1,1), (2,1), and (3,1) are considered during vertical flow computations. This will be clear when the solution procedure is explicitly stated in the steps that follow. The new moisture contents are then obtained by

$$\theta(x,z,t + \Delta t) = \theta(x,z,t) + \frac{\sum_i Q_i \times \Delta t}{\text{Bulk Volume of Element } (x,z)}$$

where Q_i is the flux through face 'i' (see Figure 9). The detailed solution procedure is explained in the following 14 steps. It is again noted that both the lateral sweep (slopewise flow) and the vertical sweep (vertical flow) are carried out within the same time step, Δt.

A. Slopewise Flow

Step 1. Flow between the element pair (1,3),(2,3), Q_1 (see Figure 9).
From here on, flow between element pair (i,j), (k,l) will be denoted by $Q_{(i,j),\,(k,l)}$ for clarity. Since both the elements (1,3) and (2,3) are saturated, the respective pressure heads are given as
$\psi(1,3,t)$ = height of water table above the element (1,3)
$\psi(2,3,t)$ = height of water table above the element (2,3)
therefore, the hydraulic head at time t is given as

$$\phi(x,z,t) = \psi(x,z,t) + z$$

The hydraulic gradient driving the flow between the element pair (1,3), (2,3) is computed as

$$\left[\frac{\partial \phi}{\partial x}\right]^t_{\{(1,3),(2,3)\}} = \frac{\phi^t_{(1,3)} - \phi^t_{(2,3)}}{\Delta x}$$

The discharge through the face between element pair (1,3),(2,3) is computed by using Darcy's law and is given by

$$Q_{\{(1,3),(2,3)\}} = -K^t_{\{(1,3),(2,3)\}}\left[\frac{\partial \phi}{\partial x}\right]^t_{\{(1,3),(2,3)\}}$$

where

$$K^t_{\{(1,3),(2,3)\}} = \frac{\Delta x_{(2,3)} + \Delta x_{(1,3)}}{\dfrac{\Delta x_{(2,3)}}{K^t_{(2,3)}} + \dfrac{\Delta x_{(1,3)}}{K^t_{(1,3)}}}$$

$$K^t_{(x,z)} = \gamma\left[\theta^t_{(x,z)}\right]^{\omega}$$

γ and ω are parameters

Step 2. Slopewise flow between the element pair (2,3),(3,3):
This is computed in the same manner as explained in step 1. The result of this step is the flux through the element pair (2,3),(3,3) denoted as $Q_{(2,3),(3,3)}$.

Step 3. Slopewise flow between the element (1,2) and the channel:
The flow through the interface of the element (1,2) and the channel boundary is computed. Since the element (1,2) is unsaturated, ψ and K are computed from the $\psi - \theta$ and $K - \theta$ relationships. Initial moisture content of the element (1,2), denoted as $\theta(1,2,t)$, is known from the initial conditions. For this known value of $\theta(1,2,t)$, $\psi(\theta)$ and $K(\theta)$ values are computed by equations (3.2) and (3.3), respectively. The hydraulic head, $\phi(1,2,t)$ is computed from

$$\phi(1,2,t) = \psi(1,2,t) + z(1,2)$$

Let BLDROP be the difference in the elevations of the center points of the left and the right boundaries of the element (1,2) (see Figure A2). Then the difference in hydraulic head between the element (1,2) and the channel boundary is taken as one-half of BLDROP plus the pressure head, $\psi(1,2,t)$, if the channel water level is below the center point of the element at the right boundary. Thus found, hydraulic

head difference is used in Darcy's equation to compute the flow from the element (1,2) towards the channel. If the channel level is above the center point then by the boundary condition, flow below the channel water level is zero. Thus the flux through the element (1,2) and the channel, $Q_{[(1,2),\ channel]}$, is computed.

Step 4. Slopewise flow between the element pair (1,2),(2,2):
Both the elements (1,2) and (2,2) are unsaturated.

Therefore,

$$\theta(1,2,t) < n(1,2)$$

and

$$\theta(2,2,t) < n(2,2)$$

Therefore, using equations (3.2) and (3.3), $\psi(1,2,t)$, $\psi(2,2,t)$, K(1,2,t), and K(2,2,t) are computed. The discharge through the face between the element pair (1,2),(2,2) is computed by using Darcy's law. The final result of this step is $Q_{(1,2),(2,2)}$.

Step 5. Slopewise flow between the element pair (2,2),(3,2):
The elements (2,2) and (3,2) are unsaturated and therefore based on water contents $\theta(2,2,t)$ and $\theta(3,2,t)$, the pressure heads $\psi(2,2,t)$, $\psi(3,2,t)$, and the hydraulic conductivities K(2,2,t), and K(3,2,t) are computed. The discharge through the face between the element pair (2,2),(3,2) is then computed using Darcy's law. The final result of this step is $Q_{(2,2),(3,2)}$.

B. Rainfall Boundary Elements

The computation of moisture content for the surface elements should incorporate the rainfall contribution. A detailed description of the procedure is given in the following steps.

Step 6. Slopewise flow between the element (1,1) and the channel:
Let $RC_{(1,1)}$ be the rainfall volume entering the element (1,1) during the period Δt.

Then,

$$RC_{(1,1)} = \text{Net precipitation X Top surface area of the element (1,1)}$$

where:

$$\text{Net precipitation} = (\text{Rainfall rate X } \Delta t) - \text{Interception}$$

Interception is taken as 0.05 inch for the dormant season (November through April) and 0.10 inch for the growing season (May through October).

Volume of water contained in the element (1,1) at time t,

$$V_{(1,1)}^{t} = \theta_{(1,1)}^{t} \text{ X Bulk Volume of the element (1,1)}$$

Therefore, the revised total volume of water contained in (1,1) is $[V_{(1,1)}^{t} + RC_{(1,1)}]$. Therefore, the revised moisture content of the element (1,1) is computed as

$$\theta_{(1,1)}^{Rev} = \frac{V_{(1,1)}^{t} + RC_{(1,1)}}{\text{Bulk Volume of the element (1,1)}}$$

The moisture content of the element (1,1), for further calculations is computed as the average of the initial moisture content, $\theta_{(1,1)}^{t}$, and the revised moisture content, $\theta_{(1,1)}^{Rev}$, which is

$$\theta_{(1,1)}^{R1} = \frac{\theta_{(1,1)}^{t} + \theta_{(1,1)}^{Rev}}{2}$$

This moisture content is used as the initial moisture content of the element (1,1) for both the slopewise flow and the vertical flow computations within the time interval Δt. Note that $\theta_{(1,1)}^{R1}$ computed above may exceed the porosity of the element, n(1,1) which results in the following two cases:

Case 1: $\theta_{(1,1)}^{R1} < n(1,1)$

In this case, the moisture content of the element (1,1) is less than its porosity. The flux through the element (1,1) to the channel is computed using the procedure for the element-channel interface in step 3.

Case 2: $\theta_{(1,1)}^{R1} \geq n(1,1)$

When the moisture content of the element (1,1) exceeds its porosity, the excess volume of water for the element (1,1) is computed as

$$V_{(1,1)}^{excess} = \left[\theta_{(1,1)}^{R1} - n(1,1)\right] \times V(1,1)$$

where: $V_{(1,1)}^{excess}$ is the excess volume of water in the element (1,1) accounted for by its porosity; and V(1,1) is the bulk volume of the element (1,1). This excess volume of water is used in conjunction with the volume of water in the element (1,1), at the end of both the slopewise and the vertical flow components, to compute the revised volume of water in the element (1,1) at time $t + \Delta t$ which is explained in detail in step 14. Volume of water so obtained is divided by V(1,1) to obtain $\theta(1,1,t + \Delta t)$. The procedure is described below.

When $\theta_{(1,1)}^{R1} > n(1,1)$ set

$$\theta_{(1,1)}^{R1} = n(1,1)$$

For this moisture content, the pressure head ψ is taken to be zero based on the ψ-θ relationship and the fact that it is the surface element. Therefore, following the procedure of step 3, the flow through the element-channel interface is computed. The final result of this step is $Q_{(1,1),channel}$.

It should be remembered that, at the end of the slopewise flow computation between the element (1,1) and the channel, $V_{(1,1)}^{excess}$ computed above still remains the same and will be dealt with later.

Step 7. Slopewise flow between the element pair (1,1),(2,1):

Rainfall contribution to the element (2,1) is computed in the same manner as used for the element (1,1) in step 6. As in the previous step, the moisture content so computed may or may not exceed the porosity of the element, n(2,1).

Case 1: $\theta_{(2,1)}^{R1} < n(2,1)$.

In this case, the hydraulic head for the element (2,1) is computed using the moisture content $\theta_{(2,1)}^{R1}$, described in step 6. The hydraulic gradient and the flux through the element pair (1,1),(2,1) are then computed using the procedure similar to those described in step 4. The final result of this step is $Q_{(1,1),(2,1)}$

Case 2: $\theta_{(2,1)}^{R1} \geq n(2,1)$

In this case, the excess volume of water, $V_{(2,1)}^{excess}$, is computed by using the procedure described in step 6, case 2; set

$$\theta_{(2,1)}^{R1} = n(2,1)$$

Following the procedure of case 2 of step 6, the pressure head ψ and the hydraulic conductivity K are computed for the saturated condition ($\theta = n$). Then, the hydraulic gradient between the elements (1,1) and (2,1) are computed as in step 3. This is used in Darcy's equation to compute the flux through the face of the element pair (1,1),(2,1). The final result of this step is $Q_{(1,1),(2,1)}$.

Step 8: Slopewise flow between the element pair (2,1),(3,1):

The procedure described in step 7 is used for both cases: (1) $\theta_{(3,1)}^{R1} < n(3,1)$, and (2) $\theta_{(3,1)}^{R1} \geq n(3,1)$. The excess volume of water that cannot be held by the element (3,1) is denoted as $V_{(3,1)}^{excess}$. The final result of this step is $Q_{(2,1),(3,1)}$.

C. Vertical Flow

Vertical flows are next computed starting from the lowermost layer on the channel side, proceeding up the slope, and then up the layers. With regard to Figure A1, first the element pair (1,3),(1,2) is considered. This is followed by the pairs (2,3),(2,2), (3,3),(3,2), (1,2),(1,1), (2,2),(2,1), and (3,2),(3,1) in that order. These are described below. It is noted that pressure heads and hydraulic conductivities are once again based on $\theta(x,z,t)$ values.

Step 9. Vertical flow between the element pair (1,3),(1,2):
Based on $\theta(x,z,t)$ for elements (1,3) and (1,2), the hydraulic gradient is computed as

$$\left[\frac{\partial \phi}{\partial z}\right]^t_{\{(1,3),(1,2)\}} = \frac{\phi^t_{(1,2)} - \phi^t_{(1,3)}}{\Delta z}$$

and the discharge is given as

$$Q_{\{(1,3),(1,2)\}} = -K^t_{\{(1,3),(1,2)\}} \times \left[\frac{\partial \phi}{\partial z}\right]^t_{\{(1,3),(1,2)\}}$$

Step 10. Vertical flow between the element pair (2,3),(2,2):
The procedure of step 9 is used to compute the hydraulic gradient between the elements (2,2) and (2,3). This is used in Darcy's equation to compute $Q_{(2,3),(2,2)}$, the vertical flow between the element pair (2,3),(2,2).

Step 11. Vertical flow between the element pair (3,3),(3,2):
Step 9 is repeated to compute $Q_{(3,3),(3,2)}$, the flow through the face of the element pair (3,3),(3,2).

Step 12. Vertical flow between the element pair (1,2),(1,1):
This vertical flow is computed based on $\theta_{(1,1)}{}^{R1}$ for element (1,1) (see step 6) and $\theta_{(1,2)}{}^{t}$ (from initial conditions) for element (1,2).

Step 13. Vertical flow between the element pairs (2,2),(2,1) and (3,2),(3,1):
The procedure of step 12 is used to obtain $Q_{(2,2),(2,1)}$ and $Q_{(3,2),(3,1)}$.
Based on steps 1-13, the fluxes through all faces of each of the 9 elements are known. The moisture contents are now revised using the continuity equation for each element. For example, for the central element (2,2) in Figure A1, $Q_{(2,3),(2,2)}$, $Q_{(1,2),(2,2)}$, $Q_{(2,2),(3,2)}$, $Q_{(2,2),(2,1)}$ are known. The initial moisture content of the element (2,2), denoted by $\theta(2,2,t)$, is also known. Therefore, the revised moisture content of the element (2,2), denoted by $\theta_{(2,2)}{}^{R2}$, is obtained as

$$\theta^{R2}_{(2,2)} = \theta(2,2,t) + \left[\frac{\pm Q_{\{(2,3),(2,2)\}} \pm Q_{\{(1,2),(2,2)\}} \pm Q_{\{(2,2),(3,2)\}} \pm Q_{\{(2,2),(2,1)\}}}{V(2,2)}\right] \times \Delta t \qquad (A.1)$$

The sign of fluxes is determined based on whether the flow is into or out of the element (2,2). If the flow is towards the element (2,2), a positive sign is chosen. Or the minus sign is selected for the computation of $\theta_{(2,2)}^{R2}$. The moisture content so obtained, $\theta_{(2,2)}^{R2}$, is once again revised adding the moisture contribution from the adjoining upstream and downstream elements, if any. This is carried out as follows.

The moisture content of the element (1,2) at the end of step 13, $\theta_{(1,2)}^{R2}$, is compared with its porosity, n(1,2). If $\theta_{(1,2)}^{R2} > n(1,2)$, set

$$\theta_{(1,2)}^{R3} = n(1,2)$$

where: $\theta_{(1,2)}^{R3}$ is the newly revised moisture content of the element (1,2). The excess volume of water that cannot be held by the element (1,2), denoted by $V_{(1,2)}^{excess}$, is computed as

$$V_{(1,2)}^{excess} = \left[\theta_{(1,2)}^{R2} - n(1,2)\right] \times V(1,2)$$

where:V(1,2) is the bulk volume of the element (1,2). It is noted that $V_{(1,2)}^{excess}$ is zero and $\theta_{(1,2)}^{R3} = \theta_{(1,2)}^{R2}$ when $\theta_{(1,2)}^{R2} \leq n(1,2)$. The excess volume of water, $V_{(1,2)}^{excess}$, so computed is used to revise $\theta_{(2,2)}^{R2}$ computed in step 13. The newly revised moisture content of the element (2,2), $\theta_{(2,2)}^{R3}$, is computed as

$$\theta_{(2,2)}^{R3} = \theta_{(2,2)}^{R2} + \frac{V_{(1,2)}^{excess}}{V(2,2)}$$

A comparison is made between $\theta_{(2,2)}^{R3}$ so obtained and n(2,2). If $\theta_{(2,2)}^{R3} > n(2,2)$, set

$$\theta_{(2,2)}^{R4} = n(2,2)$$

where: $\theta_{(2,2)}^{R4}$ is the further revised moisture content of the element (2,2). The excess volume of water that cannot be held by the element (2,2) is computed as

$$V_{(2,2)}^{excess} = \left[\theta_{(2,2)}^{R3} - n(2,2)\right] \times V(2,2)$$

For cases when $\theta_{(2,2)}^{R3} \leq n(2,2)$, $V_{(2,2)}^{excess}$ is zero and $\theta_{(2,2)}^{R4} = \theta_{(2,2)}^{R3.}$ The excess volume so computed is once again used to revise $\theta_{(3,2)}^{R2}$ (from step 13) as

$$\theta_{(3,2)}^{R3} = \theta_{(3,2)}^{R2} + \frac{V_{(2,2)}^{excess}}{V(3,2)}$$

Here again, two cases are possible. For the case when $\theta_{(3,2)}^{R3} \leq n(3,2)$,

$$\theta(3,2,t+\Delta t) = \theta_{(3,2)}^{R3}$$

If $\theta_{(3,2)}^{R3} > n(3,2)$, set

$$\theta(3,2,t+\Delta t) = n(3,2)$$

The excess volume of water that cannot be held by the element (3,2), denoted as $V_{(3,2)}^{excess}$, is given as

$$V_{(3,2)}^{excess} = \left[\theta_{(3,2)}^{R3} - n(3,2)\right] \times V(3,2)$$

This $V_{(3,2)}^{excess}$ is used along with $\theta_{(2,2)}^{R4}$ to compute $\theta_{(2,2)}^{R5}$, further revised moisture content of the element (2,2), as

$$\theta_{(2,2)}^{R5} = \theta_{(2,2)}^{R4} + \frac{V_{(3,2)}^{excess}}{V(2,2)}$$

If $\theta_{(2,2)}^{R5} \leq n(2,2)$ then

$$\theta(2,2,t+\Delta t) = \theta_{(2,2)}^{R5}$$

If, on the other hand, $\theta_{(2,2)}^{R5} > n(2,2)$, set

$$\theta(2,2,t+\Delta t) = n(2,2)$$

and the revised excess volume of water in the element (2,2), $V_{(2,2)}^{excess1}$ is obtained as

$$V_{(2,2)}^{excess1} = \left[\theta_{(2,2)}^{R5} - n(2,2)\right] \times V(2,2)$$

This excess volume of water is used along with $\theta_{(1,2)}^{R3}$ to update the moisture content of the element (1,2). A similar procedure described above is used to obtain $\theta(1,2,t+\Delta t)$ and $V_{(1,2)}^{excess1}$, if any. The excess volume of water from the element (1,2), if any, at the end of the computations above is directly added to the channel as the lateral flow contribution from the middle layer. A similar procedure is followed for the bottom layer. However, it is noted that the flow to the channel from the element (1,3) is zero because of the impermeable boundary condition. Therefore, when the revised moisture content of the element (1,3), $\theta_{(1,3)}^{R5}$, is greater than n(1,3), the excess volume of water from this element is utilized in revising the moisture content of the element (1,2) obtained from step 13 as

$$\theta_{(1,2)}^{R2} = \left[\theta_{(1,2)}^{R2}\right]_{\text{from step 13}} + \left[\theta_{(1,3)}^{R5} - n(1,3)\right] \times \frac{V(1,3)}{V(1,2)} \qquad \text{(A2)}$$

For element (1,2), the revised value of the moisture content, instead of the moisture content computed in step 13, equation (A1), is used in all computations.

Thus the moisture content of all the elements, except the elements on the surface layer, are determined at the time $t + \Delta t$.

D. Overland Flow

Step 14. The revised moisture contents of elements (1,1), (2,1) and (3,1) (see step 13) are used along with $V_{(1,1)}^{excess}$, $V_{(2,1)}^{excess}$, and $V_{(3,1)}^{excess}$ (see steps 6, 7, and 8) to compute the overland flow component. The following procedure is used.

Let $\theta_{(1,1)}^{R2}$ be the revised moisture content of the element (1,1) at the end of step 13 —equation (A1). This moisture content is revised to $\theta_{(1,1)}^{R3}$ by adding the contribution of $V_{(1,1)}^{excess}$ (see step 6) as

$$\theta_{(1,1)}^{R3} = \theta_{(1,1)}^{R2} + \frac{V_{(1,1)}^{excess}}{V(1,1)}$$

It is noted that $V_{(1,1)}^{excess}$ is zero if case 1 of step 6 is true. If $\theta_{(1,1)}^{R3}$ so obtained is greater than n(1,1), set

$$\theta_{(1,1)}^{R4} = n(1,1)$$

where: $\theta_{(1,1)}^{R4}$ is the newly revised moisture content of the element (1,1).

The revised excess volume of water, $V_{(1,1)}^{excess1}$, that cannot be held by the element (1,1) is computed as

$$V_{(1,1)}^{excess1} = \left[\theta_{(1,1)}^{R3} - n(1,1)\right] \times V(1,1)$$

This excess volume is zero if $\theta_{(1,1)}^{R3}$ is less than n(1,1). In such cases

$$\theta_{(1,1)}^{R4} = \theta_{(1,1)}^{R3}$$

Any excess volume of water from the element (1,1), denoted as $V_{(1,1)}^{excess1}$, is used to revise the moisture content of the upstream element (2,1) as

$$\theta_{(2,1)}^{R3} = \theta_{(2,1)}^{R2} + \frac{V_{(2,1)}^{excess}}{V(2,1)} + \frac{V_{(1,1)}^{excess1}}{V(2,1)}$$

where: $\theta_{(2,1)}^{R2}$ is the moisture content of the element (2,1) at the end of step 13 —equation (A1) — and $V_{(2,1)}^{excess}$ is the excess volume of water in the element (2,1) computed in step 7. It is noted that $V_{(2,1)}^{excess}$ is zero for case 1 of step 7.

Here again, $\theta_{(2,1)}^{R4}$ and $V_{(2,1)}^{excess1}$ are computed as described earlier. If $\theta_{(2,1)}^{R3}$ is less than n(2,1), then

$$\theta_{(2,1)}^{R4} = \theta_{(2,1)}^{R3}$$

and

$$V_{(2,1)}^{excess1} = 0$$

In cases when $\theta_{(2,1)}{}^{R3}$ is greater than n(2,1), set

$$\theta_{(2,1)}^{R4} = n(2,1)$$

and the revised excess volume of water in the element (2,1), $V_{(2,1)}{}^{excess1}$, is computed as

$$V_{(2,1)}^{excess1} = \left[\theta_{(2,1)}^{R3} - n(2,1)\right] \times V(2,1)$$

The moisture content of the element (3,1), $\theta_{(3,1)}{}^{R2}$ (from step 13, equation A1), is also revised to $\theta_{(3,1)}{}^{R3}$ using $V_{(3,1)}{}^{excess}$ and $V_{(2,1)}{}^{excess1}$. Any excess volume of water in the element (3,1), $V_{(3,1)}{}^{excess1}$, is computed and $\theta_{(3,1)}{}^{R4}$ is obtained by comparing it with n(3,1) and following the steps used for the element (2,1). The final moisture content of the element (3,1) so obtained, $\theta_{(3,1)}{}^{R4}$, is the required moisture content at the time $\theta(3,1,t + \Delta t)$. The revised excess volume of water in the element (3,1), $V_{(3,1)}{}^{excess1}$, is used to further revise $\theta_{(2,1)}{}^{R4}$ to $\theta_{(2,1)}{}^{R5}$ as

$$\theta_{(2,1)}^{R5} = \theta_{(2,1)}^{R4} + \frac{V_{(3,1)}^{excess1}}{V(2,1)}$$

It is noted that $V_{(3,1)}{}^{excess1}$ is zero if $\theta_{(3,1)}{}^{R3}$ is less than n(3,1). If $\theta_{(2,1)}{}^{R5}$ is less than n(2,1), then

$$\theta(2,1,t + \Delta t) = \theta_{(2,1)}^{R5}$$

and

$$V_{(2,1)}^{excess2} = 0$$

where: $\theta(2,1,t + \Delta t)$ is the moisture content of the element (2,1) at the time $t + \Delta t$, and $V_{(2,1)}{}^{excess2}$ is the further revised volume of water that cannot be held by the element (2,1). In case $\theta_{(2,1)}{}^{R5}$ is greater than n(2,1), then

$$\theta(2,1,t + \Delta t) = n(2,1)$$

and

$$V_{(2,1)}^{excess2} = \left[\theta_{(2,1)}^{R5} - n(2,1)\right] \times V(2,1)$$

This excess volume of water is used to further revise the moisture content of the element (1,1), which is denoted as $\theta_{(1,1)}^{R5}$. Depending on whether $\theta_{(1,1)}^{R5}$ is greater than or less than n(1,1), $\theta(1,1,t + \Delta t)$ and$V_{(1,1)}^{excess2}$ are computed as described above. Any excess volume of water so obtained, $V_{(1,1)}^{excess2}$, is added to the channel flow as the overland flow component. Thus, $\theta(x,z,t + \Delta t)$ for all (x,z) are determined.

FIGURE A1
Sample Problem

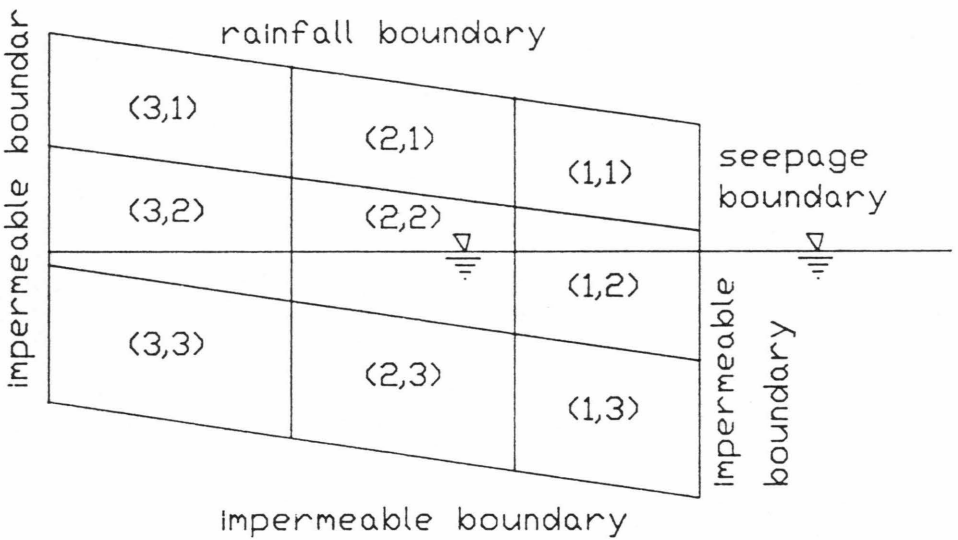

FIGURE A2
Discretization of Porous Medium

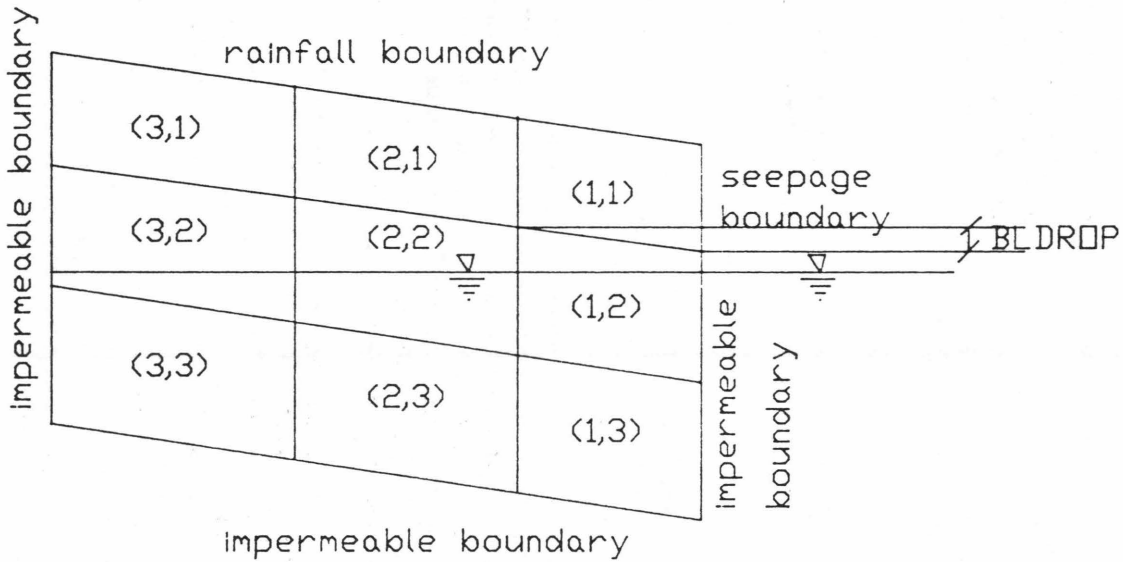

APPENDIX B: USERS' MANUAL

This is the users' manual for the model used in this report. The model requires two input data files: The first input deck contains data on the segmentation of watershed, precipitation data, and data for each segment (cards V-XIX); the second contains the initial moisture content values for all elements for each segment. Worksheets, one for each input data file, are shown in Figures B1 and B2. A step-by-step procedure on the preparation of these input decks are presented in the following paragraphs. These are described for a sample problem shown in Figure B3 whose salient features are outlined in Figure B4 and Table B1. Input files are shown in Tables B2 and B3.

I. Preparation of Input Deck 1

Card I contains the number of segments and the name of the watershed. The sample problem consists of one segment, the name of the watershed being 'Test Basin.'

Card II may contain any general remark concerning the problem or may be left blank.

Card III specifies the starting date of simulation in the order of year, month, and day. The starting hour is always 1 a.m. In the sample problem, the simulation is performed for August 8, 1988 (Table B2).

Card IV is used for rainfall information. Rainfall is provided in inches at hourly intervals. Eight rainfall data are provided in one card thereby requiring three cards per day. Blank fields indicate periods without rain whereas any value greater than or equal to 9 indicates the end of the precipitation deck. If simulation is to be performed for rainfall intensities exceeding 9 inches per hour, appropriate modifications should be made in the subroutine READ of the source code. For the sample problem, the rainfall begins on August 8, 1988 at 4 a.m. and lasts for an hour. The simulation is performed for eight hours.

Card V is the beginning of the segment description. It consists of 5 different items.

Item 1 — identifies the segment number for which simulation is to be performed.

Item 2 — tells the model the number of line pairs used to describe the segment. At least two pairs are required. Each pair describes a ridge-to-stream boundary. Internal line pairs may be added, if necessary. Here three line pairs are used to describe the segment (Table B2).

Item 3 — indicates the number of soil layers used to describe the soil profile. Usually 3 to 5 layers are used. The example problem uses 5 soil layers.

Item 4 — is the time of travel, in minutes, for a water particle generated by the segment to reach the watershed outlet. For the sample problem, this time is taken as 5 minutes.

Item 5 — the last item on this card is the area of the segment in square feet. Here, the area is 60,000 sq. ft.

Card VI provides the difference in elevation between the top of the bank and the channel level, in feet. This value is 4.5 feet for the sample problem.

Card VII — along with cards VIII, IX and X — is used to determine the segment geometry. Two lines are required to describe each layer. This card is used to describe the surface

configuration of the first line pair (pair 1 in the sample problem). This card consists of 3 different items.

Item 1 — the coefficients of the polynomial are fitted to the surface configuration of the line pair 1 (A_1, B_1, C_1, D_1, and E_1 of Figure 12). These are obtained by using the known elevations and distances from the stream as explained in chapter 3. For the sample problem, $A_1 = 6.600 \times 10^{2}$, $B_1 = 2.188 \times 10^{-1}$, $C_1 = -5.402 \times 10^{-4}$, $D_1 = 1.403 \times 10^{-6}$, and $E_1 = -1.690 \times 10^{-9}$ in the general equation

$$Z_1 = A_1 + B_1X + C_1X^2 + D_1X^3 + E_1X^4$$

in which X is the distance from the stream and Z_1 is the surface elevation (Figure 12).

Item 2 — the horizontal stream to ridge length (D in Figure 13) of the line pair 1 are expressed in feet. The horizontal stream to ridge length is 400 feet.

Item 3 — the distance in feet between two adjacent line pairs at the stream side is indicated here. For the sample problem, the distance between line pairs 1 and 2 at the stream side is 95 feet.

Card VIII is used to describe the depth configuration of the first line pair. This card also has 3 items.

Item 1 — the coefficients of the polynomial are fitted to the depth configuration of line pair 1. In the sample problem, the depth of the mantle is 10 feet throughout the length of the line pair, i.e. $A_2 = 10.0$, $B_2 = C_2 = D_2 = E_2 = 0.0$ in the general equation

$$Z_2 = A_2 + B_2X + C_2X^2 + D_2X^3 + E_2X^4$$

in which X is the distance from the stream and Z_2 is the depth of the soil mantle (Figure 12).

Item 2 — the horizontal stream to ridge length, in feet, is denoted here. For the sample problem, this has a value of 400 feet.

Item 3 — denotes the distance between two adjacent line pairs at the ridge side of the segment. For the sample problem, the distance between line pairs 1 and 2 at the ridge side is 100 feet.

Card IX repeats Cards VII and VIII, in that order, for the line pairs 2, 3, ... until all the line pairs in the segment are covered.

Card X provides information on soil mantle. The first item is the thickness of the top layer in feet. The remaining items are the thicknesses of other layers which are expressed as the fraction of the depth of the soil mantle minus the thickness of the top layer. The sample problem consists of five layers with 0.75 feet the thickness of the top layer. The second, third, fourth, and bottom layers are 1.25 ft., 2.0 ft., 3.0 ft., and 3.0 ft. thick, respectively. The second layer thickness of 1.25 ft. is a fraction of 9.25 ft. (which is the thickness of the soil mantle after subtracting the top layer thickness, i.e. 10.0-0.75 ft.) is 0.135 which is entered in card X. The other fractions are obtained similarly and are shown in card X.

Card XI provides data for channel and impervious area precipitation. The first item is the top

surface area of the stream in square feet. This is used to compute channel precipitation. The second item is the impervious surface area, if any. These are the impervious surface areas linked to the channel from which surface flow can be generated.

Card XII indicates the positions along the slopes of the zones of changing soil hydrological properties. In each layer, soil hydrological properties are allowed to change with respect to the distance from the channel. A maximum of 3 zones can be used. The upper boundary of each zone as a fraction of the total slope length is indicated here. A value of 1.0 in the first field indicates that only one type of soil exists. In the sample problem, three types of soils exist. The hydrological properties change at 20 percent and 80 percent of the total slope length (Table B2).

Card XIII contains the parameters of the pressure head-moisture content function for zone 1 of layer 1. The first item is the parameter α and the second item is the parameter β of the $\psi - \theta$ function. For the sample problem, these parameters are 4.608×10^{-3} and -8.05885, respectively. These are used in the function XMATRX to compute $\psi(\theta)$ for a known value of θ.

Card XIV indicates the parameters γ and ω for zone 1 of layer 1. These are used in the function CON along with the respective saturated hydraulic conductivity values to compute $K(\theta)$ for a known value of θ. For the sample problem, $\gamma = 2.921 \times 10^{7}$ and $\omega = 18.81997$.

Card XV repeats Cards XIII and XIV for all the five layers of zone 1.

Card XVI repeats cards XIII through XV for all three zones (for card XII). This card is not required if only one zone describes the segment.

Card XVII consists of 3 fields.

Item 1 — saturated hydraulic conductivity of soil on the top layer of zone 1, in cm per hour, is provided here. For the sample problem, this value is 51.5475 cm/hr.

Item 2 — the porosity of the top layer of zone 1. The sample problem has porosity equal to 0.4585.

Item 3 — correction factor, c, for the $\psi - \theta$ function for the top layer of zone 1. This value is 2.47038 for the example problem.

Card XVIII repeats Card XVII for all the layers of zone 1.

Card XIX repeats Cards XVII and XVIII for all the zones. This card is not required if the segment consists of only one zone.

Card XX begins the input deck for a new segment (same as Card V). Cards V through XIX are repeated for all the segments. It is NOT used in the sample problem because there is only one segment.

Card XXI marks the end of input deck 1. This is indicated by a number greater than 99 on this card.

II. Preparation of Input Deck 2

These cards provide the initial moisture contents of all the elements in the subsurface domain which are necessary to solve the boundary value problem. For the purpose of preparation of input deck 2, the segment is divided into 10 increments (from stream to ridge). The length of the first increment, d_1, is obtained by using the relationship

$$d_1 = 0.01D \tag{B1}$$

where: D is the total horizontal length of the segment slope.

The horizontal length of the nth increment is then computed by

$$d_n - d_{(n-1)} = 0.01D\left[n^2 - (n-1)^2\right] \tag{B2}$$

Equation (B2) is used to compute horizontal lengths d_2 through d_{10}. It is noted that the stream to ridge length is divided into 10 increments strictly for the preparation of input deck 2. Depending on surface saturation conditions, these increments are further subdivided internally by the subroutine RECOM (note that there are 12 increments per layer in the output file of the sample problem, Table B4, even though input data were provided for only 10 increments per layer, Table B3) The increments so obtained along with the depth of each layer define all the elements in the subsurface domain. The initial moisture contents for the 50 elements resulting from 10 increments per layer for five layers are provided through this input deck. The first number of line 1 in Table B3 represents the initial moisture content of the element (1,1) (see Figure 13 for explanation of the element (i,j)), the second number is the initial moisture content of the element (1,2), ..., the last number is the initial moisture content of the element (1,10). Similarly, the second card represents the elements on the second layer. Five cards are provided per segment. Five cards are required even if less than five layers are used to describe the segment. The initial moisture contents need be provided for only the layers describing the segments. The remaining cards are left blank. This is repeated for all segments. Figure B2 is the worksheet for this input deck.

III. Output Interpretation

Using this information, the model generates the outflow hydrograph at the watershed outlet (see Table B4). It also prints the time history of saturated areas, which aids in delineating the expansion and contraction of various parts of the basin. Saturated widths of various segments at different times can be plotted to visualize the source area dynamics. Detailed description of the model output for the sample problem is provided below.

The watershed consists of 1 segment. Simulation is performed for a 1.50 in./hr rainfall, beginning at 4 a.m. on August 8, 1988, and lasting for an hour. Duration of simulation is eight hours. A complete input data set (Tables B2 and B3) is included along with the output (Table B4).

The first four lines of the output identify the basin, total number of segments in the watershed

and the date of the rainfall event. The fifth line indicates that the simulation results are for segment 1. Following this are the elevations of soil elements, slopes of each element, depths of each element, slope lengths of each element. Elevation of soil elements are the centroidal elevations. These are internally computed in the subroutine BLKVOL based on the line pair equations, depths of layers, stream to ridge lengths and distances between line pairs. These are indicated for all the layers. Widths of increments are printed next. Note the presence of 12 increments in Table B4 even though input data were provided only for 10 increments (Table B3). This is due to the rearrangement of increments in the subroutine RECOM (this is done internally within the computer program). The centroidal elevations, slopes, depths and widths of elements were then computed, based on the updated increments, by the subroutine BLKVOL and are printed in lines 8 through 36.

Headings are printed from lines 37 through 39. Overland flow and the flow from the top layer headings are printed next. Lines 42 through 45 are the overland and subsurface flow from the top layer. Line 46 prints the simulation time, net precipitation, and the flow details. The first column represents the simulation time, the second column is the net precipitation which is computed as the total precipitation minus abstractions, if any. The third column indicates the channel precipitation and the flow from impervious areas. The next five columns are the subsurface flow components from the five soil layers. The ninth column is the sum of the surface and the subsurface flow components expressed as cubic feet per hour. The last column is the total flow in cubic feet per hour per square mile.

Line 72 is the heading indicating that the moisture contents at the end of six hours of simulation is printed next. Note that updated moisture contents are printed at six hour intervals. The program can be modified to print these moisture contents at desired intervals. The necessary modifications should be made in the SUBROUTINE OUTA of the source code. By observing the moisture content profile and noting the porosity of each element, saturated elements can be detected. This aids in determining the trend of saturated area expansion and contraction.

The process continues for a prespecified simulation period. At the end of the simulation period the outflow hydrograph, at the outlet of the watershed, is printed. These are lines 89 through 98 in the output. I's appearing in lines 93 through 97 are the base flow separation for the outflow hydrograph. The last five lines of the output indicate the total stormflow volume, total rainfall volume, and the response of the watershed. The remaining rainfall volume has gone into increasing the moisture contents of the elements of the segment. If simulation is performed for a sufficiently long duration, all the rainfall is expected to flow out of the watershed as stormflow.

FIGURE B1
Worksheet for Input Deck 1

Card number					
I	Number of segments	Name of the watershed			
	I3	15A4			
II	Remarks (may be left blank)				
	18A4				
III	Starting date of simulation (year, month, day)				
	3I2				
IV	Hourly Precipitation in inches (8 per card)				
	8F4.2				
	1	2	3	4	5
V	Segment number	Number of line pairs	Number of soil layers	Time of travel (min.)	Segment Area (sft.)
	I2	I4	I4	I5	F10.0
VI	Difference in elevation between top of the bank and the channel level (ft.)				
	F5.3				
	1	2	3		
VII	Coefficients of the polynomials fitted to the surface configuration of the first line pair	Stream to ridge length (ft.)	Distance between line pairs 1 and 2 at the the stream side (ft.)		
	5E10.4	E10.4	E10.4		
	1	2	3		
VIII	Coefficients of the polynomials fitted to the depth configuration of the first line pair	Stream to ridge length (ft.)	Distance between line pairs 1 and 2 at the the ridge side (ft.)		
	5E10.4	E10.4	E10.4		
IX	Repeat cards VII and VIII in that order for all line pairs				
X	Thickness of layer 1 (ft.)	Thickness of other layers as a fraction of the mantle depth minus the thickness of top layer			
	F8.4	4F8.4			

FIGURE B1 continued

Card number			
XI	Stream area (sft.) F9.1	Impervious surface area (sft.) F9.1	
XII	Positions along the slopes of zones of changing soil hydrological properties (maximum of 3 zones) 3F7.3		
XIII	Parameter α of the $\psi - \theta$ function for zone 1 of layer 1 E12.6	Parameter β of the $\psi - \theta$ function for zone 1 of layer 1 F12.6	
XIV	Parameter γ of the $K - \theta$ function for zone 1 of layer 1 E12.6	Parameter ω of the $K - \theta$ function for zone 1 of layer 1 F12.6	
XV	Repeat cards XIII and XIV for all the layers of zone 1		
XVI	Repeat cards XIII through XV for all the zones (not required if the first item in card XII is 1.0)		
	1	2	3
XVII	Saturated hydraulic conductivity of the top layer of zone 1 (cm/hr) F10.4	Soil porosity of layer 1 of zone 1 F10.4	Correction factor for moisture release curve (zone 1, layer 1) F10.4
XVIII	Card XVII is repeated for all layers of zone 1		
XIX	Cards XVII and XVIII are repeated for all zones (not required if the first item of card XII is 1.0)		
XX	Beginning of input for segment number 2 (repeat cards V through XIX for all segments)		
XXI	End of input deck 1 (indicated by a number greater than 99)		

FIGURE B2
Worksheet for Input Deck 2

Card number		
I	Initial moisture contents for the elements in the top layer of segment 1 {first number is for the element (1,1), the second for the element (1,2), ..., the tenth number is for the element (1,10)} (10 numbers per card)	10F6.3
II	Initial moisture contents for the second layer of segment I as in card I	10F6.3
III	Initial moisture contents for the third layer of segment I as in card I	10F6.3
IV	Initial moisture contents for the fourth layer of segment I as in card I	10F6.3
V	Initial moisture contents for the bottom layer of segment I as in card I	10F6.3
VI	Beginning of input for segment number 2	
VII	End of input deck 2	

FIGURE 3
Test Basin (Sample Problem)

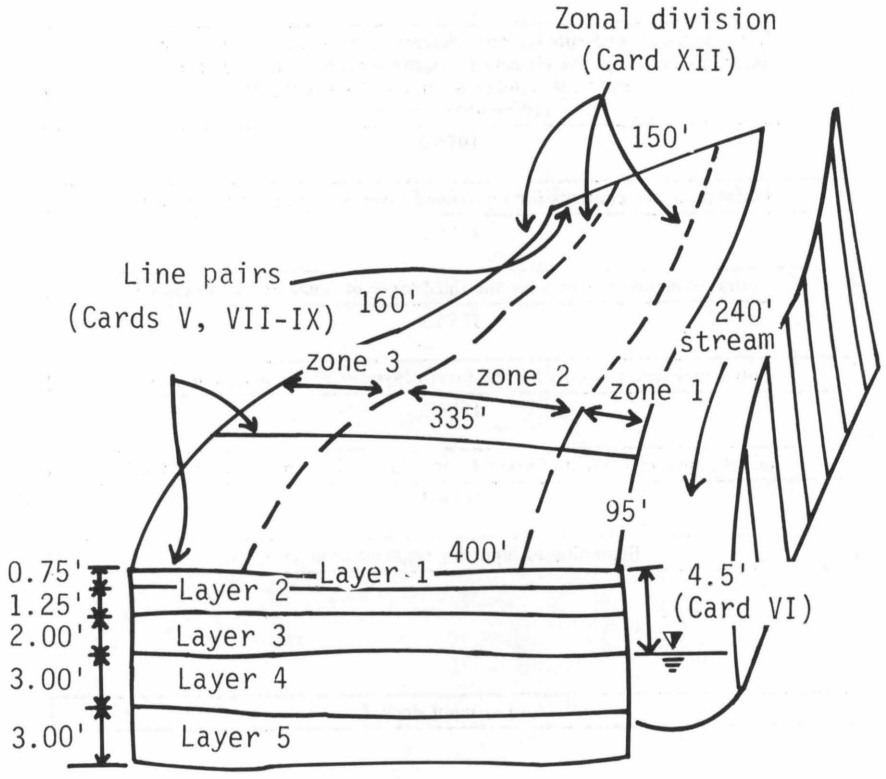

Not to Scale

FIGURE B4
Salient Features (Sample Problem)

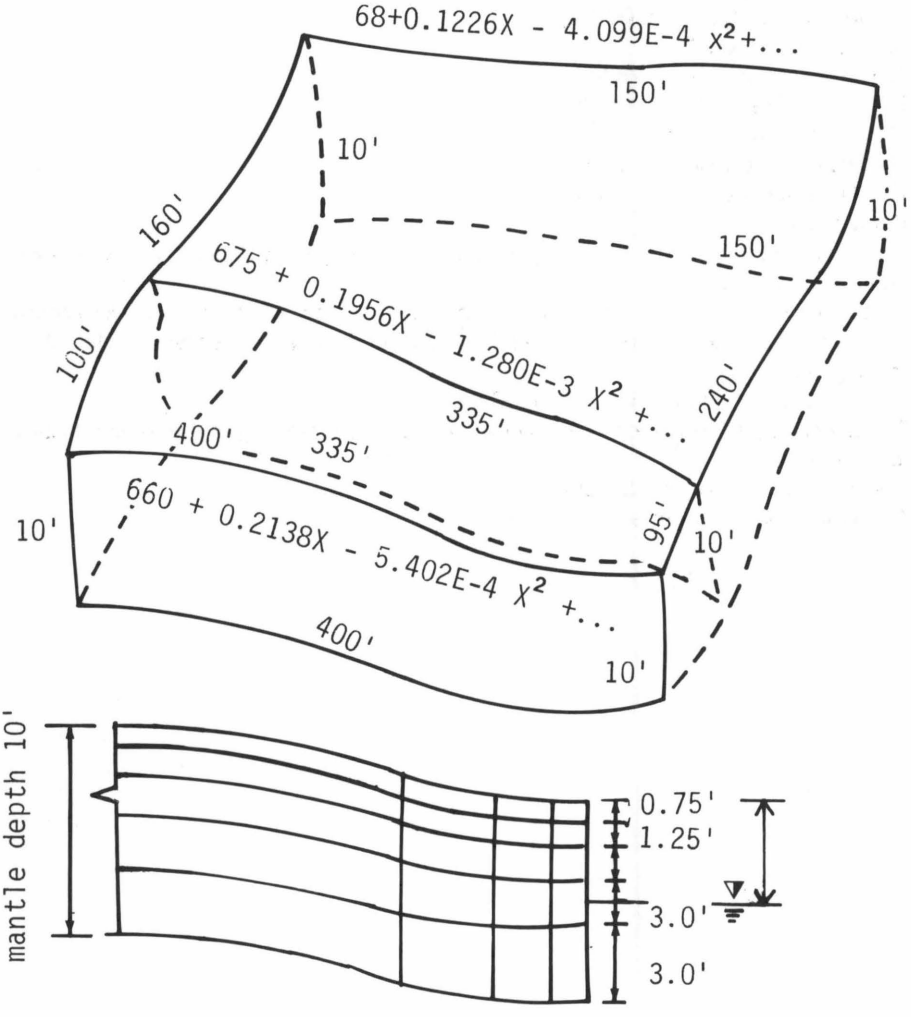

Not to Scale

TABLE B1
General Description of the Sample Problem Watershed

Name of the watershed - Test Basin
Number of segments - 1
Number of line pairs - 3
Number of soil layers - 60,000 sq. ft.
Mantle depth - 10.0 ft.
Thickness of top layer - 0.75 ft.
Thickness of second layer - 1.25 ft.
Thickness of third layer - 2.0 ft.
Thickness of fourth layer - 3.0 ft
Thickness of bottom layer - 3.0 ft.
Stream area - 500 sq. ft.
Time required for a water particle generated by the segment to reach the watershed outlet - 5 minutes
Three different soil types exist along the length of the segment, the hydrological properties changing at 20 percent and 60 percent of the total horizontal slope length of the segment.
Soil properties are shown in Table B2 (Data file 1).
Simulation is performed for a rainfall on June 8, 1988, starting at 4 a.m. and lasting for an hour.
The total precipitation is 1.5 inches.
The simulation is performed for 8 hours.

TABLE B2
Data File for Input Deck 1 (Sample Problem)

```
                                                                                                                    CARD NO.
  1TEST BASIN                                                                                                          I
THIS IS A TEST RUN TO EXPLAIN OUTPUT FILE                                                                              II
880808                                                                                                                III
            1.5                                                                                                       IV
  9.
 1   3   5    5    60000.                                                                                             V
4.5                                                                                                                   VI
  6.600E02  2.188E-1 -5.402E-4  1.403E-6 -1.690E-9  4.000E02  9.500E01                                                VII
  0.100E02                                          4.000E02  1.000E02                                              VIII
  6.750E02  1.956E-1 -1.280E-3  5.620E-6 -7.628E-9  3.350E02  2.400E02
  0.100E02                                          3.350E02  1.600E02                                               IX
  6.850E02  1.226E-1 -4.099E-4  2.142E-6 -3.408E-9  1.500E02
  0.100E02                                          1.500E02
   0.75    0.135   0.216   0.324   0.325                                                                             X
   500.                                                                                                            XI
    0.2    0.8     1.0                                                                                            XII
    4.608E-3    -8.05885      Layer 1                                                                             XIII
    2.921E07    18.81997                                                                                          XIV
    4.416E-3    -8.19369      Layer 2
    6.525E07    19.13503
    1.289E-2    -9.19313      Layer 3          Zone 1
    3.295E06    21.7547                                                                                           XV
    3.023E-2    -7.47757      Layer 4
    2.363E07    20.73710
    3.023E-2    -7.47757      Layer 5
    2.363E07    20.73710
    2.409E-2    -5.44682
    1.761E06    13.3804
    1.125E-4   -14.78649
    1.906E10    33.53633
    1.289E-2    -9.19313          Zone 2
    3.295E06    21.7547
    3.023E-2    -7.47757
    2.363E07    20.73710
    3.023E-2    -7.47757
    2.363E07    20.73710
    1.417E-3    -7.74277                                                                                          XVI
    7.119E07    18.1423
    3.862E-6   -20.22843
    9.562E10    44.2194
    4.684E-2    -8.17697          Zone 3
    5.680E05    19.60233
    3.023E-2    -7.47757
    2.363E07    20.73710
    3.023E-2    -7.47757
    2.363E07    20.73710
 51.5475   0.458500   2.47038                                                                                       XVII
  9.9600   0.497917   1.33789                                                                                      XVIII
  0.1000   0.490400   9.02102
125.2583   0.489222   6.34169
125.2583   0.489222   6.34169
 51.5475   0.458500   1.68473
  9.9600   0.497917   3.82849                                                                                       XIX
  0.1000   0.490400   9.02102
125.2583   0.489222   6.34169
125.2583   0.489222   6.34169
 51.5475   0.458500   0.59371
  9.9600   0.497917   5.16249
  0.1000   0.490400  15.88588          Note that card XX is not
125.2583   0.489222   6.34169              used because there
125.2583   0.489222   6.34169              is only one segment
                                                                                                                    XXI
```

TABLE B3
Data File for Input Deck 2 (Sample Problem)

										Card No.
.372	.397	.410	.422	.397	.393	.413	.434	.452	.458	I
.444	.498	.498	.498	.498	.475	.479	.492	.498	.498	II
.490	.490	.490	.490	.490	.490	.490	.490	.490	.490	III
.489	.489	.479	.385	.354	.335	.325	.312	.303	.296	IV
.489	.489	.489	.489	.457	.411	.371	.333	.310	.299	V

TABLE B4
Output File (Sample Problem)

Test Run of Hydrograph Simulation for Segment 1 of Test Basin to Explain Output File

ELEVATION OF EACH SOIL ELEMENT (FEET)

J , N	1	2	3	4	5	6	7	8	9	10	11	12	13	14	15	16
1	676.25	676.93	678.19	679.89	681.87	684.01	686.30	688.86	691.90	695.68	700.18	704.82	0.00	0.00	0.00	0.00
2	675.25	675.93	677.19	678.89	680.87	683.01	685.30	687.86	690.90	694.68	699.18	703.82	0.00	0.00	0.00	0.00
3	673.63	674.30	675.56	677.26	679.24	681.39	683.68	686.23	689.28	693.05	697.56	702.19	0.00	0.00	0.00	0.00
4	671.13	671.81	673.07	674.77	676.75	678.89	681.18	683.74	686.78	690.55	695.06	699.70	0.00	0.00	0.00	0.00
5	668.13	668.81	670.07	671.77	673.74	675.89	678.18	680.74	683.78	687.55	692.06	696.69	0.00	0.00	0.00	0.00

SLOPE OF EACH SOIL ELEMENT

J , N	1	2	3	4	5	6	7	8	9	10	11	12	13	14	15	16
1	0.18	0.18	0.16	0.14	0.12	0.11	0.10	0.09	0.10	0.11	0.11	0.09	0.00	0.00	0.00	0.00
2	0.18	0.18	0.16	0.14	0.12	0.11	0.10	0.09	0.10	0.11	0.11	0.09	0.00	0.00	0.00	0.00
3	0.18	0.18	0.16	0.14	0.12	0.11	0.10	0.09	0.10	0.11	0.11	0.09	0.00	0.00	0.00	0.00
4	0.18	0.18	0.16	0.14	0.12	0.11	0.10	0.09	0.10	0.11	0.11	0.09	0.00	0.00	0.00	0.00
5	0.18	0.18	0.16	0.14	0.12	0.11	0.10	0.09	0.10	0.11	0.11	0.09	0.00	0.00	0.00	0.00

DEPTH OF EACH SOIL ELEMENT (FEET)

J , N	1	2	3	4	5	6	7	8	9	10	11	12	13	14	15	16
1	0.75	0.75	0.75	0.75	0.75	0.75	0.75	0.75	0.75	0.75	0.75	0.75	0.00	0.00	0.00	0.00
2	1.25	1.25	1.25	1.25	1.25	1.25	1.25	1.25	1.25	1.25	1.25	1.25	0.00	0.00	0.00	0.00
3	2.00	2.00	2.00	2.00	2.00	2.00	2.00	2.00	2.00	2.00	2.00	2.00	0.00	0.00	0.00	0.00
4	3.00	3.00	3.00	3.00	3.00	3.00	3.00	3.00	3.00	3.00	3.00	3.00	0.00	0.00	0.00	0.00
5	3.01	3.01	3.01	3.01	3.01	3.01	3.01	3.01	3.01	3.01	3.01	3.01	0.00	0.00	0.00	0.00

SLOPE LENGTH OF EACH SOIL ELEMENT (FEET)

J , N	1	2	3	4	5	6	7	8	9	10	11	12	13	14	15	16
1	1.96	5.88	9.79	13.69	17.59	21.52	25.49	29.52	33.64	37.85	42.13	46.42	0.00	0.00	0.00	0.00
2	1.96	5.88	9.79	13.69	17.59	21.52	25.49	29.52	33.64	37.85	42.13	46.42	0.00	0.00	0.00	0.00
3	1.96	5.88	9.79	13.69	17.59	21.52	25.49	29.52	33.64	37.85	42.13	46.42	0.00	0.00	0.00	0.00
4	1.96	5.88	9.79	13.69	17.59	21.52	25.49	29.52	33.64	37.85	42.13	46.42	0.00	0.00	0.00	0.00
5	1.96	5.88	9.79	13.69	17.59	21.52	25.49	29.52	33.64	37.85	42.13	46.42	0.00	0.00	0.00	0.00

WIDTH OF EACH INCREMENT (FEET)

J , N	1	2	3	4	5	6	7	8	9	10	11	12	13	14	15	16
1	334.12	330.59	323.53	312.92	298.74	280.97	259.58	234.55	205.82	173.35	138.72	132.99	0.00	0.00	0.00	0.00

TABLE B4 continued

TIME	NET PRECIP. INCHES	Q SURFACE	Q LAYER 1	Q LAYER 2	Q LAYER 3	Q LAYER 4	Q LAYER 5	Q TOTAL	Q TOTAL CFSM	
				CU.FEET/HOUR						
OVERLAND FLOW (CFT.)		TOP LAYER FLOW (CFT.)								
		0.000								
		0.000								
		0.000								
		0.000								
100	0.00	0.0	0.0	6.9	0.8	0.0	0.0	0.0	1.0	
		0.000								
		0.000								
		0.000								
		0.000								
200	0.00	0.0	0.0	32.7	2.1	0.0	0.0	0.0	4.5	
		0.000								
		0.000								
		0.000								
		0.000								
300	0.00	0.0	0.0	34.1	2.4	0.0	0.0	0.0	4.7	
		0.000								
		0.444								
1277.448		4.322								
1591.736		18.553								
400	1.40	58.3	2892.5	85.6	2.7	0.0	0.0	0.8	392.2	
		11.088								
		3.237								
		1.352								
		0.354								
500	0.00	0.0	16.0	101.7	2.6	0.0	0.0	0.0	15.5	
		0.038								
		0.000								
		0.000								
		0.000								
600	0.00	0.0	0.0	75.3	2.2	0.0	0.0	0.0	10.0	

MOISTURE CONTENT AFTER ITERATION 6

J ; N	1	2	3	4	5	6	7	8	9	10	11	12	13	14	15	16
1	0.384	0.427	0.441	0.432	0.433	0.434	0.437	0.437	0.436	0.433	0.434	0.428	0.000	0.000	0.000	0.000
2	0.498	0.498	0.498	0.497	0.498	0.497	0.498	0.497	0.497	0.498	0.498	0.498	0.000	0.000	0.000	0.000
3	0.490	0.490	0.490	0.489	0.487	0.490	0.490	0.490	0.489	0.488	0.486	0.485	0.000	0.000	0.000	0.000
4	0.489	0.489	0.489	0.470	0.386	0.360	0.347	0.340	0.332	0.325	0.320	0.315	0.000	0.000	0.000	0.000
5	0.489	0.489	0.489	0.489	0.489	0.462	0.410	0.380	0.349	0.324	0.309	0.300	0.000	0.000	0.000	0.000

```
      0.000          0.000
      0.000          0.000
      0.000          0.000
      0.000          0.000
700     0.00         0.0      0.0     65.0     2.5      0.0      0.0      0.0      8.7
      0.000          0.000
      0.000          0.000
      0.000          0.000
      0.000          0.000
800     0.00         0.0      0.0     54.7     2.4      0.0      0.0      0.0      7.4
```

INDEX	DAY	TIME	RAIN(IN.)	FLOW(CFSM)	HYDROGRAPH
1	8	100	0.00	0.92	*
2	8	200	0.00	4.20	*
3	8	300	0.00	4.69	*
4	8	400	1.50	359.95	I *
5	8	500	0.00	46.93	I *
6	8	600	0.00	10.47 *	I
7	8	700	0.00	8.83	I *
8	8	800	0.00	7.49	I *
9	8	900	0.00	0.61 *	

SEGMENT	STORMFLOW(IN.)	RESPONSE(%)
1	0.6313	42.083

THE STORMFLOW IN INCHES OF WATER IS 0.6349

THE RAINFALL IN INCHES OF WATER IS 1.5000

REFERENCES

Aitchison, J., and J. A. C. Brown. 1957. *The Lognormal Distribution*. Cambridge University Press.

Bear, J. 1979 *Hydraulics of Groundwater*. McGraw-Hill, New York.

Bennion, D. W., and J. C. Griffiths. 1966." A Stochastic Model for Predicting Variations in Reservoir Rock Properties." *Trans AIME,* 237(2), 9-16.

Bernier, P. Y. 1985. "Variable Source Areas and Storm-Flow Generation: An Update of the Concept and a Simulation Effort." *Journal of Hydrology*, 79,195-213.

Betson, R. P. 1964. "What is Watershed Runoff?" *Journal of Geophysical Research*, 69(8), 1541-1552.

Beven, K. J., and M. J. Kirby. 1979. "A Physically-Based Variable Contributing Area Model of Basin Hydrology." *Hydrological Sciences Bulletin*, 24(1), 43-69.

Carsel, R. F., and R. S. Parrish. 1988. "Developing Joint Probability Distributions of Soil-Water Retention Characteristics." *Water Resources Research*, 24(5), 755-769. Carvallo, H. O., D. K. Cassel, J. Hammond, and A. Bauer. 1976. "Spatial Variability of *In Situ* Unsaturated Hydraulic Conductivity of Maddock Sandy Loam." *Soil Science,* 121, 1-8.

Collins, R. E. 1961. *Flow of Fluids Through Porous Materials.* Reinhold, New York.

Dagan, G., and E. Bresler. April 1983. "Unsaturated Flow in Spatially Variable Fields 1. Derivation of Models of Infiltration and Redistribution." *Water Resources Research,* 19(2), 413-420.

Darcy, H. 1956 (Translation 1983). *Les Fontaines Publiques de la Ville de Dijon.* Victor Dalmont, Paris. (Translation by R. A. Freeze. R. A. Freeze and W. Back, eds. In *Physical Hydrogeology (Benchmark Papers in Geology, Vol. 72).* Hutchinson Ross Publishing Company.

DeGroot, M. H. 1965. *Probability and Statistics.* Addison-Wesley Publishing Company, Reading, Massachussets.

De Wiest, R. J. M. 1965. *Geohydrology.* Wiley, New York.

Dunne, T. 1978. "Field Studies of Hillslope Flow Processes." In: *Hillslope Hydrology,* M. J. Kirkby, ed. John Wiley and Sons, 227-294.

Dunne, T. 1983. "Relation of Field Studies and Modeling in the Prediction of Storm Runoff." *Journal of Hydrology.* 65(1/3):25-48.

Dunne, T., and R. D. Black. 1970a. "An Experimental Investigation of Runoff Production in Permeable Soils." *Water Resources Research.* 6(2):478-490.

Dunne, T., and R. D. Black. 1970b. "Partial Area Contributions to Storm Runoff in a Small Watershed." *Water Resources Research.* 6(5):1296-1311.

Dunne, T., and L. B. Leopold. 1978. *Water in Environmental Planning.* W. H. Freeman and Company, San Francisco.

Eagleson, P. S. 1970. *Dynamic Hydrology.* McGraw-Hill, New York.

El-Kadi, A. I. 1984. "Modeling Variability in Groundwater Flow." *Institute Paper No. 31.* Holcomb Research Institute, Butler University, Indianapolis.

Engman, E. T., and A. S. Rogowski. 1974. "A Partial Area Model for Stormflow Synthesis." *Water Resources Research.* 10(3), 464-472.

Fiering, M. B., and B. B. Jackson. 1971. *Synthetic Streamflows.* Water Resources Monograph No. 1, American Geophysical Union.

Freeze, R. A. 1974. "Streamflow Generation." *Reviews of Geophysics and Space Physics.* 12(4):627-647.

Freeze, R. A. 1975. "A Stochastic-Conceptual Analysis of One-Dimensional Groundwater Flow in Nonuniform Homogeneous Media." *Water Resources Research.* 11(5), 725-741.

Freeze, R. A., and J. A. Cherry. 1979. *Groundwater.* Prentice-Hall, Inc., Englewood Cliffs, New Jersey.

Gburek, W. J., R. L. Hendrick, A. S. Rogowski, and M. L. Paul. 1977. "Predictability of Effects of a Severe Local Storm in Pennsylvania" *Journal of Applied Meteorology.* 16(2), 136-144.

Gelhar, L. W. 1986. "Stochastic Subsurface Hydrology From Theory to Applications." *Water Resources Research.* 22(9):135S-145S.

Hewlett, J. D. 1961. "Some Ideas About Storm Runoff and Base Flow, USDA Forest Service, Southeast Forest Experiment Station." *Annual Report.* 62-66.

Hewlett, J. D., and A. R. Hibbert. 1967. "Factors Affecting the Response of Small Watershed to Precipitation in Humid Areas." In: *Forest Hydrology,* W. E. Sopper and H. W. Lull, eds. Oxford Pergamon, 275-290.

Hewlett, J. D., and W. L. Nutter. 1970. "The Varying Source Area Streamflow From Upland Basins." *Proceedings of Symposium on Watershed Management.* ASCE. 65-83.

Horton, R. E. 1933. "The Role of Infiltration in the Hydrologic Cycle." *Transact' American Geophysical Union.* 14, 446-460.

Johnson, R. A., and D. W. Wichern. 1982. *Applied Multivariate Statistical Analysis.* Prentice Hall, Inc., Englewood Cliffs, New Jersey.

Leite, J. D. 1985. "Interflow, Overland Flow and Leaching of Natural Nutrients on an Alfisol Slope of Southern Bahia, Brazil. *Journal of Hydrology.* 80, 77-92.

Nielsen, D. R., J. W. Biggar, and K. T. Erh. 1973. "Spatial Variability of Field Measured Soil-Water Properties." *Hilgardia.* 42, 215-259.

Ragan, R. M. 1968. "An Experimental Investigation of Partial Area Contributions." *International Association of Scientific Hydrology.* Publications No. 76, 241-249.

Rogowski, A. S. 1972. "Watershed Physical Soil Variability Criteria. *Water Resources Research.* 8, 1015-1023.

Scheuer, E. M., and D. S. Miller. 1972. "On the Generation of Normal Random Vectors." *Technometrics.* 4, 278-281.

Sharma, M. L., G. A. Gander, and C. G. Hunt. 1980. "Spatial Variability of Infiltration in a Watershed." *Journal of Hydrology.* 45, 101-122.

Sherman, L. K. 1932. "Streamflow From Rainfall by the Unit Graph Theory." *Engineering News Record.* 108.

Silliman, S. E., and A. L. Wright. 1988. "Stochastic Analysis of Paths of High Hydraulic Conductivity in Porous Media." *Water Resources Research.* 24(11):1901-1910.

Smith, L., and R. A. Freeze. 1979a. "Stochastic Analysis of Steady State Groundwater Flow in a Bounded Domain, 1, One-Dimensional Simulations." *Water Resources Research.* 15(3):521-528.

Smith, L., and R. A. Freeze. 1979b. "Stochastic Analysis of Steady State Groundwater Flow in a Bounded Domain. 2, Two-Dimensional Simulations." *Water Resources Research.* 15(6):1543-1559.

1979b. Smith, L., and F. W. Schwartz. 1980. "Mass Transport, 1, A Stochastic Analysis of Macrospic Dispersion." *Water Resources Research.* 16(2):303-313.

Smith, L., and F. W. Schwartz. 1981a. "Mass Transport, 2, Analysis of Uncertainty in Prediction." *Water Resources Research.* 17(2):351-369.

Smith, L., and F. W. Schwartz. 1981b. "Mass Transport, 3, Role of Hydraulic Conductivity Data in Prediction." *Water Resources Research.* 17(5):1463-1479.

United States Department of Agriculture. November 1952. *Soil Survey: Culpeper County, Virginia.* Series 1941, No. 3.

van Genuchten, M. Th. 1980. "A Closed-form Equation for Predicting the Hydraulic Conductivity of Unsaturated Soils." *Journal of the Soil Science Society of America.* 44,892-898.

Virginia Water Resources Research Center. 1988. *HISARS (Hydrologic Information Storage And Retrieval System).* Virginia Polytechnic Institute and State University, Blacksburg.

Watershed Engineering Project, General Information — Ten Virginia Watersheds with Complex Land Use. USDA, ARS, SWCRD. 1968.

Zaslavski, D., and A. F. Rogowski. 1969. "Hydrologic and Morphologic Implications of Anisotropy and Infiltration in Soil Profile Development." *Soil Science Society of America, Proceedings.* 33:594-599.

Zaslavski, D., and G. Sinai. 1981. "Surface Hydrology: III — Causes of Lateral Flow." *ASCE Journal of Hydraulics Division.* 107(HY1):37-52.

The Virginia Water Resources Research Center is a federal-state partnership agency attempting to find solutions to the state's water resources problems through careful research and analysis. Established at Virginia Polytechnic Institute and State University under provisions of the Water Research and Development Act of 1978 (P.L. 95-467), the Center serves six primary functions.

- It studies the state's water and related land-use problems, including their ecological, political, economic, institutional, legal, and social implications.
- It sponsors, coordinates, and administers research investigations of these problems.
- It collects and disseminates information about water resources and water resources research.
- It provides training opportunities in research for future water scientists enrolled at the state's colleges and universities.
- It provides other public services to the state in a wide variety of forms.
- It facilitates coordinated actions among universities, state agencies, and other institutions.

More information on programs and activities may be obtained by writing or telephoning the Water Center.

Virginia Water Resources Research Center
Virginia Polytechnic Institute and State University
617 North Main Street
Blacksburg, Virginia 24060-3397
Phone (703) 231-5624